COMPARING THE EFFECTIVENESS OF HHE TWO-ELECTRODE ARRAY WITH THE SYMMETRICAL SCHLUMBERGER ARRAY OVER THE MAIN CAMPUS OF AHMADU BELLO UNIVERSITY, ZARIA

BY

YUSUF, DAVID BACHAMA

SEPTEMBER, 2000

COMPARING THE EFFECTIVENESS OF THE TWO-ELECTRODE ARRAY WITH THE SYMMETRICAL SCHLUMBERGER ARRAY OVER THE MAIN CAMPUS OF AHMADU BELLO UNIVERSITY, ZARIA

BY

YUSUF, DAVID BACHAMA
AHMADU BELLO UNIVERSITY, ZARIA

A THESIS SUBMITTED TO THE POSTGRADUATE SCHOOL, AHMADU BELLO UNIVERSITY, ZARIA

IN PARTIAL FULFILMENT FOR THE AWARD OF THE DEGREE OF MASTER OF SCIENCE IN APPLIED GEOPHYSICS.

DEPARTMENT OF PHYSICS
FACULTY OF SCIENCE
AHMADU BELLO UNIVERSITY, ZARIA

SEPTEMBER, 2000

DECLARATION

I hereby declare that, this thesis is an original work carried out by the author under the supervision of Professor C.O. Ajayi and Dr. M. N. Umego.

To the best of my knowledge, no part thereof has been submitted elsewhere for the award of a degree.

The work of others are duly acknowledged and referenced.

Yusuf David Bachama

Author

Date

CERTIFICATION

This thesis entitled: COMPARING THE EFFECTIVENESS OF THE TWO-ELECTRODE ARRAY WITH THE SYMMETRICAL SCHLUMBERGER ARRAY OVER THE MAIN CAMPUS OF A.B.U, ZARIA by YUSUF, David Bachama meets the regulations governing the award of the degree of Master of Science (Applied Geophysics) of Ahmadu Bello University, Zaria and is approved for its contribution to knowledge and literary presentation.

Prof. C.O. Ajayi
Chairman, Supervisory Committee Date 22/11/2000

Dr. M. N. Umego
Member Supervisory Committee Date 22/11/2000

Prof. I.B. Osazuwa
Head, Dept. Of Physics Date 24-11-2000

Prof. S. B. Ojo
Dean, Postgraduate School Date 17/03/01

ACKNOWLEDGEMENT

I would like to acknowledge the assistance of several people who have contributed in one way or the other to the success of this work.

First and foremost, I would like to express my profound gratitude to my supervisor Professor C.O. Ajayi who suggested the topic and supervised the work. I am extremely grateful for his understanding, co-operation and useful pieces of advice.

I wish to express my thanks to Professor I.B. Osazuwa, Professor S.B. Ojo, Dr. P. Sule and Dr. M.N. Umego for their inspiration during the course of my programme.

I cannot forget the contribution of my sister Mrs. Ruskana P.A. of the Dept. of Industrial Design, A.B.U, Zaria. My profound and sincere thanks go to her, for her moral and financial support throughout my studies. The support of her children Abba, Yusuf and Maryamu is highly appreciated.

I would also like to acknowledge the assistance of Alhaji Zakari Danbam who allowed me to use their computer for the interpretation.

To my friends and colleagues: Ibeh Stephen and Pascal Ayi, I am grateful for their co-operation, teamwork and useful pieces of advice. Mr.Aminu Lawal is also acknowledged for his useful suggestions and advice.

The effort and co-operation of my friends Mr. J.S. Doka (Jaggers) and Mr. T. Kadiri (Boy) and Dr. Alh. Nuru concerning this work are highly appreciated.

I appreciate the co-operation of Mr. B. Nwosu, O. Fagbemi and Mallan Jatau. The efforts of Mr. Ouma Roufai for the excellent typing of this work is highly appreciated.

IM RAHIM

To Rahila Ismaila, I am very greatful for her cooperation, support and understanding.

Finally and above all, I thank God the Allmighty for making this work a reality. He made it possible for me to carry out the fieldwork and interprete the collected data successfully. I thank God for granting me safe journey mercies during the course of this work.

ABSTRACT

A geoelectric investigation employing vertical electrical soundings (VES) using the Ajayi-Makinde two-electrode method, as used by Makinde (1996), and the conventional Schlumbcrger configuration was carried out in the Main Campus of Ahmadu Bello University (A.B.U.) Zaria with the aim of testing the reliability and effectiveness of the said two-electrode method.

Results of the VES interpretation obtained in this work using the two-electrode method have compared very well with those obtained from Schlumbcrger data gathered in this work at the same VES stations used for the two-electrode method. The areas of good agreement between the results of the two methods include: depth-to-basemenl values (about 86 %), layer thicknesses (about 72 %) and resistivity values of the various layers (about 52 %).

Interpretation of the two-electrode data and the Schlumbcrger data revealed that the layering in the study area varied from 3 to 4 layers. The resistivity values of the top or sueface layer, second layer and basement from the two-electrode method varied from 70 - 450 -m, 98 - 813 -m and 1000 - 3000 -m respectively while those from the Schlumberger configuration data varied from 89 - 434 -m, 59 - 634 -m and 1000 - 3300 -m for the surface layer, second layer and the basement respectively.

The two methods show that the geometry of the bedrock underlying the Main Campus is undulating with depth values increasing away from the central part of the study area towards the southern, western and eastern parts of the study area. The depth to the bedrock obtained from the two-electrode method ranges from about 11.5 m in the

central part of the study area to about 30.0 in around the southern end of the study area, while that obtained from the Schlumberger configuration ranges from about 9.0 in in the central part of the study area to about 28.0 m in the southern end of the study area.

DEDICATION

This work is dedicated to my late father, Mr. Yusufu Bachama Mwanai.

TABLE OF CONTENTS

CHAPTER			PAGE
	Declaration		ii
	Certification		iii
	Acknowledgement		iv
	Abstract		vi
	Dedication		viii
	Table of Contents		ix
	List of Tables		xiii
	List of Figures		xiv
	List of Appendices		xvi
1	INTRODUCTION		1
	1.1	Location of the Study Area	1
	1.2	Relief and Climate of the Study Area	3
	1.3	Geology of the Kubanni Basin	3
	1.4	Previous Work in the Study Area	7
		1.4.1 Geographical Studies	7
		1.4.2 Geological Studies	7
		1.4.3 Geophysical Studies	8
	1.5	Aim of the Present Work	10

2 THE ELECTRICAL RESISTIVITY METHOD OF SURVEYING....12

2.1 Basis of Electrical Resistivity Method....12

2.2 Theory of the Direct Current Resistivity Method of the Four-Electrode Arrangement....13

2.2.1 Apparent Resistivity....19

2.3 The Different Electrode Arrangements....19

2.3.1 The Four-Electrode Arrangement....19

2.3.2 The Three-Electrode (tripotential) Arrangement....23

2.3.3 The Two-Electrode Arrangement....25

2.3.4 The Five-Electrode and Six-Electrode Arrangements....26

2.4 Principle of the Two-Electrode Method Used....26

2.5 Assumptions Made in the Ajayi-Makinde Two-Electrode Method Used....28

2.6 Theory of the Ajayi-Makinde Two-Electrode Array....28

3 DATA COLLECTION AND REDUCTION....33

3.1 Types of Data Collected....33

3.2 Data Collection....33

3.2.1 The Two-Electrode Array....35

a. Instrumentation....35

b. Field Procedure.....35

3.2.2 The Schlumberger Array.....37

a. Instrumentation.....37

b. Field Procedure.....37

3.3 Data Reduction.....38

3.3.1 The Two-Electrode Array.....38

3.3.2 The Schlumberger Array.....39

4 INTERPRETATION AND RESULTS.....42

4.1 Data Interpretation.....42

4.2 Interpretation of Data Obtained Using

the Two-Electrode method.....44

4.2.1 Determination of Layer Parameters.....46

a. Number of Layers Sounded.....46

b. Depth-To-Basement Determinations.....47

c. Layer Thickness Determination.....47

d. Determination of Resistivity Values.....47

4.3 Interpretation of Data Obtained Using the

Schlumberger Array.....49

4.4 Geoelectric and Geologic Sections.....51

4.5 Contour Maps and Cross-Sections Produced.....57

4.5.1 Depth – to – Basement Contour Maps.....57

a. From the Two-Electrode Array Data.....57

b. From the Schlumberger Array Data.....62

4.5.2 3-D Cross-Sectional Diagrams of the Basement.....62

4.5.3 Surface Layer Thickness Contour Maps.....62

4.6 Comparison of Results obtained Using Interpreted Two-Electrode Array Data and Schlumberger Array Data.....65

4.7 Comparison of Results Obtained in this Work With Those Obtained by Previous Workers in the Kubanni Basin.....67

5 DEDUCTIONS, SUGGESTIONS AND CONCLUSIONS.....77

5.1 Deductions from Results.....77

5.1.1 Reliability of the Two-Electrode Array.....77

5.1.2 The Geometry of the Basement Beneath the Main Campus of A.B.U., Zaria.....78

5.1.3 Groundwater Potential of the Study Area.....79

5.2 Suggestions for Future Research.....82

5.3 Conclusions.....82

References.....85

Appendix A.....88

Appendix B.....97

LIST OF TABLES

Table		Page
1	Typical Reduced and Plotted Data Obtained Using the Two-Electrode Array for VES Station 25	40
2	Typical Reduced and Plotted Data Obtained Using the Schlumberger Array for VES Station 25	41
3	Resistivity values of Rock Types in the Nigerian Basement Areas	43
4	Resistivity Values of Materials in the Kubanni Basin	43
5	Summary of Results Obtained from the Interpretation of both Sets of Data	69

LIST OF FIGURES

Figure		Page
1.1	Location of the Project Area Within the Geological Map of the Kubanni Basin	2
1.2	Simplified Geological Map of Nigeria	4
2.1	Four-Electrode Arrangement in Resisitivity Measurement	17
2.2	Some Common Four-Electrode Configurations	21
2.3	Some Three-Electrode Arrangements	24
2.4	Field Layout of Some Two-Electrode Configurations	24
2.5	Some Other Electrode Arrangements	24
2.6	Laboratory Determination of Ohm's Law and its 2-Electrode "Sounding " Analog	27
3.1	Map of the Area Under Study Showing the Sounding Points	34
3.2	Arrangement of the Field Equipment Used for the Two-Electrode Method	36
4.1	Plot of Bulk Resistivity Against L/2 and Interpretation of Data Obtained Using Two-Electrode Array for VES Station 25	45
4.2	Interpretation of Apparent Resistivity Obtained Using Schlumberger Array for VES Station 25	50
4.3	Geoelectric and Geologic Sections Along Profile A-A'	52
4.4	Geoelectric and Geologic Sections Along Profile B-B'	57

4.5 Geoelectric and Geologic Sections Along Profile C-C' 55

4.6 Geoelectric and Geologic Sections Along Profile D-D' 56

4.7(a) Depth-To-Basement Contour Map of the Project Area Obtained from the Interpreted Two-Electrode Data..... 58

4.7(b) Depth-To-Basement Contour Map of the Project Area Obtained from the Interpreted Schlumberger Data..... 59

4.8(a) 3-D Cross-Sectional View of the Basemnet Underlying the Project Area from Interpreted Two-Electrode Data..... 60

4.8(b) 3-D Cross-Sectional View of the Basemnet Underlying the Project Area from Interpreted Schlumberger Data..... 61

4.9(a) Contour Map of Surface Layer Thickness from Interpreted Two-Electrode Data..... 63

4.9(b) Contour Map of Surface Layer Thickness from Interpreted Schlumberger Data..... 64

5.1(a) Contour Map of Aquifer Thickness of the Project Area from Interpreted Two-Electrode Data..... 80

5.1(b) Contour Map of Aquifer Thickness of the Project Area from Interpreted Schlumberger Data..... 81

LIST OF APPENDICES

Appendix		Page
A	Plots of Bulk Resistivity against L/2 and Interpretation of Data Using Two-Electrode Array	88
B	Interpretation of Schlumberger Data	97

CHAPTER 1

INTRODUCTION

1.1 LOCATION OF THE STUDY AREA

The Main Campus of Ahmadu Bello University (A.B.U.) Zaria is the project area investigated in this study. It is part of the Kubanni River Basin which is situated in the north-central part of Nigeria (Fig. 1.1). The Kubanni River Basin is situated in the centre of the SouthEast quadrant of the 1:50,000 Zaria sheet No. 102 S.W. of Nigeria Ordinance Survey Map. The Main Campus is located in the north-western part of the Kubanni Basin, which occupies about 9 % of the area of the basin. The Main Campus is situated north-west of Zaria city at a distance of about 15.5 km from the City and just to the left of the Zaria - Funtua road.

The Main Campus is approximately bounded by latitude $11^0 09'$ N and $11^0 10'$ N and longitudes 7^0 38' E and 7^0 39' E (Fig. 1.1). It is a built-up area and the part investigated in this work is the western half of the Main Campus which includes: Area 3, Area A (parts I and II) Staff quarters, Danfodio Hall, Ramat and ICSA Halls, Suleiman Hall, Akenzua Hall, Amina Hall, Ribadu and Alexander Halls. It also includes the Staff School, A.B.U. Demonstration Secondary School, the Faculties of Human Medicine, Veterinary Medicine, Pharmaceutical Sciences, Sciences, Arts, Social Sciences, Engineering, Education and Environmental Design. The PostGraduate School, the Senate Building, Kashim Ibrahim Library (K.I.L.) and the Athletic and Football Fields are also included in the study area for this work. The exact area covered by the study area is shown in Fig. 1.1.

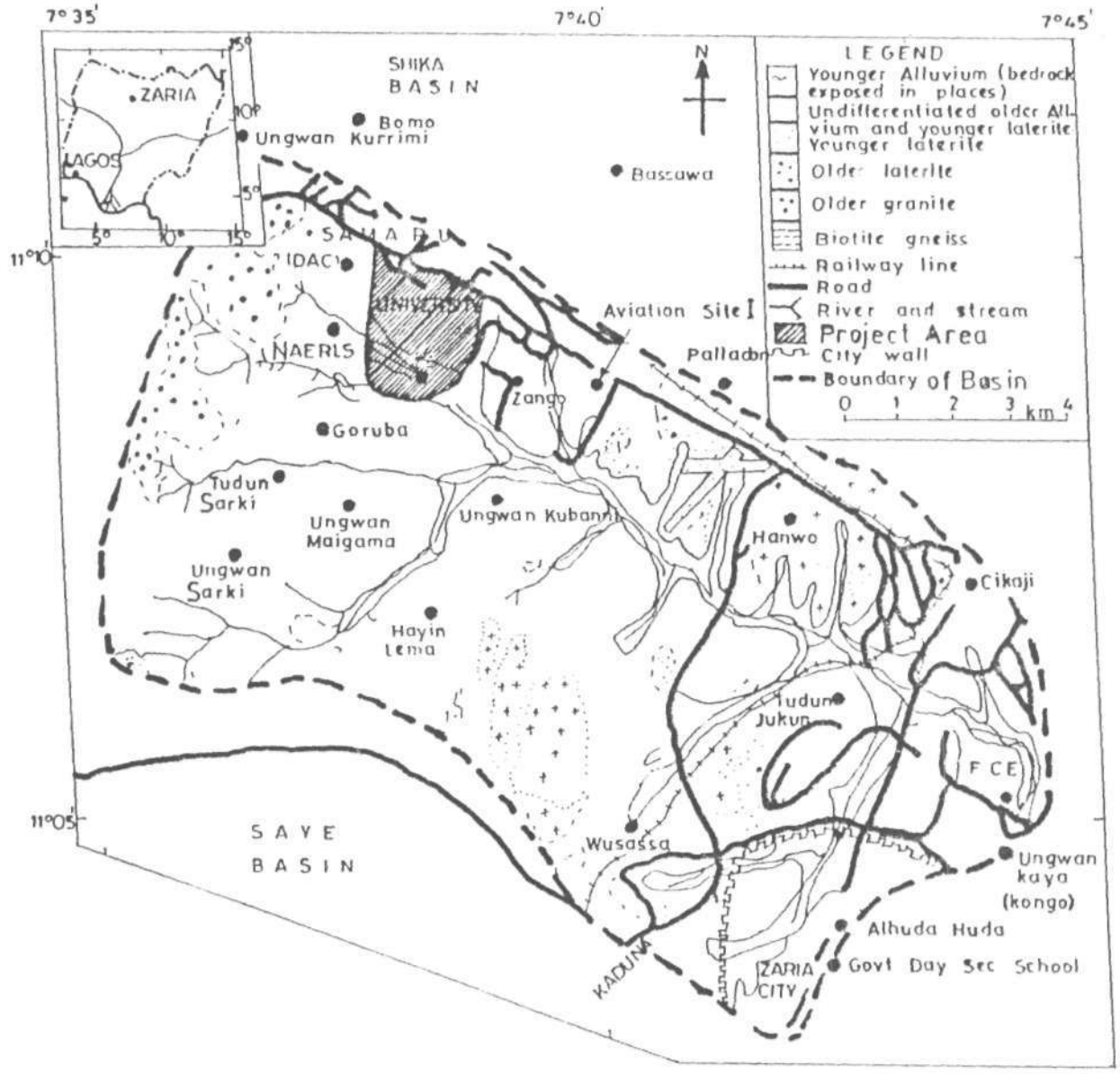


Fig. 1.1 Location of the Project Area Within the Geological Map of the Kubanni Basin (Modified from Shemang, 1990)

1.2 RELIEF AND CLIMATE OF THE STUDY AREA

According to Thorp (1970), Zaria, which contains the Main Campus of A.B.U. Zaria, is a part of the gently undulating peneplain that extends east-west from Lake Chad to Sokoto and northwards from the southern parts of Kaduna to Tiquodi in the Republic of Niger.The Kubanni basin is located on a Plateau at a height of about 570 m above sea level (Ologe 1971).

Zaria, which includes the Main Campus (the study area) is located within the tropical Savannah region and it is, thus, associated with distinct wet and dry seasons. The wet season begins around April/May and ends around October/November. The highest rainfall in the area is normally recorded in August while the highest peak of the dry season is around March/April (Ologe, 1971). The annual rainfall per annum ranges from 100 cm to 200 cm.

1.3 GEOLOGY OF THE KUBANNI BASIN

As reported by McCurry (1970), the Nigerian basement complex rocks are exposed over more than half of the land surface of Nigeria. The rocks are exposed mostly in the northern part, western part and the eastern flank of Nigeria that has border with the Republic of Cameroun (Fig.1.2).

As stated by Oyawoye (1964), the Nigerian basement complex is the end result of at least two major orogenic cycles. The last of the cycles probably extended from Late Precambrian to Lower Paleozoic. The cycles were believed to be initiated by the deposition of thick sands, mud and greywackes on igneous material cover and eroded metamorphic basement during the preceding cycle. As a result of extensive re-metamorphism and partial mobilization of the underlying basement, the accumulated

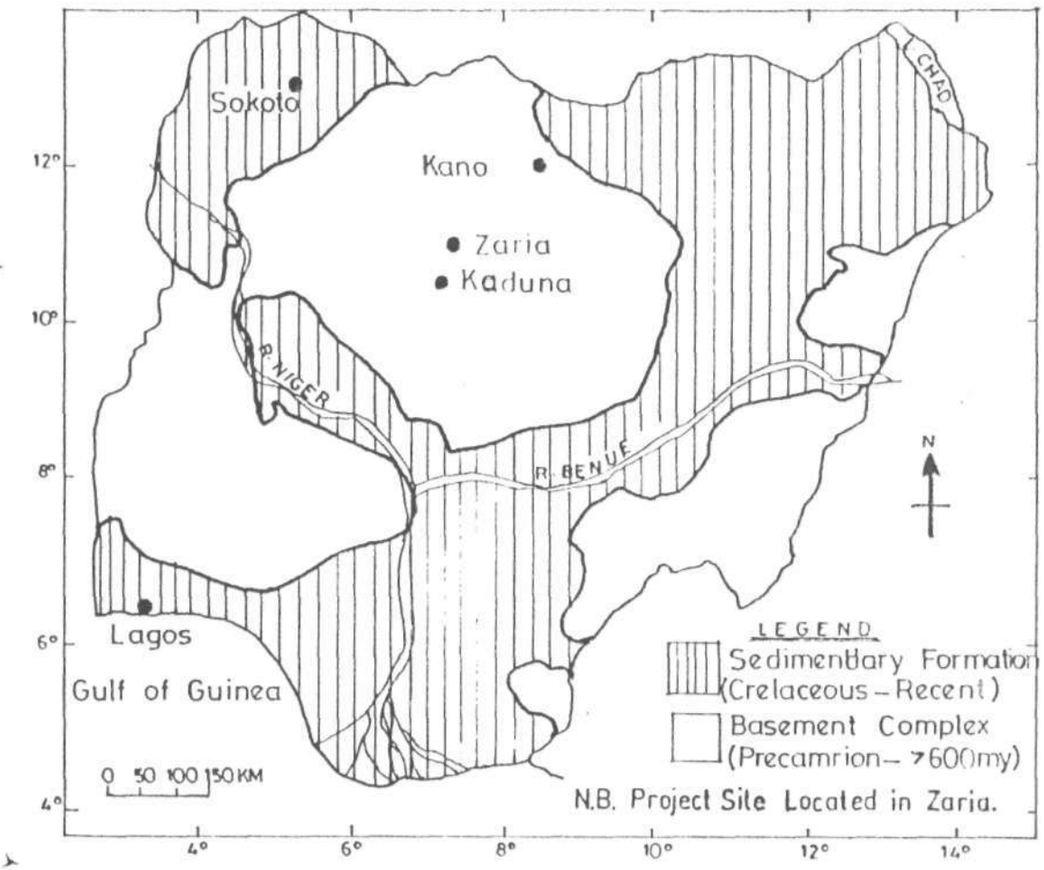


Fig.1.2 Simplified Geological Map of Nigeria (After G.S.N., 1970).

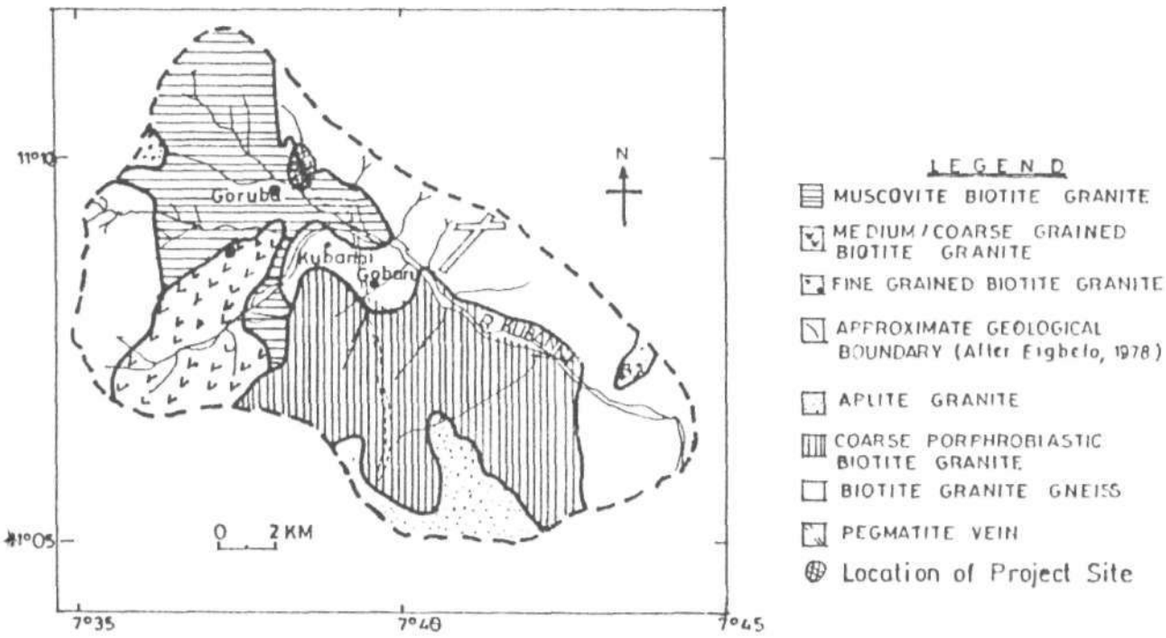


Fig. 1-3 Basement Geology Map of the Kubanni Basin, Zaria (After Eigbefo, 1978).

materials were developed into high-grade gneiss, migmatites and Older granite (Truswell and Cope, 1963; Wright and McCurry, 1970).

Fig.1.3 shows the basement geology map of the Kubanni Basin. The basin is underlain by rocks of the Precambrian age. Biotite gneiss predominates in the area and outcrops mainly in stream valleys where they are deeply weathered (Wright, 1970). The biotite gneiss complex consists of medium to coarse grained and moderate to weakly foliated rocks which constitute about 30 - 40 % of the basement complex rocks exposed in the basin (Wright and McCurry, 1970).

The different basement complex rocks found in the Kubanni basin are mostly covered by Quarternary to Recent deposits. They were summarised by Eigbefo (1978) as follows:

(i) Coarse porphyritic-biotite granite

(ii) Medium-coarse grained biotite granite gneiss

(iii) Aplite granite with pegmatite and quartz veins cutting across most of the bodies.

The superficial deposits that cover most of the basement rocks in the Kubanni Basin act as recharge areas where they are underlain by weathered basement (Eigbefo, 1978). Also, according to Eigbefo (1978), two phases of deformation took place in the basin. The first was along an E-W axis while the second was roughly along a N-S axis. The latter was of greater intensity, which obliterated evidence of the former and left a dominant N-S structural trend. Wright and McCurry (1970) also observed the basement structure in the basin to be relatively simple because of the uniform regional foliation trends. They also found that numerous joints and fractures have occurred in the basin after the Pan-African orogeny.

The Main Campus of A.B.U. Zaria, being part of the Kubanni Basin, is, therefore, underlain by Precambrian rocks of the Nigerian basement complex. As shown in Fig. 1.3, muscovite biotite-gneiss occupies the southern and western parts of the Campus while the rest or northern and eastern parts is underlain by biotite granite-gneiss (Eigbefo, 1978). Tokarski (1972) classified the main elements of the Kubanni Basin, which includes the Main Campus as: Acolin cover, Upper Savannah Loam, Younger laterite and Lower Savannah Loam. He divided the Quarternary sequences into three types of terraces according to their ages of deposition, relationship between their mineral content and the mineralogy of the underlying basement complex rocks as follows:

(i) Terrace III: This is the oldest deposit which is made up of Acolin cover, Upper Savannah Loam, the Younger laterite and the Lower Savannah Loam.

(ii) Terrace II: This consists of sandy Loam and ordinary level sands, which are products of the most recent erosion cycles.

(iii) Terrace I: This consists of hydroclastic material and "drift".

According to Olowu (1967) and Eigbefo (1978), the weathered basement is the main storage element for groundwater in the Kubanni Basin. As the case in the entire basin, the aquifer in the Main Campus is covered by laterite loam (Wright and McCurry, 1970; Eigbefo, 1978). The laterite contain little water which are mostly unconsolidated and, because they are shallow, they receive direct recharge from rainfall. The alluvial deposit in Zaria area consists of gravels, sands, silts and clay which are mostly found along stream channels. Their thicknesses ranges from 5 - 15 m (Olowu, 1967).

1.4 PREVIOUS WORK IN THE STUDY AREA

A lot of studies have been carried out in the Kubanni River Basin. These researches are in various fields, which include: geography, geology, geophysics and hydrogeology. Some of them are briefly discussed below.

1.4.1 GEOGRAPHICAL STUDIES

Hore (1970) studied the weather and climate of Zaria region for a span of over 30 years. His work has shed more light on the seasonal fluctuations of rainfall and the annual variations of temperature. Klikenbera (1970) also studied the soils in Zaria area and concluded that they belong to the class of the leached ferruginous tropical soils with weakly developed soils near the inselbergs and hydromorphic soils which form the Fadama soils. Also, he reported that most of these soils contain 30 - 40 % clay at reasonable depths. Thorp (1970) studied the landscape evolution of the Zaria region. According to him, the features of Zaria area include inselbergs and ruwares which he described as distinctively shaped hills of more or less bare rock that belong to the general category of residual hills, the mesas and the plains. The gully development in the Zaria area with emphasis on the Kubanni drainage basin was studied by Ologe (1971).

1.4.2 GEOLOGICAL STUDIES

Geological studies in the Kubanni Basin, according to Hassan (1987), dates back to 1967 when Olowu carried out a study of the surface water and its effect on the groundwater in Zaria area. He found that all the streams in the area are seasonal except the Galma river.

McCurry (1970) and Wright and McCurry (1970) carried out a study of the basement geology of the Zaria Sheet 102 S.W. They found the the basement complex rock is mostly made up of biotite granite-gneiss and Older granites.

Akpoborie (1972) studied the hyrogeological structures, which control underground water in the Samaru Creek. He found that the flow of groundwater into the Creek is controlled by structures like joints and fractures developed in the rocks.

Tokarski (1972) carried out one of the major geological investigations in the Zaria area which includes the basin just to the west of A.B.U. Zaria Main Campus. He worked out the heterogeneous terrace arrangement and the groundwater occurrences in the area.

The hydrogeology of the Kubanni Basin, with emphasis on the extent and variation in the thicknesses of the existing aquifer, was studied by Eigbefo (1978). Even though his work was mainly on the surface, he used the existing hand dug wells in the area and deduced the depths to the water table at various points in the area to vary from 3 - 10 m. Also, he concluded that the thicknesses of the weathered basement aquifer in the basin varies from 1 - 30 m.

1.4.3 GEOPHYSICAL STUDIES

The earliest electrical resistivity survey carried out in the Kubanni Basin is that of Jones and Du Preez (1952). The authors reported the presence of well developed steep dipping joints, which contain water in some granite outcrops in the basin but did not give their locations.

Ososami (1968) carried out a groundwater assessment of part of the northwestern part of the Kubanni Basin, mainly around the Main Campus of A.B.U. Zaria using vertical electrical soundings. He found that the aquifer in the area has variable thickness

and that the depth to the bedrock varies from less than a metre to a maximum depth of about 30 m.

Messrs. Preussag Limited carried out a resistivity survey from 1981 - 1982 in Jama'a Kubanni village for borehole siting (Olufemi, 1985). From the results of the resistivity data, they found the presence of faults within the bedrock which has caused a downthrow of certain parts of the bedrock. Olugbemiro (1985) also estimated the depth to the bedrock around Jama'a Kubanni village in the basin to be about 36 m.

Hassan (1987) carried out a geoelectric investigation of the western half of the Kubanni Basin. He reported that the resistivity values of the first layer (topsoil), second layer and third layer varied from 36 - 600 Ω-m, 20 - 350 Ω-m and 26 - 180 Ω-m respectively while the resistivity value of the bedrock ranged from 1000 - 8000 Ω-m. Also, he reported that the bedrock is undulating and concluded that the depth to the basement in the area is generally increasing towards the southern part. The depth to the bedrock as reported by Hassan (1987) in the western part of the Kubanni Basin ranges from less than 5 m in the northern end of the area and may reach up to 60 m in the south easthern part of the area.

Shemang (1990) conducted electrical depth soundings at selected well sites within the Kubanni River basin and reported that the resistivity values of the topmost layer in the basin ranged from 50 Ω-m at Cikaji to 781 Ω-m at Government Day Secondary School, Zaria City. He estimated the range of the depth to the basement to be about 3 m just to the west of A.B.U. Zaria dam, to about 44 m around Unguwan Kubanni while the average depth to basement in the basin is about 12 m. Shemang's interpreted VES data suggest that the overburden is mostly made up of clays, silts and sands, fresh laterite and weathered laterite.

Bajeh (1992) conducted a ground magnetic survey of the Kubanni Basin. Results of his work, in most cases, corroborated those of Shemang (1990). Bajeh (1992) also established that the depth to the basement within the basin is between 0 to about 50 m, which is about 6 m deeper than that of Shemang (i.e. between 3 m and 44 m).

Recently, Makinde (1996) carried out field investigation of a variant of the two electrode d.c. resistivity array within the Kubanni Basin. The results of his work show that this method has the capability to correctly estimate layer thicknesses and the depth to basement. Also, the depth-to-basement values obtained from his work compared well with those obtained by previous workers in the Kubanni Basin. Results from his interpretation of the collected data using the C-C mode show that the depth to basement within the basin varied from 7.9 m to about 36 m on the average.

1.5 AIM OF THE PRESENT WORK

As earlier discussed in section 1.1, the Main Campus of A.B.U. Zaria is situated in the Kubanni River Basin. It is chosen as the project area in this work because the geology of the basin is well known.

The C-C mode of the two-electrode array used by Makinde (1996) which is also the method employed in this work is a new method currently under development.

The primary aim of this work is to test the reliabilty and effectiveness of the new C-C mode of the two electrode method by comparing its results with those previously obtained using other well-known and well-tested geophysical methods in an area with known geology. The degree of agreement between the two sets of data (results) will determine whether or not the new method (array) is good enough for use in electrical geophysical prospecting. This aim was achieved through the following specific procedures:

(i) Carrying out vertical electrical soundings at selected points within the Main Campus of A.B.U. Zaria using the two-electrode array and the Schlunberger array at each sounding point and

(ii) Producing geoelectric sections obtained by interpretations of the two sets of data collected at each sounding point.

The secondary aims of this work are: (i) to determine the geometry of the basement beneath the Main Campus of A.B.U. Zaria and (ii) to determine the groundwater potential of the Main Campus. These aims were achieved by; (a) producing depth to basement contour maps and 3-D cross-sectional views from the interpreted VES data and (b) producing aquifer thickness contour maps from the interpreted VES data.

Interpretations made in this work from the VES data collected are reliable since a sound knowledge of the geology of the Kubanni Basin is available. As no geophysical information of the same detail as this work currently exists on the Main Campus of this University, results of this work are expected to give a better picture of the basement geometry of the campus for engineering (construction) purposes and for the purpose of groundwater exploitation within the Main Campus of A.B.U. Zaria.

CHAPTER II

THE ELECTRICAL RESISTIVITY METHOD OF SURVEYING

2.1 BASIS OF ELECTRICAL RESISTIVITY METHOD

In geophysical investigations for ore prospecting, water exploration, depth – to – bedrock determination, sand and gravel exploration, etc., the electrical resistivity method can be quickly and economically used to obtain details about the location, depth and resistivity of the targets of interest. The basis of the electrical resistivity method is that when current is applied into the ground through electrodes, any subsurface variation, in conductivity alters the current flow pattern within the earth and this, in turn, affects the distribution of the resulting electric potential in the earth. The degree to which the potential at the surface is affected by the current flow depends on the size, location, shape and conductivity of the material within the ground. It is therefore, possible to obtain information about the subsurface distribution of the earth's material from measurements of the electric potential made at the surface.

The usual practice is to pass current into the ground by means of two electrodes and to measure the potential difference between a second pair placed in line between them. The ratio of the voltage output (i.e. the potential difference) to the current input gives the resistance R of the ground, i.e.,

$$R = V/I \quad \ldots\ldots (2.1)$$

If V is expressed in volt (V) and I in ampere (A), then R is in Ohms (Ω). Equation (2.1) is a simple expression of Ohm's law, which is the basis of all the electrical resistivity method.

2.2 THEORY OF THE DIRECT CURRENT RESISTIVITY METHOD OF THE FOUR–ELECTRODE ARRAGEMENT

According to Keller and Frischknecht (1966), the simplest approach to the theoretical study of earth resistivity measurements is to consider first the case of a completely homogeneous isotropic earth. An equation, which gives the potential about a single point current source, can be developed from Ohm's law and the divergence condition. Ohm's law states that the electric field strength, E, at a point in a material is proportional to the current density, j, at that point, i.e.,

$$\vec{E} = \rho \vec{j} \quad \cdots\cdots (2.2)$$

where ρ is the resistivity of the medium. E is expressed in Volt per metre (Vm^{-1}), j in Ampere per square metre (Am^{-2}) and ρ in Ohm - metre (Ω - m). E is the gradient of a scalar potential function, V in volts, thus

$$\vec{E} = -\nabla V \quad \cdots\cdots\cdots\cdots (2.3)$$

Substituting for E from equation (2.3) into equation (2.2) gives

$$\vec{J} = -\nabla (V/\rho) \quad \cdots\cdots\cdots\cdots (2.4)$$

The divergence condition to be applied here according to Keller and Frischknecht (1966), states that all the current flowing into a chunk of material must leave the other side provided there is no current source or sink within the chunk. The divergence of the current density vector must therefore be zero except at the current source, i.e.,

$$\nabla \vec{j} = O \cdots\cdots\cdots\cdots (2.5)$$

Applying the divergence condition (i.e. equation (2.5)) to equation (2.4) gives

$$\nabla \vec{j} = -\nabla(\nabla V / \rho) = O$$

$$or \quad \nabla \frac{1}{\rho} . \nabla V + \frac{1}{\rho} \nabla^2 V = O \cdots\cdots\cdots\cdots (2.6)$$

Since ρ is a constant, the first term in equation (2.6) vanishes, hence

$$\nabla^2 V = O \cdots\cdots\cdots\cdots (2.7)$$

Equation (2.7) is Laplace's Equation.

In polar coordinates, Laplace's equation is

$$\frac{\partial}{\partial r}\left(r^2 \frac{\partial V}{\partial r}\right) + \frac{1}{r^2 \sin\theta} \frac{\partial}{\partial \theta}\left(\sin\theta \frac{\partial V}{\partial \theta}\right) + \frac{1}{r^2 \sin^2\theta}\left(\frac{\partial^2 V}{\partial \psi^2}\right) = 0 \quad \cdots\cdots\cdots (2.8)$$

For a single current source, it is assumed that there is complete symmetry of current flow with respect to the 0 and φ directions. The derivative with respect to these directions are zero or may be eliminated, hence equation (2.8) becomes

$$\frac{\partial}{\partial r}\left(r^2 \frac{\partial V}{\partial r}\right) = O \cdots\cdots\cdots\cdots (2.9)$$

Integrating equation (2.9) twice gives

$$r^2 \frac{\partial V}{\partial r} = C \cdots\cdots\cdots\cdots (2.10)$$

and

$$V = -\frac{C}{r} + D \cdots\cdots\cdots\cdots\cdots\cdots (2.11)$$

where C and D are constants and r is the distance of the single current electrode to where measurement is taken.

If the level of potential considered at a great distance from the current source is Zero, then, the constant of integration, D, must also be zero. Equation (2.11) reduces to

$$V = -\frac{C}{r} \cdots\cdots\cdots\cdots\cdots\cdots (2.12)$$

The current flows radially outwards in all directions from the point current source or electrode. The total current crossing the surface of the sphere drawn around the current source can be expressed as the integral of the current density over the surface, i.e.,

$$I = \int_s \vec{j}\, ds = \int_s \frac{\vec{E}}{\rho}\, ds = \int_s \frac{C}{\rho r^2}\, ds \cdots\cdots\cdots\cdots (2.13)$$

For a single current electrode at the surface of the earth, all the current flows through a hemispherical surface of area $2\pi r^2$, hence equation (2.13) becomes

$$I = \int_s \frac{C}{\rho r^2} ds = -\frac{2\pi C}{\rho}$$

so that

$$C = -\frac{I\rho}{2\pi} \cdots\cdots\cdots\cdots\cdots\cdots (2.14)$$

Substituting for C from equation (2.14) into equation (2.12) for the potential function gives

$$V = \frac{I\rho}{2\pi r} \cdots\cdots\cdots\cdots\cdots\cdots (2.15)$$

Potential functions are scalars, and so if there are many current sources at the surface of the earth, the total potential at an observation point is the algebraic sum of the potential contributions from each source considered independently. Hence, the potential at an observation point O due to n current sources distributed in a uniform medium is

$$V_0 = \frac{\rho}{2\pi}\left(\frac{I_1}{r_1} + \frac{I_2}{r_2} + \cdots\cdots\cdots\cdots + \frac{I_n}{r_n}\right) \cdots\cdots (2.16)$$

where I_n is the current from the n^{th} source and r_n is its distance from the point of observation O. Fig.2.1 shows the arrangement of the four-electrode spread normally used in resistivity measurements.

Applying equation (2.16), the potential at M due to both current electrodes A and B is

$$V_M = \frac{I\rho}{2\pi}\left(\frac{1}{AM} - \frac{1}{BM}\right) \cdots\cdots\cdots\cdots (2.17)$$

The negative sign arise because the current in the two current electrodes, A and B are equal and opposite in direction. While one current electrode is a source, the other is a sink.

Similarly, the potential at N due to both current electrodes, A and B is

$$V_N = \frac{I\rho}{2\pi}\left(\frac{1}{AN} - \frac{1}{BN}\right) \cdots\cdots\cdots\cdots (2.18)$$

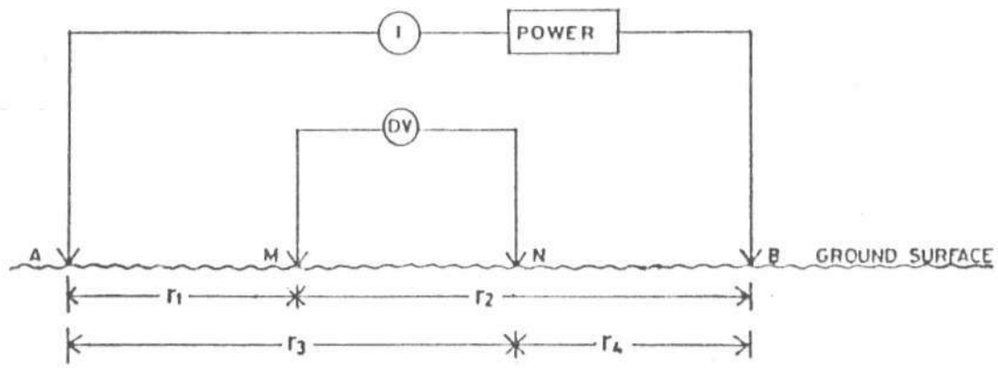


FIG. 2.1. FOUR-ELECTRODE ARRANGEMENT IN RESISTIVITY MEASUREMENT. A AND B ARE CURRENT ELECTRODES WHILE M AND N ARE POTENTIAL ELECTRODES (AFTER KELLER AND FRISCHKNECHT, 1966).

The potential difference, ΔV, between M and N is

$$\Delta V = V_M - V_N$$

$$= \frac{I\rho}{2\pi}\left\{\left(\frac{1}{AM} - \frac{1}{BM}\right) - \left(\frac{1}{AN} - \frac{1}{BN}\right)\right\} \quad \cdots\cdots\cdots (2.19)$$

The resistivity of the ground is therefore

$$\rho = \frac{\Delta V}{I}\left\{\frac{2\pi}{\left(\frac{1}{AM} - \frac{1}{BM}\right) - \left(\frac{1}{AN} - \frac{1}{BN}\right)}\right\} \quad \cdots\cdots\cdots\cdots\cdots\cdots (2.20)$$

Equation (2.20) can further be written in terms of a factor that represent the effect of electrode separation distance, k, known as the geometric factor, i.e.,

$$\rho = \frac{\Delta V}{I} \cdot k \quad \cdots\cdots\cdots\cdots (2.21)$$

where

$$k = \frac{2\pi}{\left(\frac{1}{AM} - \frac{1}{BM}\right) - \left(\frac{1}{AN} - \frac{1}{BN}\right)} \quad \cdots\cdots\cdots\cdots\cdots\cdots\cdots (2.22)$$

In the determination of earth resistivity, two quantities are measured and these are; the current, I, passed into the ground between two current electrodes, the potential difference, ΔV, between the electrodes. These measured quantities are substituted into equation (2.20) to determine the earth resistivity. This is the practical importance of equation (2.20).

2.2.1 APPARENT RESISTIVITY (ρ_a)

The resistivity obtained using equation (2.20) is always constant over homogeneous isotropic medium, no matter the separation of the electrodes. On the other hand, if the medium is inhomogeneous, the resistivity will vary as the electrode array is moved about. This measured resistivity is called "apparent resistivity" (ρa), which is a response function defined in most resistivity techniques. As keller and Frischknecht (1966) observed, the apparent resistivity may bear no relation to any actual value of resistivity in a heterogeneous earth. The apparent resistivity may be larger or smaller than the real resistivity, or in rare cases, identical with one of the true resistivity value in a heterogeneous subsurface (Telford et al, 1976). The value of apparent resistivity obtained for small electrode spacing is called the surface resistivity. The apparent resistivity, ρ_a, can therefore be written as

$$\rho_a = \frac{\Delta V}{I} .k \cdots\cdots\cdots\cdots (2.23)$$

2.3 THE DIFFERENT ELECTRODE ARRANGEMENTS.

There are quite a number of different electrode arrangements used in electrical D.C. resistivity survey. These include the two-electrode arrangement, the three-electrode arrangement, the common four- electrode arrangement and the six-electrode arrangement (Jain and Roy, 1973). Some of these electrode arrangements are discussed below.

2.3.1 THE FOUR ELECTRODE ARRANGEMENT

The four-electrode arrangement is actually the most widely used electrode arrangement for electrical resistivity surveys. Other common forms of arrays of the four- electrode

arrangements are the Wenner Configuration, the Schlumberger Configuration, the Lee-partition configuration, the Polar dipole-dipole (axial or end on) system and the Equatorial dipole-dipole (broadside) system. These are shown in Figs. 2.2(a), (b), (c), and (d).

In the Wenner Configuration (used for measuring potential difference) the four electrodes are arranged along a straight line with equal spacing, L, between them, Fig.2.2(a). Using equation (2.22), the geometric factor for this configuration is

$$k = 2\pi L \quad \cdots\cdots\cdots\cdots (2.24)$$

and hence the apparent resistivity is given by

$$\rho_a = 2\pi L \frac{\Delta V}{I} \quad \cdots\cdots\cdots\cdots (2.25)$$

The Schlumberger Configuration measures approximately the potential gradient. In this configuration, the two potential electrodes are placed closely together and midway between the two current electrodes as shown in Fig.2.2 (b). The electrode spacing, L, is taken as half the distance between the current electrodes (i.e.L=AB/2). Applying equation (2.22), the geometric factor for this configuration is

$$k = \pi\left(\frac{L^2}{l} - \frac{l}{4}\right) \quad \cdots\cdots\cdots\cdots (2.26)$$

The apparent resistivity, ρ_a, is therefore

$$\rho_a = \pi\left(\frac{L^2}{l} - \frac{l}{4}\right)\frac{\Delta V}{I} \quad \cdots\cdots\cdots\cdots (2.27)$$

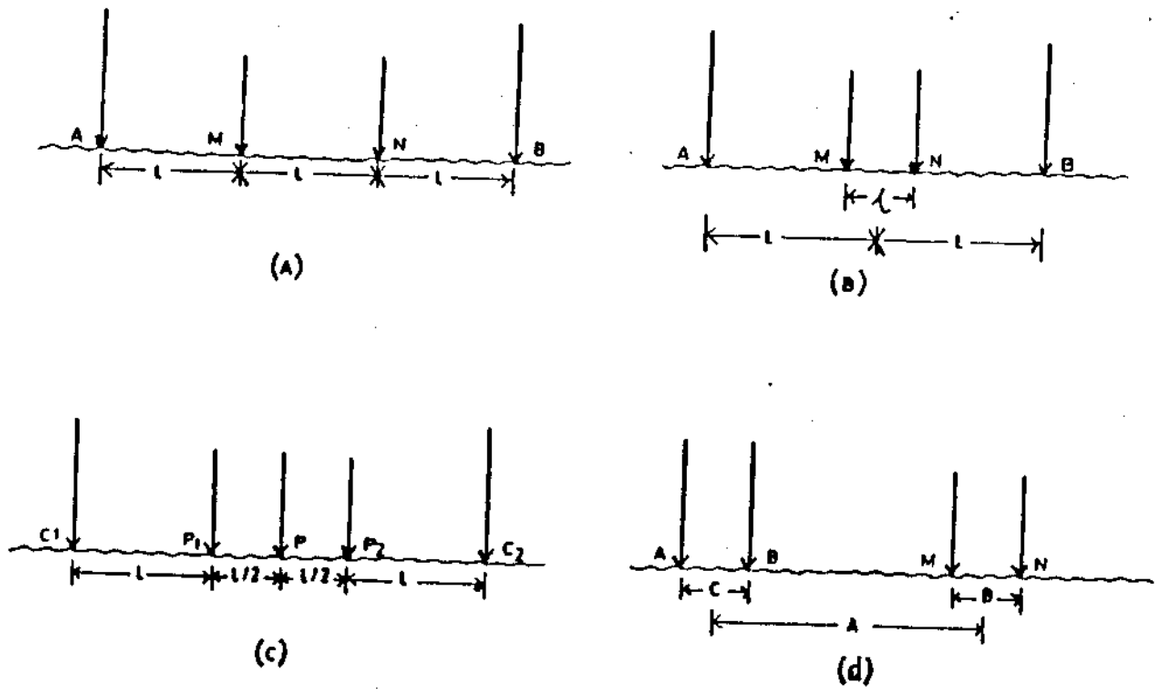


Fig. 2.2 Some Common Four – Electrode Configurations (A) Wenner Array (B) Schlumberger Array (C) Lee Partitioning Array (D) Dipole-Dipole (Polar) Array. (After Keller and Frischknecht, 1966).

The Lee-partition spread shown in Fig. 2.2 (c) is a modification of the Wenner Configuration. It uses a third potential electrode P that is located at the centre of the Wenner array. Two measurements of potential are made; one between M and P and the other between N and P. The geometric factor for each half of the array is

$$k = 4\pi l \quad \cdots\cdots\cdots\cdots (2.28)$$

and hence the apparent resistivity for each half of the array are;

$$\left.\begin{aligned} \rho_{a1} &= 4\pi l \frac{\Delta V_1}{I} \\ \rho_{a2} &= 4\pi l \frac{\Delta V}{I} \end{aligned}\right\} \quad \cdots\cdots\cdots (2.29)$$

where ΔV_1 = potential difference between M and P

and ΔV_2 = potential difference between N and P

The advantage of this system is that horizontal changes in resistivity can be recognized by comparing the resistivity of each half of the array.

The other arrays use dipoles (i.e. closely spaced electrode pairs) in which the curvature of the potential field is measured. These methods are not commonly used as the Wenner and Schlumberger arrays. In the dipole-dipole methods, the two current electrodes are closely spaced together as a pair and the two potential or measuring electrodes are also closely spaced together as another pair. In the equatorial system, shown in Fig. 2.2 (d) the current electrode pair and the potential electrode pair are arranged along a straight line such that the distance between the two pairs is very much

greater than the distance between the closely spaced electrodes. If the separation between both pairs of electrodes is the same, the geometric factor is given by

$$k = \pi\left(\frac{a^3}{b^2} - a\right) \cdots\cdots\cdots\cdots\cdots\cdots (2.30)$$

The apparent resistivity is given by

$$\rho_a = \pi\left(\frac{a^3}{b^2} - a\right)\frac{\Delta V}{I} \cdots\cdots\cdots\cdots\cdots\cdots (2.31)$$

2.3.2 THE THREE-ELECTRODE (TRIPOTENTIAL) ARRANGEMENT.

If one of the electrodes in a four-electrode arrangement is located at a point sufficiently far to approximate to infinity, the arrangement is referred to as a three-electrode configuration. This type of array can either consist of two current electrodes and one potential electrode or two potential electrodes and one current electrode. The Assymetrical Wenner array, the Modified Unipole array, the Pole-Dipole array and the Lögn array are common examples of the three electrode array (Katsube and Collett, 1973).

The principle of the three-electrode array is the same as that of the four-electrode array except that in the case of the three - electrode array, only the relative positions of the three electrodes are considered. Fig. 2.3(a) and 2.3(b) show the arrangement of the Assymetrical Wenner array and the Logn array. The apparent resistivities for the Assymetrical and Logn arrays are respectively given as

$$\rho_{a\ wenener} = 4\pi a\frac{\Delta V}{I} \cdots\cdots\cdots\cdots\cdots\cdots (2.32)$$

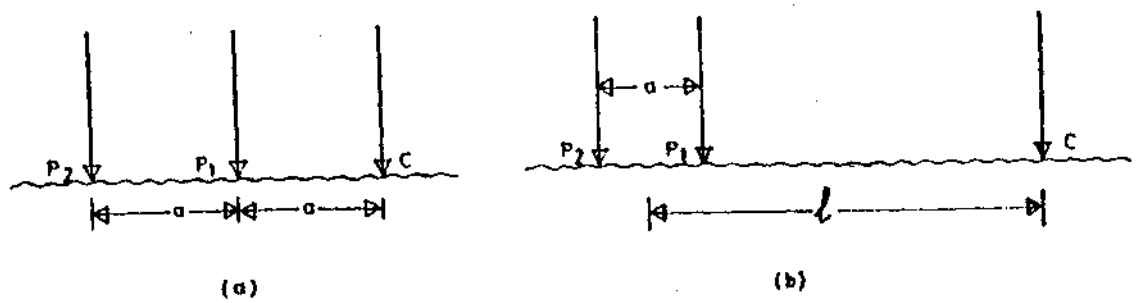


Fig. 2.3 Some Three – Electrode Arrangements

(a) The Assymetrical Wenner Array

(b) The Lögn Array (After Van Nostrand and Cook, 1966).

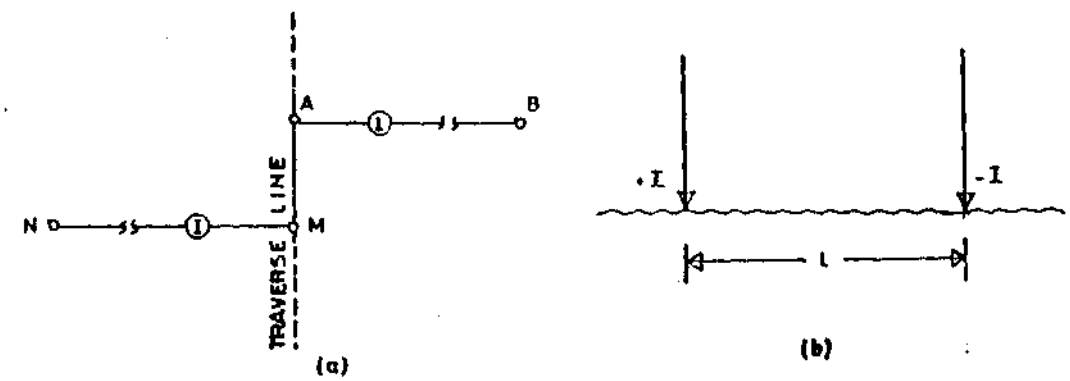


Fig. 2.4 Field Layout of Some Two-Electrode Configurations.

(a) The Sink - I and the other Potential Electrode N Placed Normal to Traverse Line at Distances that Approximate to Infinity.

(b) The Ajayi – Makinde Two – Electrode System Used in this Work. (Each Electrode Serves As Both Current and Potential Electrodes).

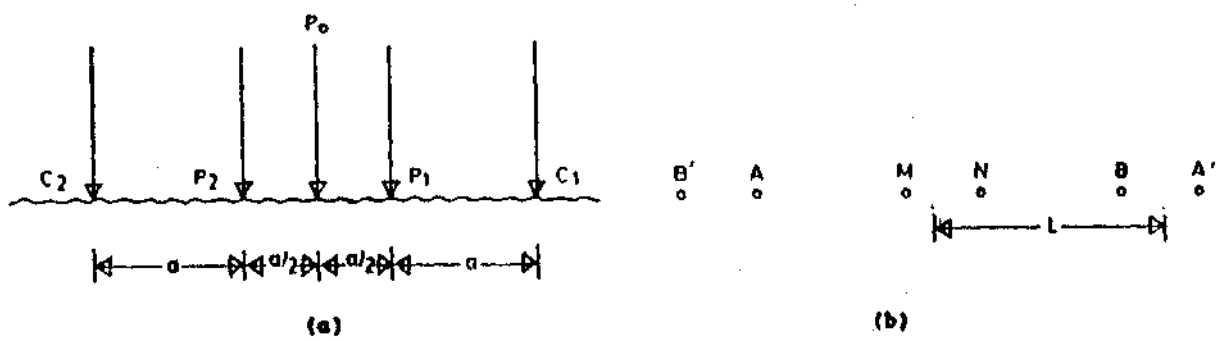


Fig. 2.5 Some other Electrode Arrangements

(a) The Lee Arrangement (After Van Nostrand and Cook, 1966)

(b) The Differential Arrangement (After Zhody, 1969).

and

$$\rho_{a\log n} = \frac{2\pi l^2}{a}\frac{\Delta V}{I} \quad \text{.....(2.33)}$$

2.3.3 THE TWO-ELECTRODE ARRANGEMENT.

The two-electrode configuration simply consists of a combination of two current electrodes or one current electrode and one potential electrode. Apparao and Roy (1973) and Kumar (1974) worked on a combination which consists of one current electrode and one potential electrode with the other current electrode and potential electrode placed at sufficiently large distance that can approximate to infinity from the measuring environment.

Gupta and Bhattacharya (1963) and Brizzolari and Bernabini (1979) reported on a combination that consists of two current electrodes in which the two current electrodes feed current into the ground with none acting as a return current electrode.

The electrode combination used by Makinde (1996) consists of only two electrodes, both of which serve as current electrodes and potential electrodes. One of the current electrodes feed current into the ground while the other electrode acts as a current return electrode. The two electrodes also serve as potential electrodes. Fig. 2.4 shows some two-electrode arrangements.

2.3.4 THE FIVE-ELECTTRODE AND SIX-ELECTRODE ARRANGEMENTS.

According to Makinde (1996), this class consists of the newly developed arrays of Zhody (1969) and the relatively obscure ones such as the five - electrode Lee-partition, tri -potential, resistolog array. Fig.2.5 shows a sketch of some of these electrode configurations.

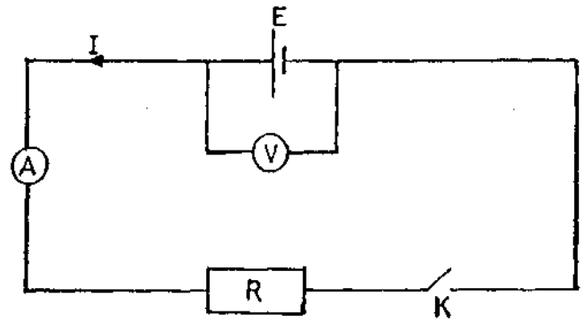
2.4 PRINCIPLE OF THE TWO-ELECTRODE METHOD USED.

The two–electrode method used in this work is that used by Makinde in 1996. The configuration is now referred to as the Ajayi – Makinde two – electrode array (Ajayi and Makinde, 2000).

The circuit diagrams shown in Figs. 2.6 (a) and (b) are used to discuss the principles underlying the two–electrode array.

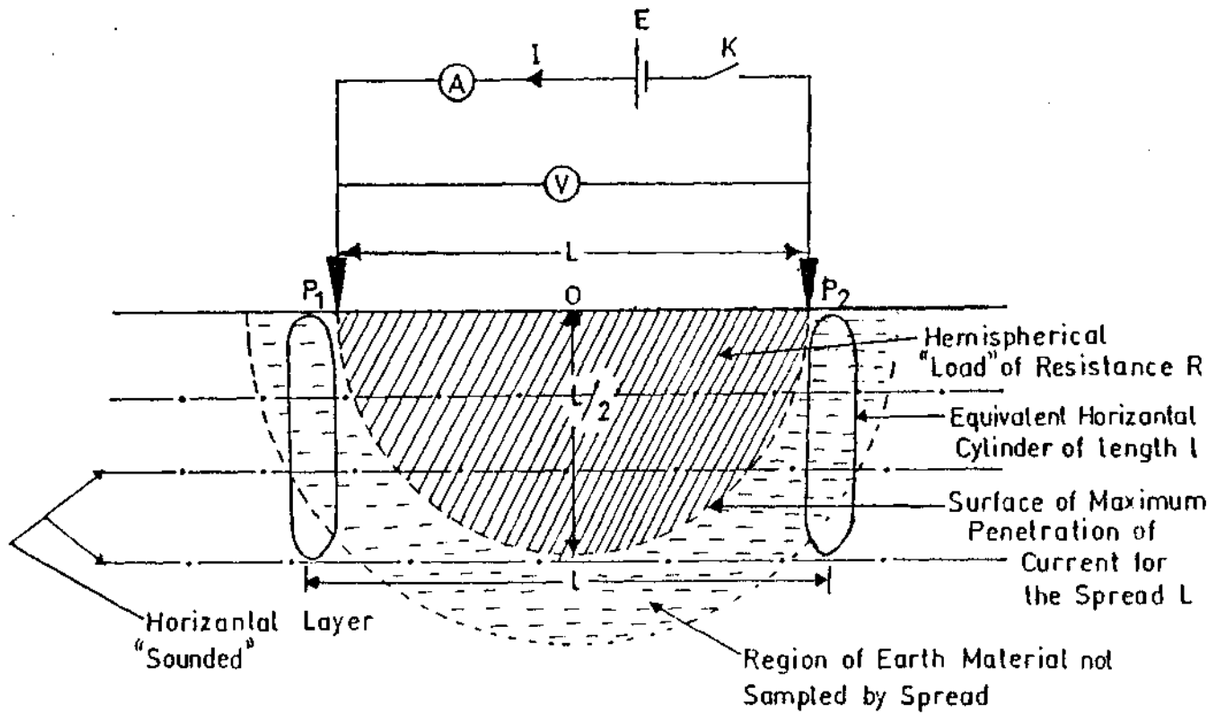
The Ajayi – Makinde two–electrode array, just like other geoelectric arrays is based on Ohm's law which states that the potential difference between the ends of a metallic conductor is directly proportional to the current passing through the conductor provided temperature and other physical conditions are kept constant.

In the Ajayi – Makinde two–electrode array, Ohm's law is applied to the simple electrical circuit in which R, the resistance or load in the circuit represents the portion of the earth " sampled" or "sounded" by the current I flowing in and out of the ground (earth material) through the two electrodes P_1 and P_2 across which a potential difference, or voltage V is applied as in Fig. 2.6(a) (Ajayi and Makinde, 2000). As the separation P_1 P_2 or L, (i.e the electrode spacing), increases, the current I penetrates the earth deeper and deeper, thereby, sampling the various layers underlying the point O "sounded", Fig. 2.6 (b) (Ajayi and Makinde, 2000).



(a) Simple Circuit to Verify Ohm's Law

K = Key; E = Applied e.m.f.; I = Current;
R = Cylindrical Load of Resistance R (Ω);
A = Ammeter for Indicating Current I;
V = Volmeter for Indicating P.D. Across R.



(b) The 2-Electrode "Sounding" or as an Analog of Fig.2.6(a).
O = Point being "Sounded" or "Sampled"; P_1P_2 = Current Electrodes;
$L = P_1P_2$ = Electrode Separation; E = Applied e.m.f.;
I = Current through Ammeter A; V = Voltage Across P_1P_2;
l = Length of Equivalent Cylinder of Diameter L/2

Fig. 2.6 Laboratory Determination of Ohm's Law and its 2-Electrode "Sounding" Analog (After Ajayi and Makinde, 2000).

2.5 ASSUMPTIONS MADE IN THE AJAYI-MAKINDE TWO-ELECTRODE METHOD USED.

In deriving the theory of the proposed method (array) for the depth-sounding mode, Ajayi and Makinde (2000) made the following assumptions:

i. As the method is based on Ohm's law, ohmic conduction is assumed for the sampled earth.

ii. The earth materials beneath the point being "sounded" are horizontally layered and each layer is assumed homogeneous.

iii. The portion of the earth being sounded by electrodes P_1 and P_2 is a hemisphere with diameter P_1 P_2 and the volume of this hemisphere can be approximated by a horizontal cylinder of the same volume but whose diameter is L/2 as in Fig.2.6.

iv. While one of the electrodes is a current source, the other is a current sink. That is, whatever current is fed into the ground through one of the two electrodes, leave the ground through the other electrode.

v. For each "sounding" or reading, the pattern of the current flow is always assumed to be hemispherical, irrespective of the number of layers encountered. In reality, this will not be true whenever a new layer is encountered.

2.6 THEORY OF THE AJAYI-MAKINDE TWO-ELECTRODE ARRAY

Based on the earlier stated assumptions, Makinde (1996) and Ajayi and Makinde (2000) derived a suitable formula for calculating the "bulk" or "apparent" resistivity of the earth material trapped within each current hemispherical "bowl" of earth material sampled as the electrode separation L is varied. Ajayi and Makinde (2000) arrived at an equation relating the volume of the assumed hemisphere formed by the sampled earth material to that of the approximate equivalent cylinder as follows:

Applying the simple expression of Ohm's law (i.e. equation (2.1)) earlier given in section 2.1 to Fig. 2.6(a) and by extension to Fig. 2. 6 (b), for a cylindrical load of uniform cross– section, the resistivity of the load is

$$\rho = \frac{RA}{l} \quad \cdots\cdots\cdots\cdots\cdots\cdots (2.34)$$

where R is the resistance of the load, A its cross-sectional area and l its length. Equation (2.1) is V = IR. Substituting for R = V/I into equation (2.34) gives

$$\rho = \frac{A}{l} \cdot \frac{V}{I} \quad \cdots\cdots\cdots\cdots\cdots\cdots (2.35)$$

The volume of a sphere of radius r is $(4/3)\pi r^3$, hence the volume, v, of the hemisphere shown in Fig. 2.6(b) is

$$v = \frac{2}{3}\pi r^3$$

But $r = \frac{L}{2}$

Therefore

$$v = \frac{2\pi(L/2)^3}{3} \quad \cdots\cdots\cdots\cdots\cdots\cdots (2.36)$$

$$v = \frac{\pi L^3}{12} \quad \cdots\cdots\cdots\cdots\cdots\cdots (2.37)$$

From the third assumption, the volume, v, in equation (2.37) is also the volume of the equivalent cylinder of the load, i.e.,

$$\pi\left(\frac{L}{4}\right)^2 l = \frac{\pi L^3}{12}$$

where l is the length of the cylinder.

This implies that $$l = \frac{4L}{3} \quad \cdots\cdots(2.38)$$

The cross-sectional area, A, of the cylinder is

$$A = \pi x^2$$

$$= \pi\left(\frac{L}{4}\right)^2 \quad \text{where } x = \frac{L}{4} = \text{radius of cylinder}$$

Therefore $$A = \frac{\pi L^2}{16} \quad \cdots\cdots(2.39)$$

Substituting for equations (2.39) and (2.38) into equation (2.36) gives

$$\rho = \frac{\pi L^2/16}{4L/3} \cdot \frac{V}{I}$$

$$\rho = \frac{3\pi}{32} \cdot \frac{L}{2} \cdot \frac{V}{I} \quad \cdots\cdots(2.40)$$

$$\rho = \frac{3\pi}{64} \cdot L \cdot \left(\frac{V}{I}\right) \quad \cdots\cdots(2.41)$$

or $$\rho = k \cdot \frac{V}{I} \quad \cdots\cdots (2.42)$$

where $$k = \frac{3\pi L}{64} \quad \cdots\cdots(2.43)$$

"k" is the geometrical factor of the array. Since the various layers being sampled as the electrode spacing increases are not of the same material, ρ in equation (2.42) is actually the "bulk" or apparent resistivity ρ_a of the layers sounded. Hence equation (2.42) is better written as

$$\rho_b = k \cdot \frac{V}{I} \quad \text{.....(2.44)}$$

From equation (2.40), a plot of ρ_b against L/2 is expected to give a set of straight lines whose slope is given by

$$S_n = \pm \frac{3\pi}{32}\left(\frac{V}{I}\right) \quad \text{.....(2.45)}$$

where n is an integer denoting the nth straight line.

According to Keller and Frischneht (1966), the resistivity of the earth may be considered to vary in the vertical direction according to the law

$$\rho_z = \rho_1 e^{\pm \alpha z} \quad \text{.....(2.46)}$$

where ρ_z is the resistivity at depth z, ρ_1 is the resistivity at the surface or top and α is a parameter defining the rate of increase or decrease with depth.

Taking the logarithm of both sides of equation (2.46) gives

$$\ln \rho_z = \ln \rho_1 \pm \alpha z \quad \text{.....(2.47)}$$

It therefore follows that a plot of $\ln \rho_z$ against z is expected to give a straight line whose slope is α and intercept $\ln \rho_1$. The values of ρ_b as determined from equation (2.44) and their corresponding values of L/2 plotted on a semi-log graph sheet is expected according to equation (2.46) to give a series of straight lines joined end-to-end. A typical example of such a plot is shown in Fig. 4.1

Equation (2.44) is consistent with the expression for the resistivity of the earth material sampled in the other common electrode arrays such as the Wenner and Schlumberger arrays in which the resistivity is always expressed in the form of equation (2.21) i.e. $\rho = (\Delta V/I)\, k$ where k is the geometric factor of the configuration. Equation (2.40) is the expression for calculating the bulk resistivity of the earth material sampled for a particular value of the electrode spacing L.

CHAPTER III

DATA COLLECTION AND REDUCTION

3.1 TYPES OF DATA COLLECTED

This project involved a fieldwork, which was undertaken in the month of March 1997. Two types of resistivity data were collected during the exercise. The first type was collected using the two-electrode method while the second type was collected using the Schlumberger configuration. The latter sets of data were collected at the points in which the first sets (of data) were collected. Hence, two different types of equipment were employed for the fieldwork.

3.2 DATA COLLECTION

A total of thirty-seven (37) points were "sounded" in this study. The points "sounded" or "stations established" were carefully selected to ensure adequate and uniform coverage of the project area. Prior to conducting the "soundings", the stations concerned were, in a reconnaissance survey, initially surveyed for accessibility. Points originally chosen that could not be easily accessed were relocated. Fig.3.1 shows the distribution of the 37 sounding points within the study area.

Vertical electrical soundings (VES) were carried out at each of the 37 stations established using first, the two-electrode method and then followed by the Schlumberger configuration. Thus seventy-four (74) VES were carried out in this work.

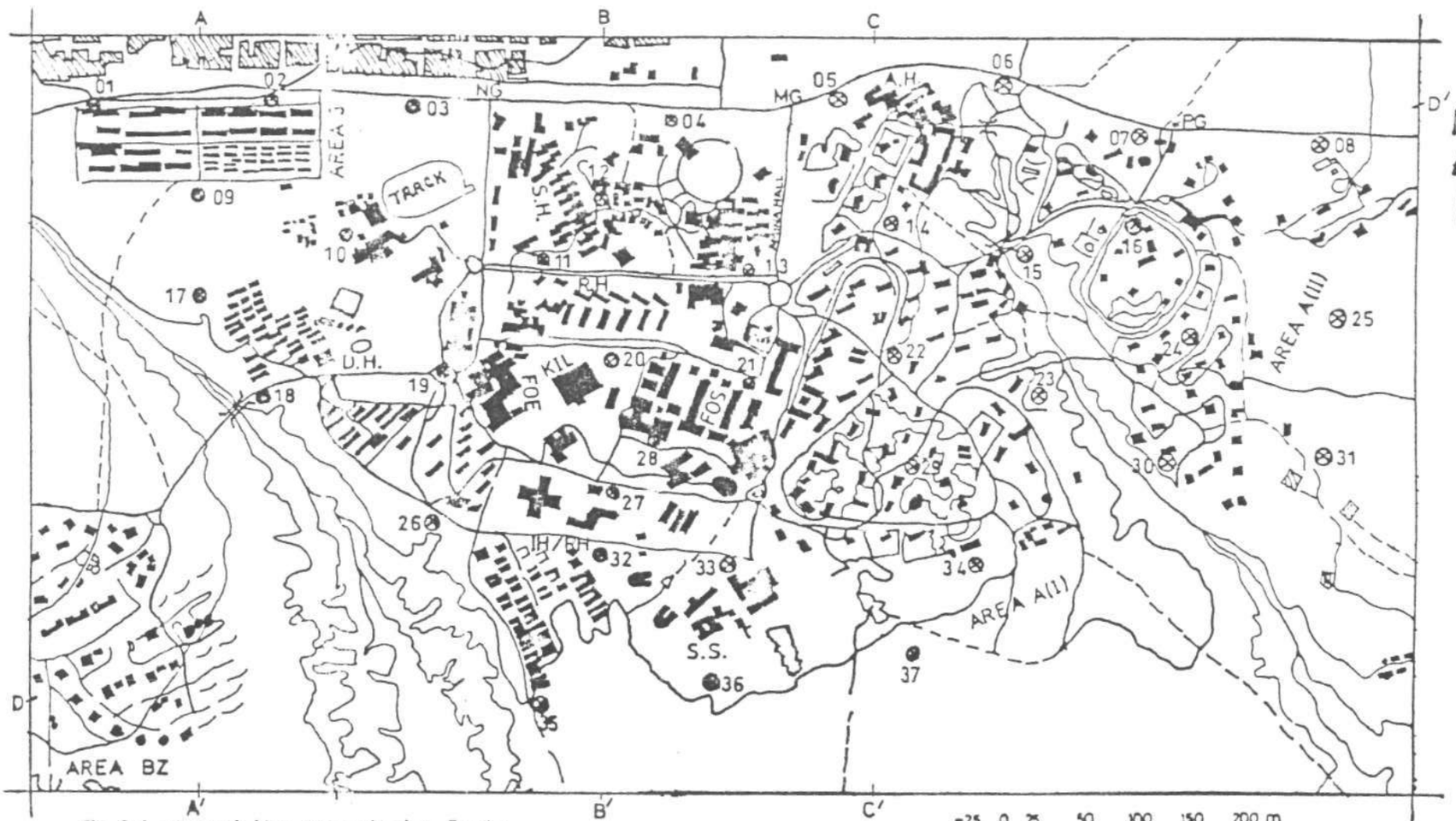


Fig.3.1 Map of the Area Under Study Showing the Sounding Points (Courtesy of U.R.P. DEPT., A.B.U. ZARIA).

3.2.1 The Two-Electrode Array

a. Instrumentation

As the two-electrode used in this work is a new array, no equipment had, as at the time of the fieldwork, been fabricated for it. Hence, the arrangement of the field equipment used for the fieldwork in this project is that shown in Fig.3.2. The arrangement basically consists of an electric generator as the power source, a voltmeter, an ammeter, two copper electrodes, two reels of wire and connecting wires. The electric generator is an ET 500 YAMAHA generating with an output voltage of 250 Volts, 50 Hz, capable of delivering a maximum current of 300 mA. A high-tension laboratory power pack was used to convert the alternating current (AC) to direct current (DC.), which was then passed into the ground through the copper electrodes. A voltmeter, with a range of 0-300 Volts was used to measure the potential difference across the electrodes while an ammeter with a range of 0 – 300 mA, was used to measure the current passed into the ground.

b. Field Procedure

The field procedure involved the expansion of L/2 (half the current electrode spacing) symmetrically about the centre point or point being sounded. Half the current electrode spacing L/2 was expanded in steps from 0.5 m to a maximum of 100 m. For each reading, the current I passed into the ground, the potential difference V across the electrodes and the electrode spacing L were measured. The ratio of the potential difference., V, to the current, I, is a measure of the electrical resistance of the ground between the electrodes at the corresponding given spacing.

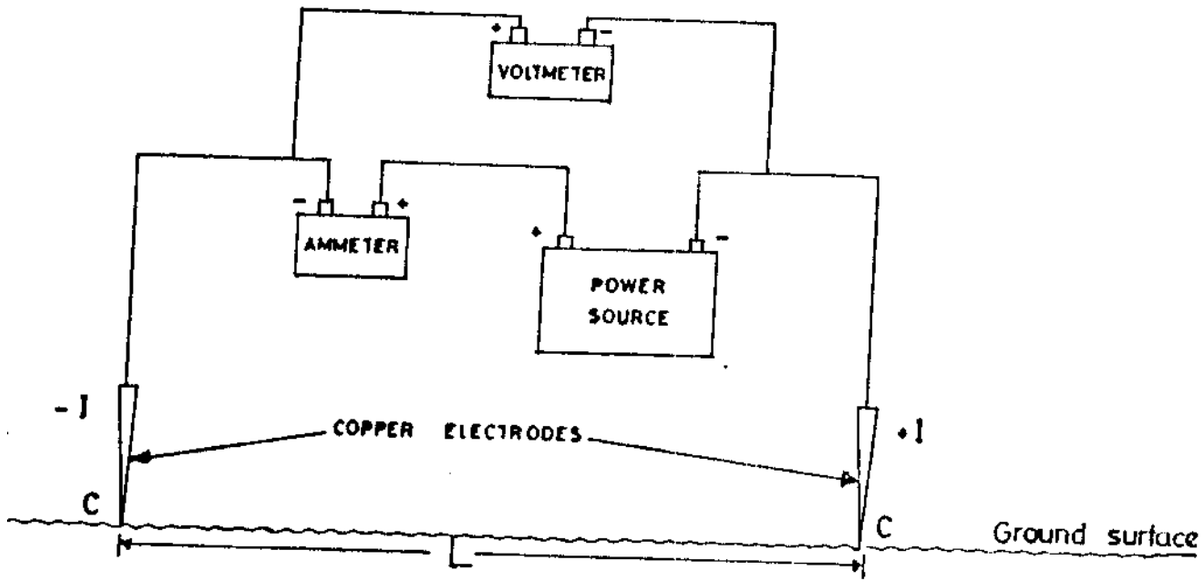


Fig.3.2 Arrangement of the field equipment used for the two – electrode method. L is the electrode separation.

3.2.2 The Schlumberger Array

a. Instrumentation

The field equipment used for the Schlumberger configuration consists of an ABEM Terrameter SAS 300, copper electrodes, four reels of wire and connecting wires. The layout of the equipment on the field for the Schlumberger configuration is shown in Fig. 2.2 (b), (section 2.3.1).

The Terrameter SAS 300 is a basic unit, which can be, used for self-potential (SP) and resistivity surveys. SAS stands for "Signal Averaging System", which is a method whereby consecutive readings are taken and the results, are automatically averaged continuously. The continuously updated running average is presented automatically in digital form as the resistivity of the ground. The Terrameter SAS 300 has three main units, all housed in a single case. These units are; the transmitter, the receiver and the microprocessor. The electrically isolated transmitter sends out well-defined and regulated current signal. The receiver discriminates noise and measures voltages correlated with the transmitted current signal. The microprocessor monitors and controls operations and calculates results to ensure optimal accuracy and sensitivity and to make certain that the instrument is used correctly.

b. Field Procedure

In this case, the field procedure consisted of expanding AB/2 symmetrically about the centre of the spread while keeping the potential electrodes relatively fixed. For each passage of current into the ground, through the current electrodes, a potential difference is set up between the potential electrodes (MN). As the expansion of the current electrodes get larger, the potential difference set up between MN will decrease and eventually exceed the capability of the measuring instrument. As stated by Kunetz

(1966), this is due to the fact that the field at the centre of the configuration varies inversely as the square of the length of the configuration (i.e. AB). Mooney (1980) suggested that when this happens, a new value for MN, typically about 3 times larger than the preceding value, should be established. The procedure is then continued by duplicating the last L (or AB/2) value with the new MN value. The magnitude of AB/2 was chosen so as to have about six points per decade in this work. This therefore implies that each value of L (i.e. AB/2) was more or less equal to the previous value multiplied by $10^{1/6}$ though rounded off for more convenient distance measurements. The maximum electrode spacing reached was 100 m as the depth of interest in the study area was estimated and reported by previous workers to be less than 40 m (Hassan, 1987).

3.2 DATA REDUCTION

3.2.1 The Two-Electrode Array

The data collected using the two – electrode method consists of the measured current, I, passed into the ground, the voltage,V, across the power source and the electrode spacing L. The resistance of the ground between the electrodes was calculated using equation (2.1) while the bulk resistivity ρ_b was calculated using equation (2.40).

The computed "bulk resistivity" values were plotted against their corresponding L/2 values on a semi-log graph paper. These plots were made for each VES station and used for interpretation. Table 1 is a typical reduced and plotted data obtained using the two-electrode array for VES station 25.

3.3.2 The Schlumberger array

The data collected using the Schlumberger configuration consists of the resistance values read from the Terrameter, the AB/2 and their corresponding MN values. Equation (2.27) was used to reduce the collected data. The computed "apparent resistivity" values formed the resistivity data for that particular station. The computed apparent resistivity values with their corresponding electrode spacing were used for interpretation. Table 2 is a typical reduced and plotted data obtained using the Schlumberger array for VES station 25.

TABLE 1: TYPICAL REDUCED AND PLOTTED DATA OBTAINED USING THE TWO-ELECTRODE ARRAY FOR VES STATION 25

L(m)	L/2(m)	V(Volts)	I(mA)	$\rho_b(\Omega\text{-m})$
1.0	0.50	188	42	659.2
2.0	1.00	174	32	1601.5
3.0	1.50	147	54	1202.6
4.0	2.00	173	34	2997.2
5.0	2.50	135	45	2208.9
6.0	3.00	120	48	2208.9
7.5	3.75	113	46	2713.2
8.0	4.00	106	39	3202.0
9.0	4.50	91	43	2804.8
10.0	5.00	120	55	3212.9
15.0	7.50	101	52	4290.4
20.0	10.50	122	49	7333.1
25.0	12.50	116	51	8373.7
30.0	15.00	105	56	8283.5
35.0	17.50	103	53	10016.6
40.0	20.00	72	44	9638.9
45.0	22.50	75	45	11044.7
50.0	25.00	45	35	9466.9
75.0	37.50	52	38	15113.8
100.0	50.00	39	40	14358.1
150.0	75.00	48	40	26507.2
200.0	100.00	183	45	119773.2

TABLE 2: TYPICAL REDUCED AND PLOTTED DATA OBTAINED USING THE SCHLUMBERGER ARRAY FOR VES STATION 25

MN(m)	AB/2(m)	R(Ω)	ρ_a(Ω-m)
1.0	1.00	193.024	454.8
	1.50	68.4525	430.1
	2.50	22.505	424.2
	3.75	8.5013	368.9
	5.00	4.1271	320.9
	7.50	1.189	209.2
	10.00	0.6111	191.5
3.0	7.50	3.9470	223.2
	10.00	1.627	166.5
	15.00	0.5179	120.8
	25.00	0.1852	120.8
	37.50	0.1131	166.5
	50.00	0.0721	188.8
10.0	37.50	0.389	1.68.9
	50.00	0.283	220.1
	75.00	0.1677	295.1
	100.00	0.1194	374.1

CHAPTER IV

INTERPRETATION AND RESULTS

4.1 DATA INTERPRETATION

The end products of any resistivity survey include a set of models and contour maps. The interpretation of the resistivity data involves expressing the information obtained from the curves, models and contour maps into geological terms which requires;

(i) a sound knowledge of the geology of the area under study and

(ii) a good practical experience of the method used.

Both of these facts were taken into consideration in this work to ensure the interpretations made are reliable.

The interpretation of resistivity data may be carried out in terms of an exponential change in resistivity with depth (Keller and Frischnecht, 1966). According to Keller and Frischnecht (1966), the resistivity of the earth may be considered to vary in the vertical direction according to equation (2.46) in section 2.6 of Chapter II. The resistivity of rock layers vary considerably not only from formation to formation but also within any one particular layer and, in particular, the variations can be very large for near surface unconsolidated sediments (Vingoe, 1972). No specific correlation, therefore, exists between lithology and resistivity. According to Vingoe (1972), it is possible to generalise and say that the order of increasing resistivity is ore deposits, clay, sand and gravel, limestone and then crystalline rocks which are still higher. Table 3 gives the resistivity values of rock types in the Nigerian basement complex. The resistivity values deduced by Shemang (1990) for different rock types in the Kubanni Basin given in table 4 were used for the geological interpretations of the geoelectric layers obtained in this work.

TABLE 3: Resistivity values of rock types in the Nigerian Basement areas (After Shemang, 1990).

Rock Type	Resistivity Range (Ω - m)
Fadama Loam	30-90
Clay, Silt and Gravel	100-200
Sand and Gravel	100-180
Weathered laterite	200-500
Fresh laterite	500-600
Weathered Basement	20-100
Fresh Basement	> 1000

TABLE 4: Resistivity values of materials in the Kubanni Basin (After Shemang, 1990)

Rock Type	Resistivity Range (Ω - m)
Fadama Loam	30 –70
Clay, Silt and Gravel	71 –200
Sand and Gravel	100-180
Weathered laterite	181-500
Fresh laterite	501-800
Weathered Basement	20 –150
Fractured Basement	600-1000
Fresh Basement (Crystalline)	>1000

4.2 INTERPRETATION OF DATA OBTAINED USING THE TWO-ELECTRODE METHOD.

The interpretation of the reduced data obtained using the two-electrode method was carried out using the method adopted by Makinde (1996). A new approach was, however, used for determining the resistivity value(s) of the underlying layers in this work.

The reduced data of section 3.3.1 obtained using the two-electrode method consists of the computed "bulk resistivity" (ρ_b) values plotted against their corresponding (L/2) values on logarithmic-linear (semi-log) graph papers. Such graphs consist of straight-line segments indicating the number of geo-electric segmentations that exist with depth. A typical example of such a plot is shown in fig. 4.1 for VES station 25.

The procedure as used by Makinde (1996) to determine the different layer parameters from the (ρ_b) against L/2 plots, and as used in this work, involves;

- Determining the intercept values of the segments on the vertical (i.e.ρ_b) axis and designating them as C_1, C_2, C_3,.....C_n
- Calculating the slope value(s) of the segments and designating them as S_1, S_2, S_3,.....S_n.
- Determining the intercept values on the horizontal (i.e. L/2) axis projected from the point of intersection of adjacent segments and designating them as h_1, h_2, h_3,.....h_n.

How each of these parameters were determined is briefly discussed below.

VES 25

C_1 =450 (Ω - m) h_1 = 3.0 m
C_2 =1,550 (Ω - m) h_2 = 20.0 m
C_3 =6,800 (Ω - m) H = 23.0 m

S_1 = (ln 1,700 – ln 450) / 1.5 m = 0.44305 m^{-1}
S_2 = (ln 5,000 – ln 1,550) / 8.0 m = 0.07320 m^{-1}
S_3 =(ln 10,000 – ln 6,800) / 22.5 m = 0.00857 m^{-1}

$\rho_1=C_1$= 450 (Ω - m)
$\rho_2=C_2 S_2 h_1$=340.38 (Ω - m)
$\rho_3=C_3 S_3 h_2$ =1,165.52 (Ω - m)

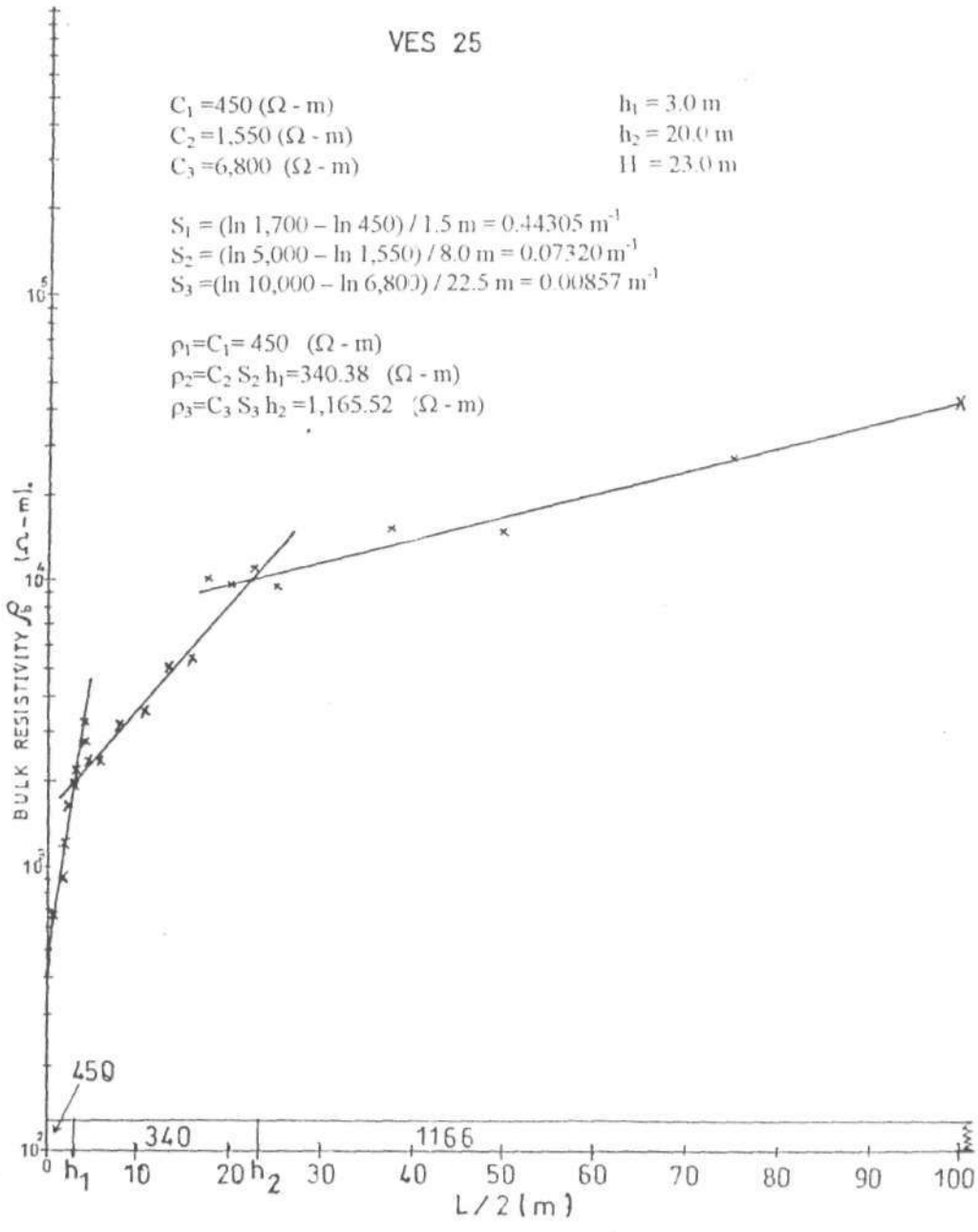


Fig.4.1 Plot of Bulk Resistivity Against L/2 and Interpretation of Data Obtained Using Two-Electrode Array for VES Station 25.

4.2.1 DETERMINATION OF LAYER PARAMETERS

Having deduced the intercept and slope values of the segments, the layer parameters which include the number of layers sounded at a VES station, the depth to basement values, the different layer thickness and the layer resistivity values were then determined as given below.

a. Number of layers Sounded

As adopted by Makinde (1996) and Ajayi and Makinde (2000), the number of layers sounded at a VES station can easily and quickly be determined by inspection of the (ρ_b) against L/2 plots. The number of straight line segments on the plot gives the number of layers sounded at that VES station since it is expected that the slope of a straight line graph (based on equation (2.45) always change, when the underlying bed is of a different material or composition from that of the overlying bed. The number of layers sounded at a VES station is therefore equal to the number of straight line segments obtained from the plot of the (ρ_b) against L/2. Therefore, the (ρ_b) against L/2 plot for VES station 25 in Fig. 4.1 has three segments. Hence, it implies that three layers were sounded at that VES station.

b. Depth to Basement Determination

The depth to basement value at each VES station was determined in this work as adopted by Makinde (1996) by reading off the intercept on the horizontal (i.e. L/2) axis projected from the point of intersection on the last two adjacent segments. The depth to basement value at each VES station can also be determined by adding up the h values of that VES station down to the point of intersection of the last two adjacent segments of the plot.

c. Layer Thickness Determination

The thickness of the layers sounded at a VES station were deduced by working out necessary subtractions from the h-values obtained from the (ρ_h) against L/2 plots. The thickness of the surface (top) layer, t_1, is h_1. The thickness of the second layer, t_2 is given as $t_2=h_2-h_1$, while that of the third layer, t_3 is $t_3=h_3-h_2$. It, therefore, follows that the thickness of the nth layer, t_n, is given as $t_n=h_{n+1}-h_n$ where n is an integer given as n=1,2,3,.....The thickness of the layers sounded at VES 25 shown in Fig. 4.1 were determined as follows;

$$t_1 = h_1 = 3.0 \text{ m}$$

$$t_2 = h_2 - h_1 = 20.0 \text{ m} - 3.0 \text{ m} = 17.0 \text{ m}$$

Similar procedure was used to determine the thickness of the different layers in all the other VES stations.

(d) Determination of Resistivity Values

The top or surface layer resistivity value at each VES station was determined by reading off the intercept, C_1, of the first segment on the vertical (i.e. ρ_h) axis as adopted by Makinde (1996). C_1 is therefore taken as the resistivity when L/2 is zero.

Hence,

$$\rho_1 = C_1 \ (\Omega - m) \qquad (4.2)$$

For example, the resistivity value of the surface layer for VES station 25, Fig. 4.1 is 450 Ω - m

Makinde (1996) computed the resistivity value(s) of the underlying layers(s) by multiplying the computed resistivity value of the overlying layer with either the slope value or its reciprocal for the layer. He used these values in such a way that the basement value will not be too low or too high. Makinde (1996), therefore, had to decide whether

to use the slope value or its reciprocal for each layer so that the resistivity value would match the composition.

A new approach was adopted in this work for determining the resistivity value(s) of the underlying layer(s). In this approach, it is assumed that the resistivity value of the nth layer (i.e. ρ_n) depends on the following:

i. The slope of the nth layer (S_n),

ii. The intercept of the nth layer (C_n) on the vertical (ρ_a) axis and

iii. The thickness of the $(n-1)^{th}$ layer

Using dimensions, it was found that the unit of ρ_n could be deduced by multiplying the three parameters above. That is,

$$\rho_n = C_n(\Omega - m) \times S_n(m^{-1}) \times h_{n-1}(m)$$

$$= C_n S_n h_{n-1} (\Omega - m) \quad \ldots\ldots(4.3)$$

where n =2,3,4,...

From equation (4.3), the resistivity value of the second layer can be determined as

$$\rho_2 = C_2 S_2 h_1 (\Omega - m) \quad \ldots\ldots(4.4)$$

And that of the third layer as

$$\rho_3 = C_3 S_3 h_2 (\Omega - m) \quad \ldots\ldots(4.5)$$

The intercepts (C and h) values, and the slope values for VES station 25, Fig. 4.1, were determined and given as below;

C_1 =450 (Ω - m) h_1 = 3.0 m

C_2 =1,550 (Ω - m) h_2 = 20.0 m

C_3 =6,800 (Ω - m) H = 23.0 m

S_1 = (ln 1,700 – ln 450) / 1.5 m = 0.44305 m^{-1}

S_2 = (ln 5,000 – ln 1,550) / 8.0 m = 0.07320 m^{-1}

S_3 =(ln 10,000 – ln 6,800) / 22.5 m = 0.00857 m^{-1}

From the above data for VES station 25, Fig. 4.1, the resistivity values of the surface (top) layer, second layer and third layer are deduced as follows;

$\rho_1=C_1= 450 \quad (\Omega - m)$

$\rho_2=C_2\ S_2\ h_1=340.38 \quad (\Omega - m)$

$\rho_3=C_3\ S_3\ h_2 =1,165.52 \quad (\Omega - m)$

By applying this procedure to all the VES data collected using this method, the resulting layer parameters determined for all the VES stations sounded are given in Appendix A. The plots of the "bulk resistivity", ρ_b, against the electrode spacing, L/2, for all the VES points and from which the layer parameters were deduced are also given in Appendix A.

4.3 INTERPRETATION OF DATA OBTAINED USING THE SCHLUMBERGER CONFIGURATION.

The data obtained using the Schlumberger configuration were interpreted using a computer program, which performs an automatic iterative curve matching process. The computer program (Offix Version 2.0, April 1990) was developed by Interpret Limited, Golden Colorado, U.S.A. in conjunction with Campus Geophysical Instrument Limited U.S.A. The program is designed to interpret D.C. resistivity sounding data for Offset Wenner Sounding System measurements, Schlumberger, Polar and Equatorial dipole, "a – na – a" dipole-dipole and pole-dipole arrays. The results of the interpretation are in terms of a layered-earth model.

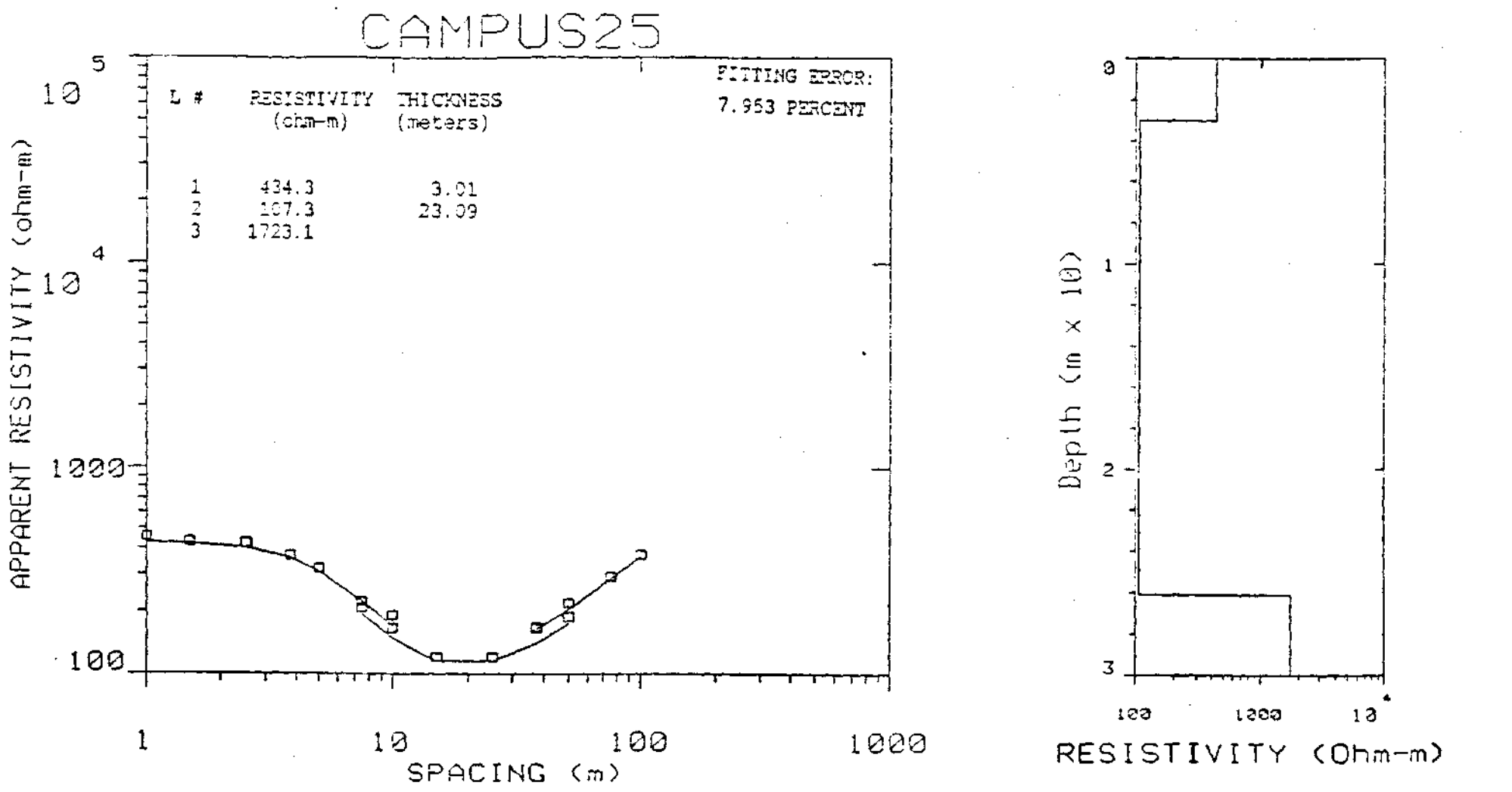


Fig. 4.2 Interpretation of Apparent Resistivity Obtained Using Schlumberger Array for VES Station 25.

A typical example of such interpretation carried out by using the computer program, which shows the curve and model for VES station 25, is given as Fig.4.2. The other curves and their corresponding model interpretations for all the other VES points surveyed in this work are given in Appendix B.

4.4 GEOELECTRIC AND GEOLOGIC SECTIONS

The geoeclectric and geologic sections presented in this work were drawn on the basis of the individual geoelectric interpretations obtained for each VES point. A brief description of each of the resulting net geoelectric and geologic sections taken along four profiles is given below.

(a) Profile A-A'

This is a N – S profile extending the gate of Area 3 (point A) to the SW of ICSA and Ramat Halls (point A'). Fig. 4.3 shows the net geoelectric and geologic sections obtained along the profile for the two arrays used. While Fig. 4.3(a) shows the geoelectric section for the two – electrode method, Fig. 4.3(b) shows that for the Schlumberger configuration. In both cases, the geoelectric sections show that three geoelectric layers underlie the profile. The surface layer (topsoil) is most likely made up of clays, silts and sands while the second layer is weathered laterite. The third layer forms the basement. The thickness of the surface layer ranges from 3.0 m to 6.0 m for the two –electrode array while, for the Schlumberger configuration, it ranges from 2.5 m to 5.5 m. The thickness of the second layer obtained for the two-electrode array ranges from 18.5 m to 22.0 m while for the Schlumberger array, it ranges from 15.5 m to 23.5 m. The thickness values for two-electrode array and Schlumberger arrays are in agreement to about 87 %.

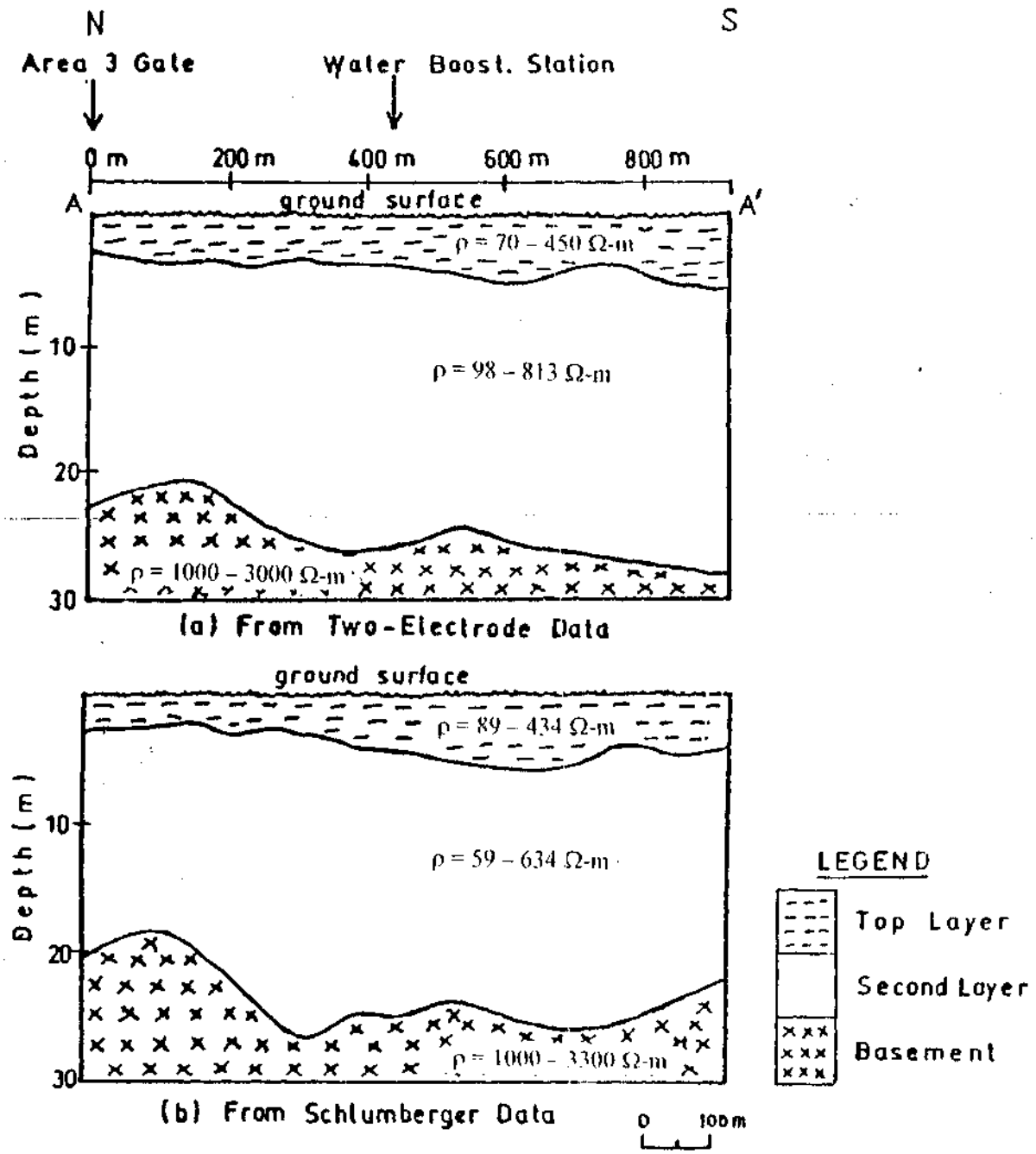


Fig. 4.3 Geoelectric and Geologic Sections Along Profile A – A′

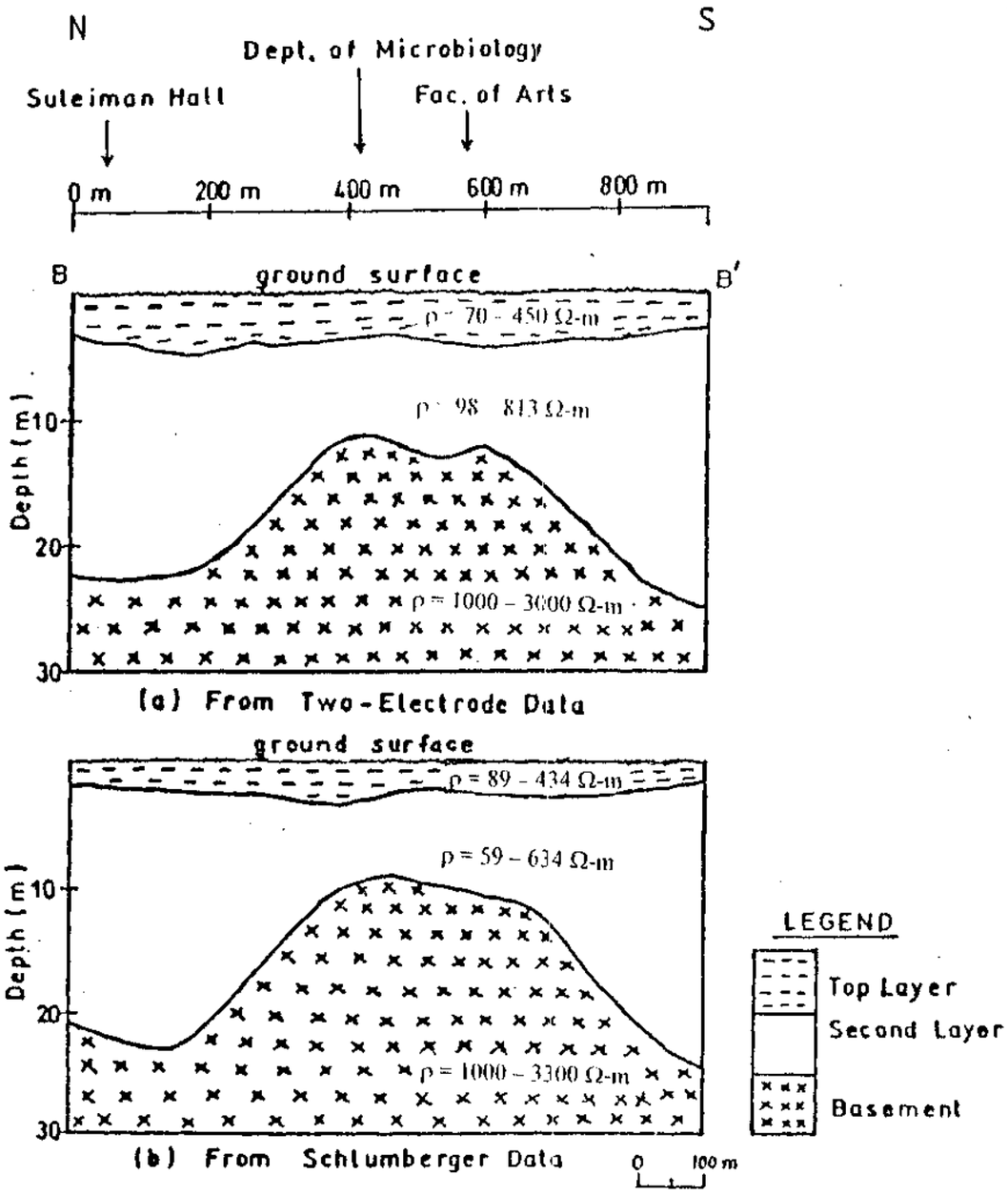


Fig. 4.4 Geoelectric and Geologic Sections Along Profile B – B′

(b) Profile B-B'

This is a N-S profile extending the northern end of Suleiman Hall to the southern end of Ramat/ICSA Halls. The net geoelectric sections obtained along Profile B-B' for the two-electrode method and Schlumberger configuration are given as Figs. 4.4 (a) and (b) respectively. Both geoelectric sections show that three layers underlie the profile. The top or surface layer is most likely clays, silts and sands, the second layer is most likely made up of weathered laterite and fresh laterite while the third layer forms the bedrock. The thickness of the top layer ranges from 3.0 m to 5.0 m for the two-electrode method while for the Schlumberger configuration, it ranges from 2.0 m to 4.0 m. The second layer thickness for the two-electrode array ranges from 7.0 m to 22.5 m while for the Schlumgerger configuration, it ranges from 6.0 m to 22.5 m. These thickness values have agreed to about 78 %.

(c) Profile C-C'

Figs. 4.5 (a) and (b) are the net geoelectric sections along profile C-C' for the two-electrode array and Schlumberger configurations respectively. As shown in the figures, profile C-C' which extends from the northern end of Akenzuwa hall to the southern end of the Botanical garden is also underlain by three layers. The surface layer most likely comprises of clays, silts and sands while the second layer is most likely weathered laterite and fresh laterite. The third layer forms the bedrock. The thickness of the top layer ranges from 2.5 m to 5.0 m for the two-electrode array and 1.5 m to 4.5 m for the Schlumberger configuration, while the thickness of the second layer ranges from 10.0 m to 27.5 m for the two-electrode array and 7.0 m to 24.0 m for the Schlumberger configuration. The thickness values obtained along profile C-C' for the two arrays have agreed to about 66 %.

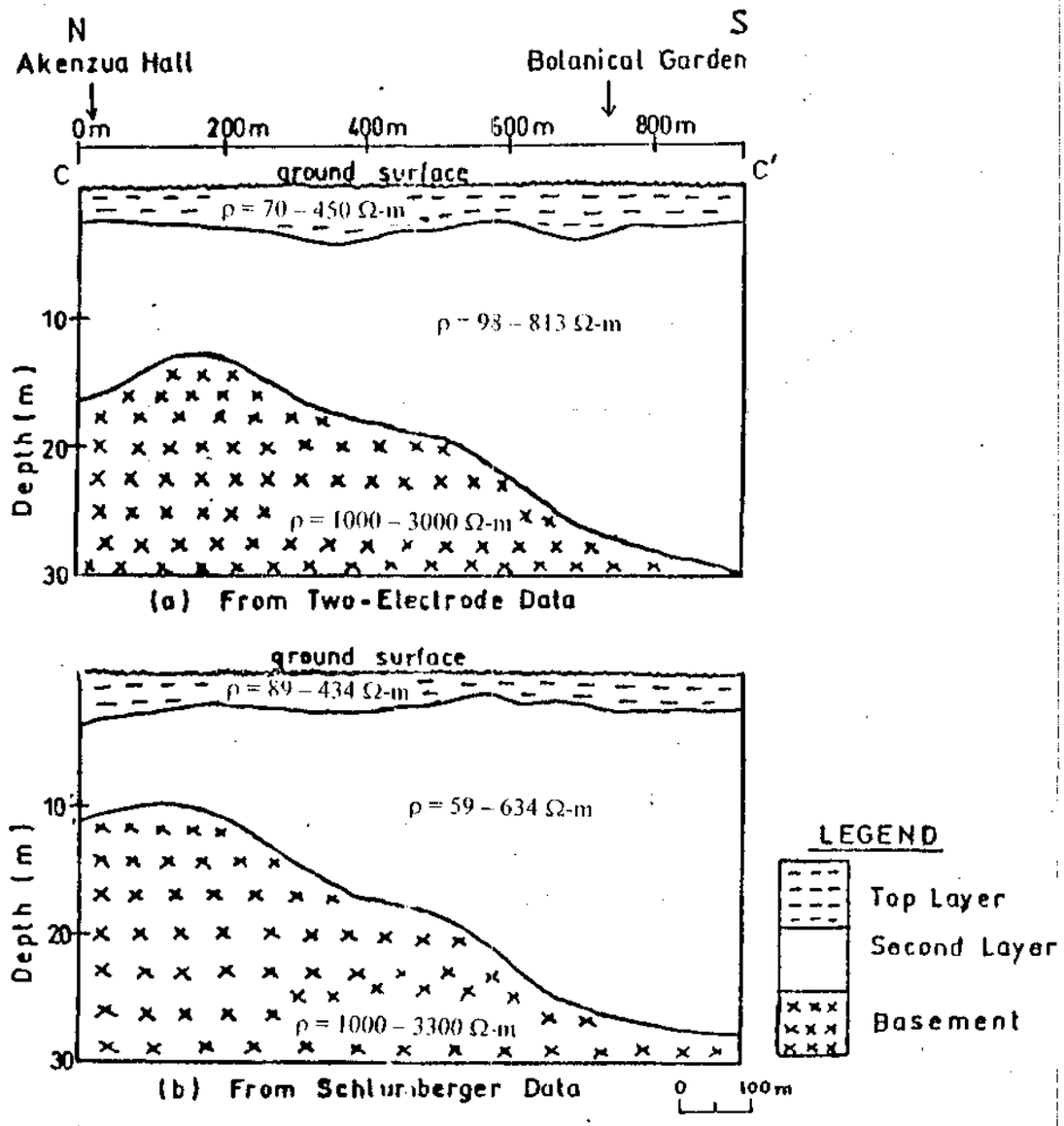


Fig. 4.5 Geoelectric and Geologic Sections Along Profile C – C′

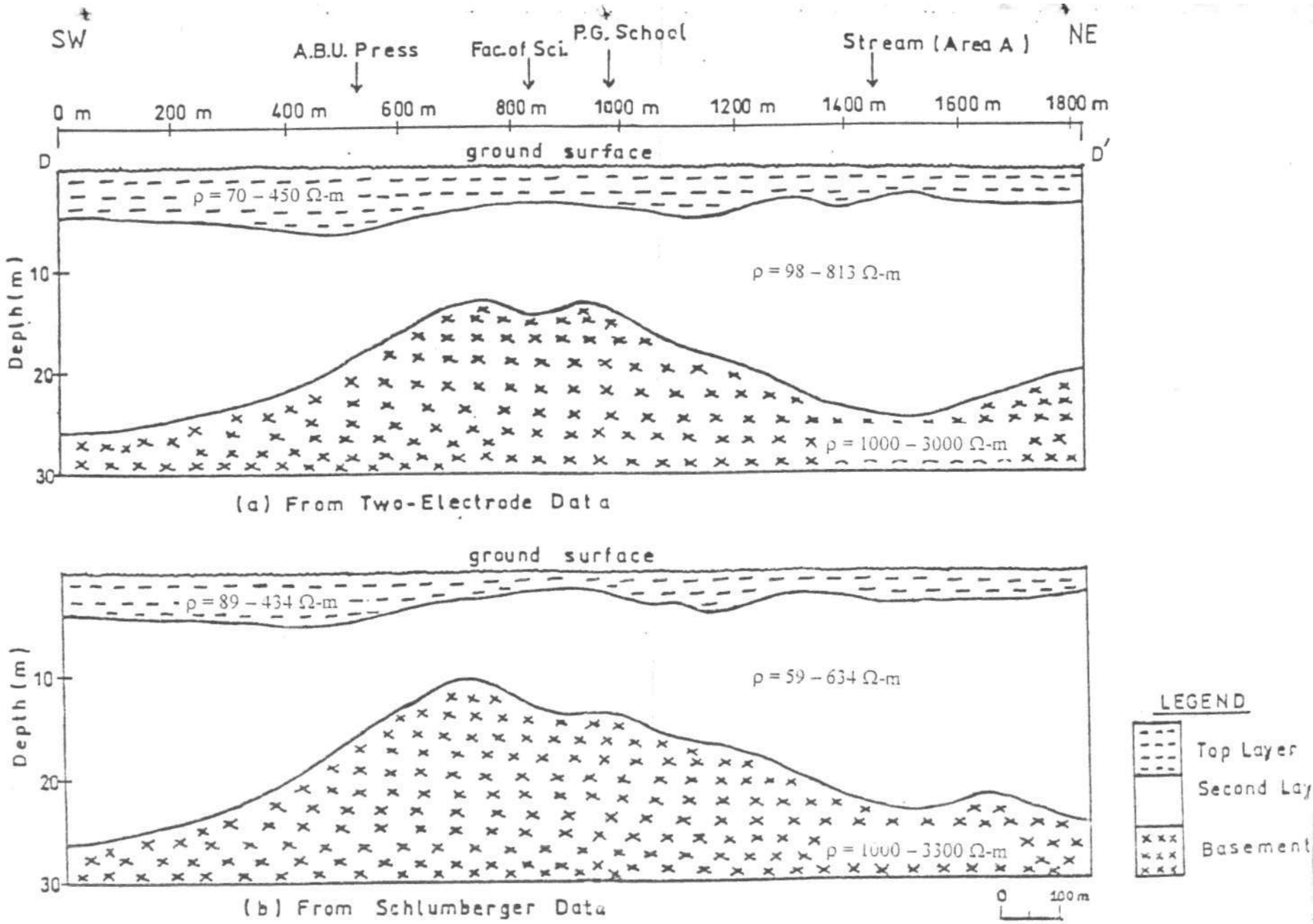


Fig. 4.6 Geoelectric and Geologic Sections Along Profile D – D′

(d) Profile D-D'

Profile D-D' has a different orientation to the other three profiles described above. Profiles A-A', B-B' and C-C' were taken along the north to south direction while profile D-D' is taken from the southwest to the north east of the Main Campus. The net geoelectric sections obtained along profile D-D' are given as Figs. 4.6 (a) and (b) respectively for the two-electrode array and Schlumberger configuration. As for the other three profiles, profile D-D' is also underlain by three layers. The top layer is most likely clays, silts and sands while the second layer is most likely weathered laterite and fresh laterite. The third layer forms the bedrock. The thickness of the top layer ranges from 2.5 m to 6.5 m for the two-electrode method while for the Schlumberger configuration, it ranges from 1.5 m to 5.5 m. The thickness of the second layer ranges from 9.0 m to 22.5 m for the two-electrode array while for the Schlumberger configuration, it ranges from 7.5 m to 22.5 m. The thickness values deduced for profile D-D' for both arrays are in agreement to about 71 %.

4.5 CONTOUR MAPS AND CROSS-SECTIONS PRODUCED

Results of the VES interpretations for all the points sounded were used to produce contour maps and cross sections using the computer program **"SURFER"** for both the two-electrode method and the Schlumberger configuration. To plot the contour maps and cross-section diagrams with the computer program, all the VES points were assigned coordinate values based on the map of the study area with VES station 26, at the southern end of A.B.U. Press, serving as the origin.

4.5.1 Depth-To-Basement Contour Maps

(a) From the Two-Electrode Array Data

Fig. 4.7 (a) is the depth-to-basement contour map obtained from the two-electrode data. The map is characterised by closures of low and high depth-to-basement values. The depth-to-basement is shallower, about 13.0 m around the central part of the

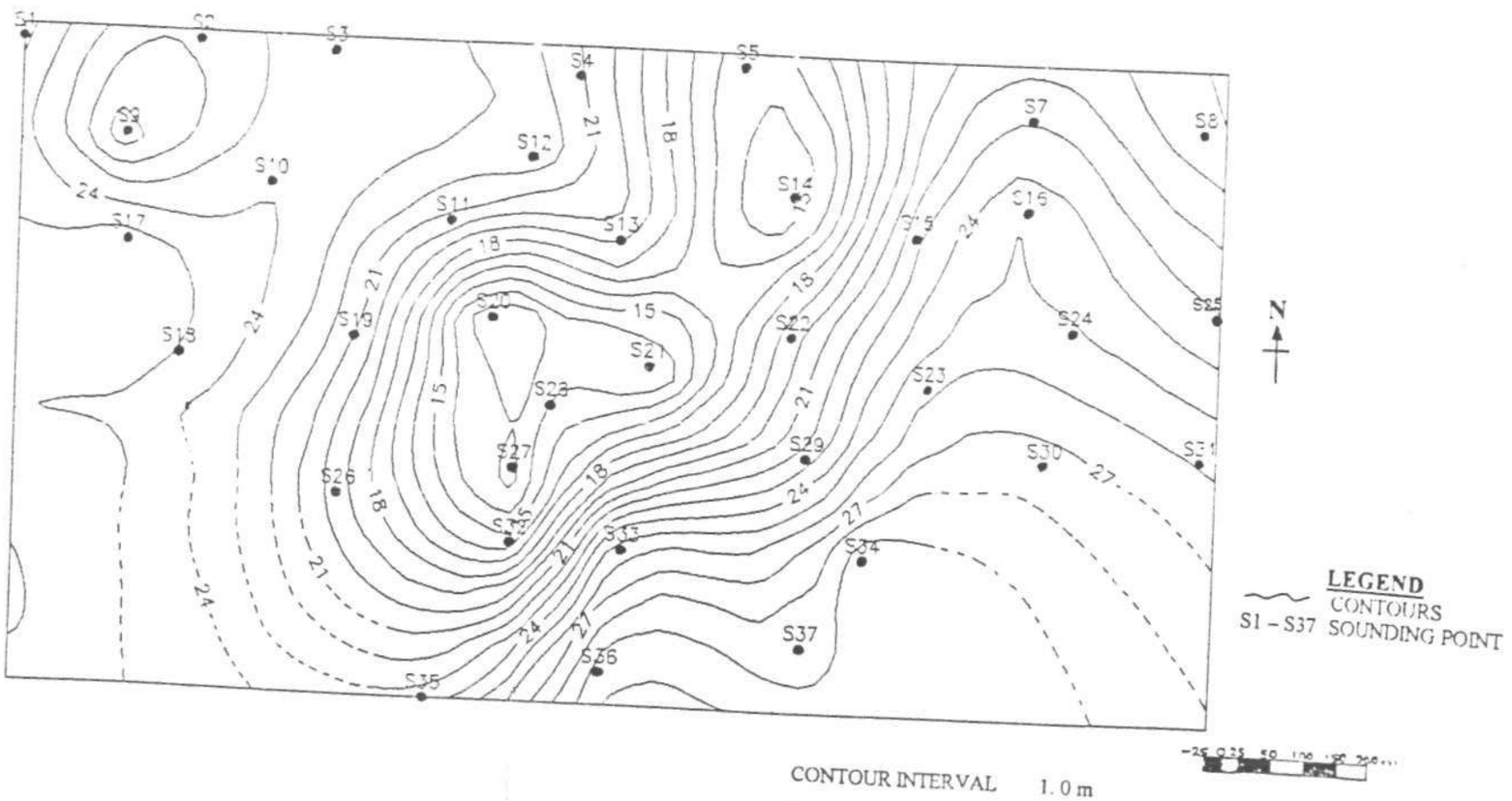


Fig. 4.7 (a) Depth – to – Basement Contour Map of the Project Area Obtained from Interpreted Two – Electrode Data.

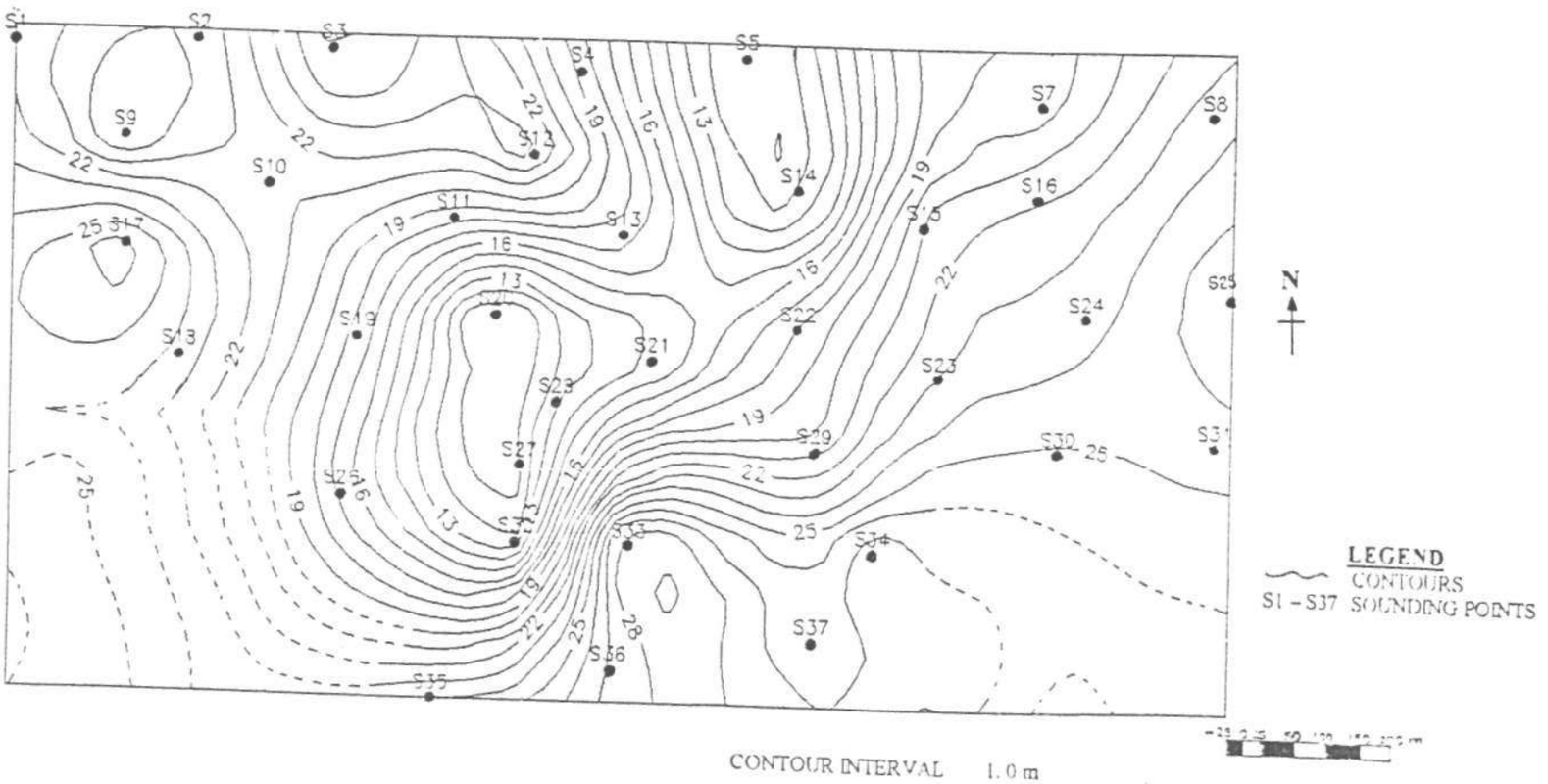


Fig. 4.7 (b) Depth – to – Basement Contour Map of the Project Area Obtained from Interpreted Schlumberger Data.

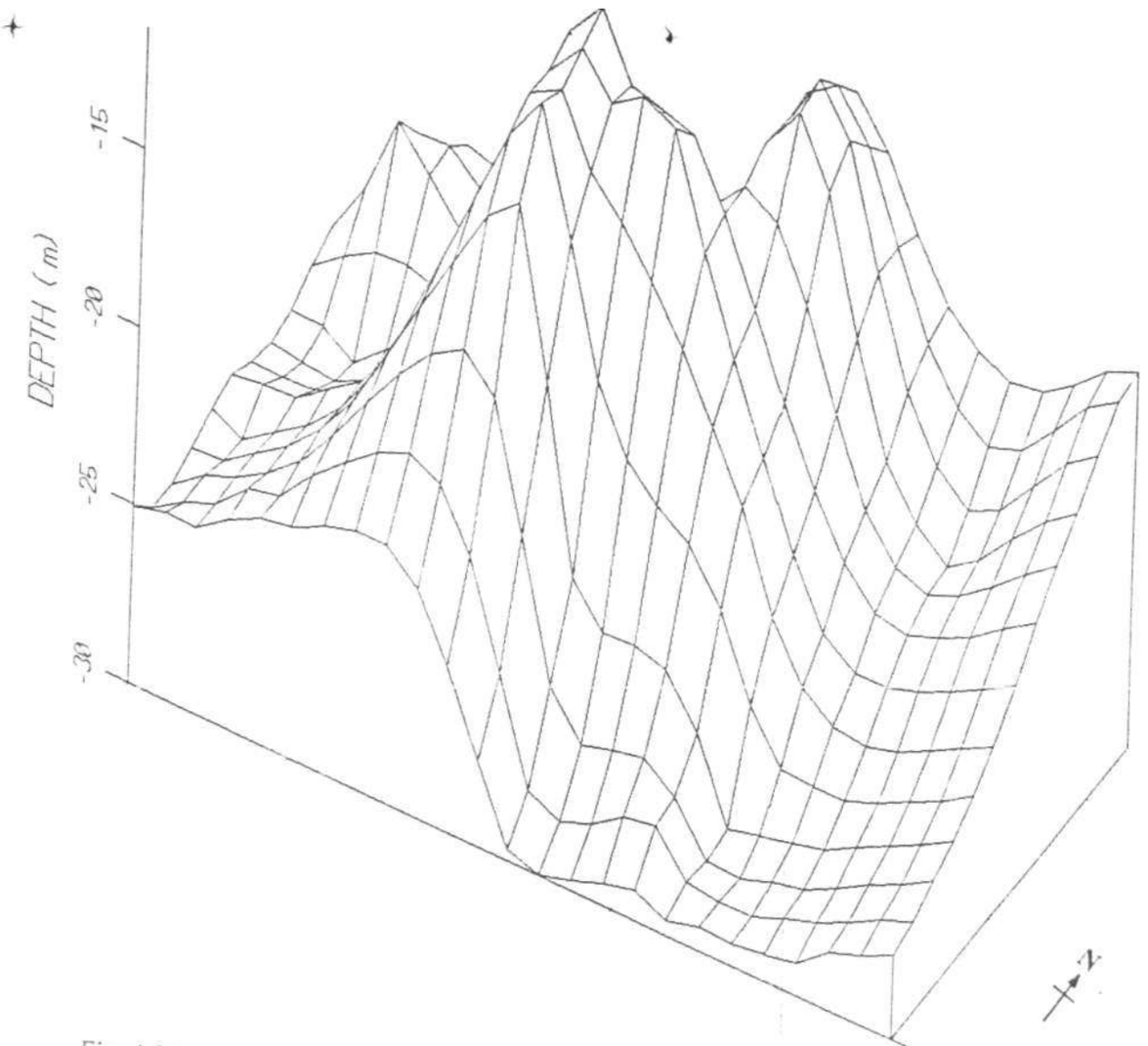


Fig. 4.8 (a) 3 – D Cross – Sectional View of the Basement Underlying the Project Area from Interpreted Two – Electrode Data.

Fig. 4.8.(b)3 – D Cross – Sectional View of the Basement Underlying the Project Area From Interpreted Schlumberger Data.

Main Campus (i.e. around KIL and Senate building), and, about 15.0 m around the area between Amina hall and Akenzua hall. The depth-to-basement is deeper, abut 25.0 m, 29.0 m and 30.0 m respectively to the west of Danfodio hall, the area west of Botanical garden area to the south of A.B.U. Staff School.

(b) From The Schlumberger Array Data

The depth-to-basement contour map obtained for the Schlumberger array is given as Fig. 4.7 (b). The map is also characterised by closures of high and low depth-to-basement values. The closures are observed around the central, northeastern and northern past of the Main Campus. The central part of the Main Campus, around KIL and the Senate Building, has depth-to-basement value of about 11.0 m while that at the northern part around Akenzua Hall is about 12.0 m. The basement is deeper to the southern end of A.B.U. Staff School with a value of about 29.0 m while that of the northeastern part between Danfodio Hall and Area 3 is about 26.0 m.

4.5.2 3-D Cross-Sectional Diagrams of the Basement

Figs. 4.8 (a) and (b) are respectively the 3-D cross-sectional diagrams for the two-electrode array and Schlumberger configuration. In both diagrams, the undulating shape of the basement in the study area is shown. The peaks or "high rises" show areas of shallow depth-to-basement while the troughs indicate areas where the basement is deeper in the study area. There is a close resemblance to the undulating nature of the basement in both cross-sections for the two-electrode array, Fig. 4.8 (a) and that for the Schlumberger configuration, Fig. 4.8 (b).

4.5.3 Surface Layer Thickness Contour Maps

(a) From Two-Electrode Array Data

The contour map of the surface or top layer thickness obtained from the two-electrode data is given as Fig. 4.9 (a). The map is characerised by closures within the

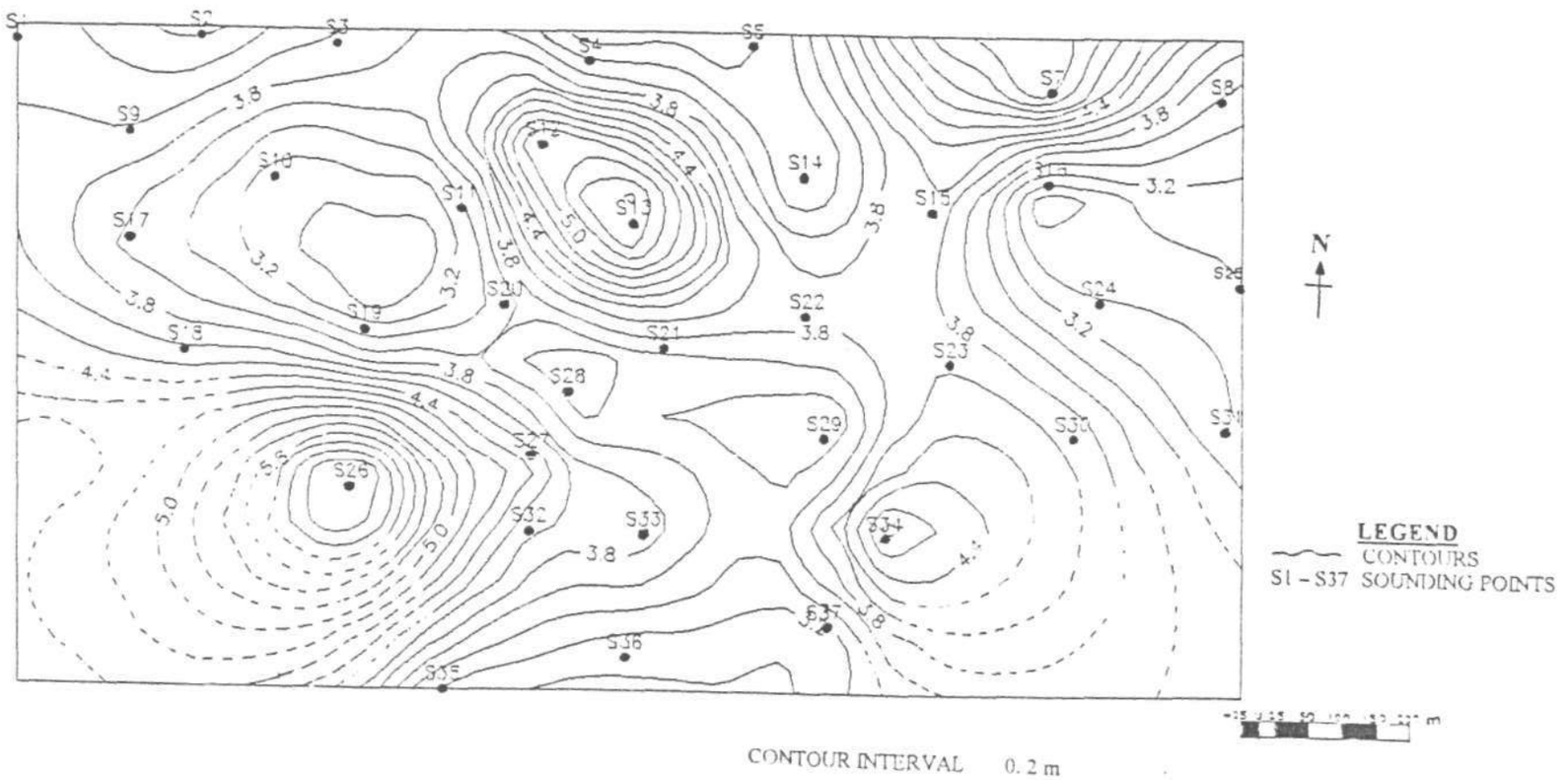


Fig. 4.9 (a) Contour Map of the Surface Layer Thickness from Interpreted Two – Electrode Data

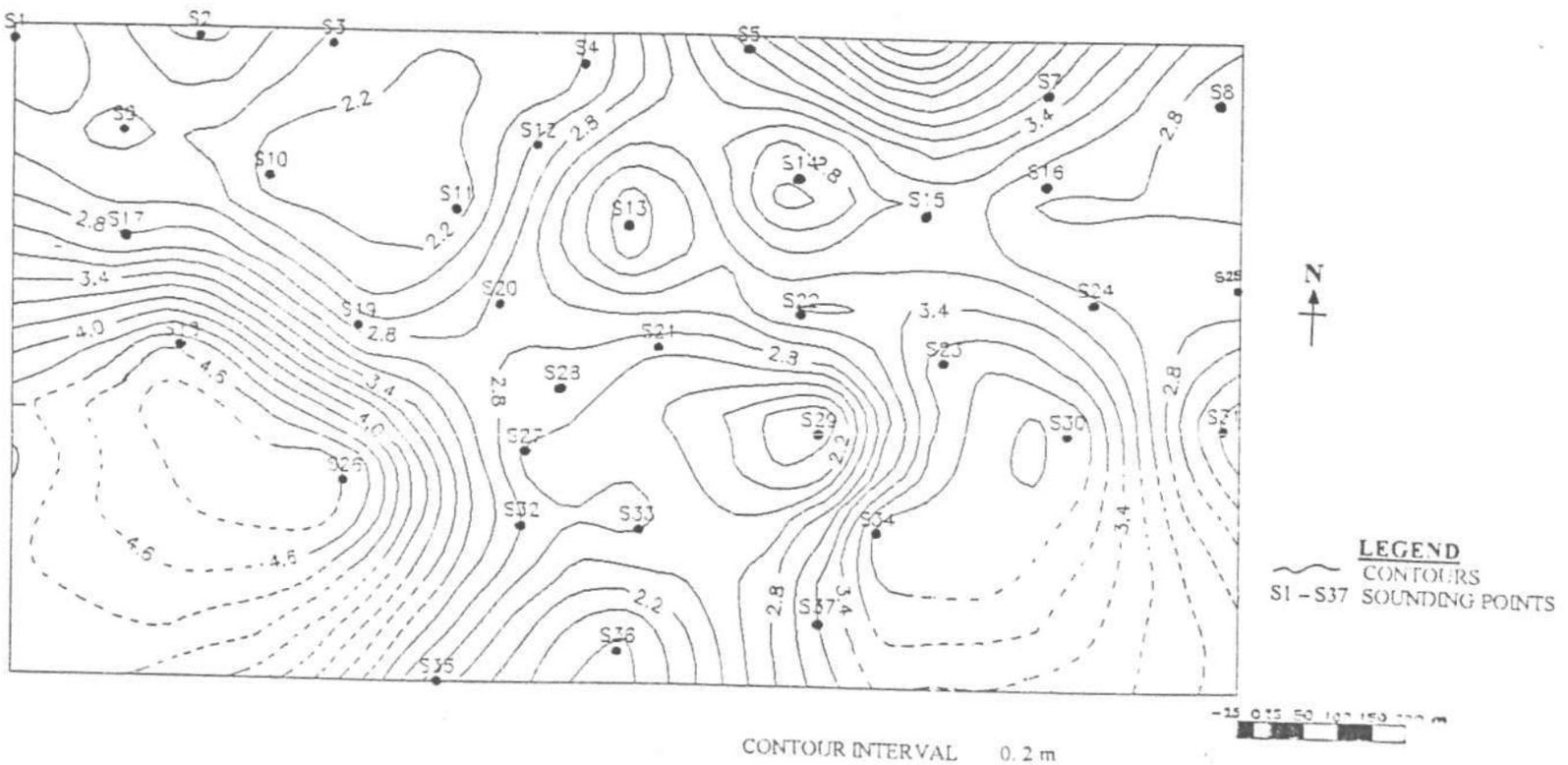


Fig. 4.9 (b) Contour Map of the Surface Layer Thickness from Interpreted Schlumberger Data.

study area. The thickness of the surface layer ranges from 2.8 m to about 6.2 m.

(b) From The Schlumberger Data

Fig. 4.9 (b) is the contour map of the surface layer thickness obtained from the Schlumberger data. As in Fig. 4.9 (a), the contour map is also characterised by closures within the Main Campus. The thickness of the surface layer varies from 2.2 m to about 4.8 m.

4.6 COMPARISON OF RESULTS OBTAINED USING INTERPRETED TWO-ELECTRODE ARRAY DATA AND THE SCHLUMBERGER ARRAY DATA.

The primary aim of this work is to test the reliability and effectiveness of the two-electrode method, which is currently under development. To achieve this aim, the interpretations obtained from the two-electrode method are, hereby, compared with those obtained from the Schlumberger array in this work.

Table 5 is a summary of the results obtained from the interpretations of both sets of data for the two-electrode method and Schlumberger configuration. The comparison of results given in table 5 is discussed below.

(i) Number of Layers

As given in table 5, the number of layers sounded varied from 3 to 4 layers. Results obtained from the two-electrode data show that all the VES stations sounded had 3 layers except for VES stations 4, 11, 31 and 34 that had 4 layers while results from the Schlumberger data show that all the VES stations sounded had 3 layers except for VES stations 4, 11 and 31 that had 4 layers. The two-electrode method has therefore compared very well with the Schlumberger configuration in terms of the number of layers sounded to about 97 % of agreement.

(ii) Thickness of Layers

The thickness of the various layers sounded at each VES station are given under the column with subheading h (m) in table 5. For instance, the thickness of the surface layer and second layer for VES station 01 are given in table 5 as 4.0 m and 21.5m respectively for the two-electrode array while that for the Schlumberger configuration for the same VES station are 2.21 m and 17.57 m respectively for the surface and second layer. The thickness of the surface layer within the Main Campus varied from 2.5 m to 7.0 m for the two-electrode array while that for the Schlumberger varied from 1.36 m to 5.25 m. The second layer thickness values also varied from 7.0 m to 27.0 m for the two-electrode array while that for the Schlumberger configuration varied from 5.41 m to 28.0 m. Thickness values obtained from the two-electrode array as given in table 5 are generally higher than those obtained from the Schlumberger configuration. This implies that the depth of penetration is greater for the two-electrode method than that of the Schlumberger configuration. The third or fourth layer which forms the basement, as the case may be, has infinite thickness, hence it is represented by the symbol (∞). The layer thickness values for the two sets of interpreted results have agreed to about 72 %.

(iii) Resistivity Values

The resistivity values of the various layers deduced from the interpretation of the two-electrode data and Schlumberger configuration data are given in table 5. There is a good correlation between the resistivity values of the various layers obtained from the two-electrode data and that obtained from the Schlumberger data. For instance, the resistivity value of the surface layer for VES station 01 is 96 Ω-m for the two-electrode array while that for the Schlumberger configuration is 87 Ω -m. The resistivity value of the second layer for the same VES point is 498 Ω-m for the two-electrode array while

that for the Schlumberger configuration is 300 Ω -m. The resistivity value for the third layer which forms the basement is 1973 Ω-m for the two-electrode array while that for the Schlumberger configuration is 2782 Ω-m. However, resistivity values of the basement for the two-electrode array are lower than those obtained for the Schlumberger configuration for VES stations 05, 06, 07, 08, 09, 20, 21 and 33. In general, the resistivity values from the two sets of interpreted results have agreed to about 52 %. The agreement is better about 82 % for the surface layer resistivity values.

4.7 COMPARISON OF RESULTS OBTAINED IN THIS WORK WITH THOSE OBTAINED BY PREVIOUS WORKERS IN THE KUBANNI BASIN

Previous geophysical studies carried out by workers in the Kubani Basin such as Ososami (1968) and Makinde (1996) reported on the undulating nature of the bedrock with depth values varying from about 0.0 m to about 60 m. Ososami (1968) deduced that the depth-to-basement within the Main Campus varies from less than a metre to about 30 m. Also Hassan (1987) deduced that the depth to the bedrock ranges from 5 m and may reach up to 60 m to the southern part of the Main Campus. Shemang (1990) found that the depth-to-the basement is about 3 m just to the west of A.B.U. dam and 44 m around Unguwan Kubanni.

Results of the interpretation of both sets of VES data in this work, as given in section 4.5.1 and table 5, show that the depth to the basement values varies from about 13.0 m to about 30.0 m, for the two-electrode array data, while that from the Schlumberger configuration varies from about 11.0 m to about 29.0 m. These values are within the range of the depth-to-basement values obtained by previous workes in the Kubanni Basin. Also, as reported by Hassan (1987), the basement is undulating. Sections 4.4 and 4.5.1 in this work reveal the undulating nature of the basement. The resistivity

values deduced by Hassan (1987) in the Western half of the Kubanni Basin as 36 - 600 Ω-m, 20 - 350 Ω-m and 1000 - 8000 Ω-m respectively for the surface layer, second layer and the basement corroborated those obtained in this work which are 70 - 450 Ω-m, 98 - 812 Ω-m and 1035 - 3680 Ω-m respectively for the surface layer, second layer and the basement using the two-electrode array while that using the Schlumberger configuration are 87 - 434 Ω-m, 59 - 633 Ω-m and 1098 - 3602 Ω-m respectively for the surface layer, second layer and basement. The overburden within the Main Campus, as deduced in this work, is most likely made up of clays, silts, sand, weathered laterite, weathered basement and fresh laterite which corroborated the results of Shemang (1990) within the Kubanni Basin.

TABLE 5: SUMMARY OF RESULTS OBTAINED FROM THE INTERPRETATION OF BOTH SETS OF DATA

VES STATION NO.	LAYER NO.	TWO-ELECTRODE METHOD			SCHLUMBERGER ARRAY			PERCENTAGE DIFFERENCE		
		ρ(Ω-m)	h(m)	H(m)	ρ (Ω-m)	h(m)	H(m)	ρ (Ω-m)	h(m)	H(m)
01	1	96	4.0		89.65	2.21		7	-8	
	2	498.45	21.5		300.00	19.78		66	8.7	
	3	1,663.71		25.5	2781.60	∞	21.99	40		16
02	1	130	4.5		104.8	2.98		24	51	
	2	430.35	17.5		302.2	17.02		42	2.8	
	3	2353.32		22.0	3602.6	∞	20.00	35		10.0
03	1	190	4.0		201.3	2.36		5.6	-69.5	
	2	346.94	20.0		468.9	23.39		26	14.5	
	3	1061.61		24.0	3395.1	∞	25.75	68		6.8
04	1	135	3.0		122.6	2.22		10	35	
	2	191.90	10.0		200.0	5.99		4.1	66.9	
	3	639.69	8.0	21.0	2496.8	9.81		74	18.5	16.5
	4	308.67			834.6	∞	18.02	63		
05	1	400	3.0		327.8	3.66		22	18.7	
	2	194.04	12.0		165.2	6.45		17.5	86	47.9
	3	385.29		15.0	1098.0	∞	10.14	64.9		

VES STATION NO.	LAYER NO.	TWO ELECTRODE METHOD			SCHLUMBERGER ARRAY			PERCENTAGE DIFFERENCE		
		ρ(Ω-m)	h(m)	H(m)	ρ (Ω-m)	h(m)	H(m)	ρ (Ω-m)	h(m)	H(m)
06	1	170	5.0		180.0	5.25		5.6	4.8	
	2	254.68	15.0		121.3	13.01		110	15.3	
	3	554.95		20.0	1635.0	∞	18.26	66		9.5
07	1	310	5.5		305.8	3.57		1.4	54.1	
	2	177.04	17.5		154.7	15.74		14.4	11.2	
	3	503.05		23.0	1079	∞	19.31	53.3		19.1
08	1	320	3.5		285.7	2.58		12	35.7	
	2	144.51	16.5		103.1	21.09		39.1	21.8	
	3	556.48		20.0	2537.1	∞	23.67	78.1		15.5
09	1	220	4.0		205.6	2.34		7	70.9	
	2	178.89	16.0		93.3	16.26		91.7	1.6	
	3	508.46		20.0	1395.0	∞	18.60	63.6		7.5
10	1	170	3.0		212.5	2.05		20	46.3	
	2	128.06	21.0		133.3	18.96		3.9	10.8	
	3	1182.78		24.0	2721.5	∞	21.01	56.5		14.2

VES STATION NO.	LAYER NO.	TWO ELECTRODE METHOD			SCHLUMBERGER ARRAY			PERCENTAGE DIFFERENCE		
		ρ(Ω-m)	h(m)	H(m)	ρ (Ω-m)	h(m)	H(m)	ρ (Ω-m)	h(m)	H(m)
11	1	170	3.0		141.6	2.02		20	48.5	
	2	418.82	4.5		387.5	4.81		8.1	6.5	
	3	75.54	13.5		115.9	11.56		34.8	16.8	
	4	985.01		21.0	1675.0	∞	18.39	41.2		14.2
12	1	130	5.5		141.5	2.65		8.1	107.5	
	2	368.61	17.5		385.9	21.31		4.5	17.9	
	3	1155.21		23.0	1748.1	∞	23.96	33.9		4.0
13	1	300	6.0		278.0	3.99		7.9	50.4	
	2	591.20	14.0		122.3	13.95		383.4	0.36	
	3	1058.77		20.0	1479.3	∞	17.94	28.8		11.5
14	1	300	3.0		252.8	2.19		18.7	37	
	2	450.64	10.0		112.0	8.28		302.4	20.8	
	3	609.55		13.0	1527.3	∞	10.47	60.1		24.2
15	1	70	4.0		99.3	2.98		29.5	35.6	
	2	227.63	19.0		162.3	18.44		40.3	3.0	
	3	679.54		23.0	975.5	∞	21.42	30.3		7.4

VES STATION NO.	LAYER NO.	TWO ELECTRODE METHOD			SCHLUMBERGER ARRAY			PERCENTAGE DIFFERENCE		
		ρ(Ω-m)	h(m)	H(m)	ρ (Ω-m)	h(m)	H(m)	ρ (Ω-m)	h(m)	H(m)
16	1	200	2.5		208.0	2.73		3.9	8.4	
	2	379.43	22.5		450.2	19.31		11.7	16.5	
	3	1861.61		25.0	1868.6	∞	22.04	0.37		13.4
17	1	180	3.5		171.6	2.71		4.9	29.2	
	2	355.68	22.5		357.1	24.29		0.40	7.4	
	3	1418.40		26.0	2511.0	∞	27.00	43.5		3.7
18	1	100	4.0		86.9	4.73		15.1	46.5	
	2	259.50	21.0		207.9	18.94		24.8	10.9	
	3	1311.41		25.0	1655.6	∞	23.67	20.7		10.1
19	1	100	3.0		105.3	2.54		5.0	18.1	
	2	233.84	18.5		329.6	15.52		29.1	19.2	
	3	1309.80		21.5	3305.5	∞	18.06	8.9		19.1
20	1	120	3.5		106.8	2.91		12.4	20.3	
	2	338.50	7.0		68.1	5.41		397.1	29.4	
	3	308.88		10.5	1387.6	∞	8.32	77.7		26.2

VES STATION NO.	LAYER NO.	TWO ELECTRODE METHOD			SCHLUMBERGER ARRAY			PERCENTAGE DIFFERENCE		
		ρ(Ω-m)	h(m)	H(m)	ρ (Ω-m)	h(m)	H(m)	ρ (Ω-m)	h(m)	H(m)
21	1 2 3	260 576.77 924.20	3.5 8.0	11.5	233.3 356.8 1905.0	2.53 10.53 ∞	13.06	11.5 61.7 51.5	38.3 24.0	11.9
22	1 2 3	156 429.18 349.34	4.0 16.0	20.0	109.5 380.7 2387.3	3.66 14.78 ∞	18.44	41.6 12.7 46.3	9.3 8.3	8.5
23	1 2 3	190 568.60 2469.06	4.0 22.0	26.0	170.1 275.2 2670.6	3.76 19.33 ∞	23.09	11.7 106.6 7.6	6.4 13.8	12.6
24	1 2 3	140 97.52 1115.18	3.0 22.0	25.0	241.8 59.1 1803.0	3.0 20.48 ∞	23.48	42.1 65.0 38.1	0 7.4	6.5
25	1 2 3	450 340.38 1165.52	3.0 20.0	23.0	4343 107.0 1723.1	3.01 23.09 ∞	26.10	3.6 218.1 32.4	0.33 13.4	11.9

VES STATION NO.	LAYER NO.	TWO ELECTRODE METHOD			SCHLUMBERGER ARRAY			PERCENTAGE DIFFERENCE		
		ρ(Ω-m)	h(m)	H(m)	ρ (Ω-m)	h(m)	H(m)	ρ (Ω-m)	h(m)	H(m)
26	1	150	7.0		132.5	5.19		13.2	34.9	
	2	407.97	12.5		242.6	11.53		68.2	8.4	
	3	1377.00		19.5	1919.3	∞	16.72	28.3		16.4
27	1	230	4.5		275.2	2.48		16.4	81.5	
	2	812.68	7.5		128.8	7.57		531.0	0.93	
	3	1033.71		12.0	1205.1	∞	10.05	14.3		52.9
28	1	230	3.0		171.1	2.66		34.4	12.8	
	2	711.42	12.0		560.4	10.69		27.0	12.3	
	3	1839.55		15.0	3263.5	∞	13.35	43.6		12.4
29	1	200	3.0		376.5	1.36		46.9	120.6	
	2	145.72	19.0		145.6	18.56		0.082	2.4	
	3	2321.27		22.0	1489.4	∞	19.92	55.9		10.4
30	1	90	4.0		179.3	4.15		49.8	3.6	
	2	195.97	23.5		97.36	20.99		101.3	12.0	
	3	1015.89		27.5	1585.9	∞	25.14	35.9		9.4

VES STATION NO.	LAYER NO.	TWO ELECTRODE METHOD			SCHLUMBERGER ARRAY			PERCENTAGE DIFFERENCE		
		ρ(Ω-m)	h(m)	H(m)	ρ (Ω-m)	h(m)	H(m)	ρ (Ω-m)	h(m)	H(m)
31	1	120	3.0		129.7	1.96		7.5	53.1	
	2	440.93	5.0		329.0	4.22		34.0	18.5	
	3	195.83	18.0		49.62	18.31		294.7	1.7	6.2
	4	1527.76		26.0	1387.9	∞	24.49	10.1		
32	1	200	4.0		232.3	2.81		13.9	42.4	
	2	390.95	11.0		410.2	8.86		4.9	24.2	
	3	1244.70		15.0	1133.1	∞	11.67	9.8		28.5
33	1	280	4.0		207.7	2.71		34.8	47.6	
	2	137.36	22.5		124.6	28.03		10.2	19.7	
	3	1012.35		26.5	1960.3	∞	30.74	48.4		13.8
34	1	90	5.0		140.0	3.97		35.7	25.9	
	2	101.95	9.5		90.26	21.90		13.0	60.4	
	3	240.59	15.5	30.0	1843.5	∞	27.96	86.9		7.3
	4	546.71								
35	1	270	3.0		201.7	2.44		33.9	23.0	
	2	548.68	20.5		633.9	21.90		13.4	6.4	
	3	1375.45		23.5	1786.5	∞	24.34	23.0		3.5
36	1	230	3.0		214.8	1.55		7.1	93.6	
	2	116.99	27.0		128.1	25.52		8.7	6.0	
	3	1747.17		30.0	2334.6	∞	27.07	25.2		10.8
37	1	250	3.0		202.3	3.2		23.6	6.3	
	2	115.53	25.0		126.8	22.66		8.9	10.3	
	3	1629.42		28.0	2704.3	∞	25.86	39.8		8.3

Average percentage difference of ρ_1 values = 18 % => 82 % agreement

Average percentage difference of ρ_2 values = 78 % => 22 % agreement

Average percentage difference of ρ_3 values = 49 % => 51 % agreement

Average percentage of agreement of ρ values = 52 %

Average percentage difference of h_1 values = 40 % => 60 % agreement

Average percentage difference of h_2 values = 17 % => 83 % agreement

Average percentage of agreement of h values = 72 %

Average percentage difference of H values = 14 % => 86 % agreement

CHAPTER V

DEDUCTIONS, SUGGESTIONS AND CONCLUSION

5.1 DEDUCTIONS FROM RESULTS

Deductions which include: the reliability of the two-electrode method used in giving true and reliable information about shallow subsurface conditions, geometry of the basement and groundwater potential of the Main Campus were made on the basis of the interpretation of the VES data presented in Chapter IV. These deductions are given below.

5.1.1 RELIABILITY OF THE TWO-ELECTRODE ARRAY

Results obtained using the two-electrode method used in this work, discussed in section 4.3, 4.4, 4.5 and 4.6 in Chapter IV suggest that the results compare very well with those obtained from interpreted Schlumberger data at each corresponding VES station. The two sets of interpreted results are found to agree very well (about 70 %) both in terms of the number of layers sounded, the thickness of each layer and resistivity value of each of the layers sounded.

It must be mentioned that the interpretation of the data collected by the two-electrode method in this work was very simple and straightforward. For instance, no computer analysis is required. Also, the number of layers sounded is obtained by just inspecting the number of segments on the ρ_h against L/2 plots. The thicknesses of the various layers were obtained by reading off the intercept values on the L/2-axis projected from the points of intersections of the segments on the ρ_h against L/2 plots. The new approach employed in this work to determine the resistivity values of the underlying layers has yielded good results that compared well with those obtained from the Schlumberger interpretation.

The two-electrode method used in this work is, therefore, a very reliable and effective method for carrying out vertical electrical resistivity survey.

5.1.2 THE GEOMETRY OF THE BASEMENT BENEATH THE MAIN CAMPUS OF A.B.U. ZARIA

From the interpretations of the VES data obtained using the two-electrode method and the Schlumberger configuration, depth-to-basement values were deduced at each VES point as earlier described in Chapter IV. These depth-to-basement values were used to plot contour maps and 3-D cross-sectional views of the basement beneath the Main Campus of A.B.U. Zaria given as Figs. 4.3 - 4.5.

The Geoelectric sections drawn along the four profiles described in sections 4.4 and 4.5, revealed that the bedrock in the Main Campus of A.B.U. Zaria is undulating. For the interpreted two-electrode array data, the depth to the bedrock varies from about 11.5 m around the central part of the Main Campus (i.e. the area around KIL and the Senate Building) to about 30.0 m around the southern end (i.e around the southern parts of Staff School and Ramat/ICSA Halls). On the other hand, the interpreted Schlunberger data show that the basement depth beneath the Main Campus varies from about 9.0 m to about 28.0 m in the same locations above. Profile C-C′ also shows that the bedrock is shallow (about 13.0 m) in the area around Akenzua Hall which then increases gradually to the Botanical Garden where it attains a value of about 28.0 m. It is observed from the contour maps and geoelectric sections along the profiles that the depth to the basement increases away from the central part of the Main Campus towards the southern, western and eastern parts of the area.

5.1.3 GROUNDWATER POTENTIAL OF THE STUDY AREA

The structural geology of an area has a very important effect on the groundwater potential of the area, more especially in areas of crystalline rocks such as the ones underlying the Kubanni Basin.

Previous workers as Olowu (1967) and Eigbefo (1978) have classified the aquifer components in the Kubanni Basin into three categories as:

(i) Weathered basement and fractures in the basement rocks.

(ii) The laterised (Older laterite) deposits which contain limited quantity of water and

(iii) The alluvial deposits.

The aquifer thickness below each VES station was determined by substracting the thickness of the first layer (topsoil) from the total depth to the basement at that VES point. These values were then used to plot contour maps for the aquifer thickness as Figs.5.1 (a) and (b), for the two-electrode method and Schlumberger configuration respectively. Both maps show a close resemblance between them and the basement maps (Figs 4.7(a) and (b)). The areas of maximum aquifer thickness shown by the maps are:

(i) The southern end of the Main Campus,

(ii) The area just to the west and southwest of Danfodio Hall and

(iii) The area around the stream dividing Area A (part I) to Area A (part II) staff quarters.

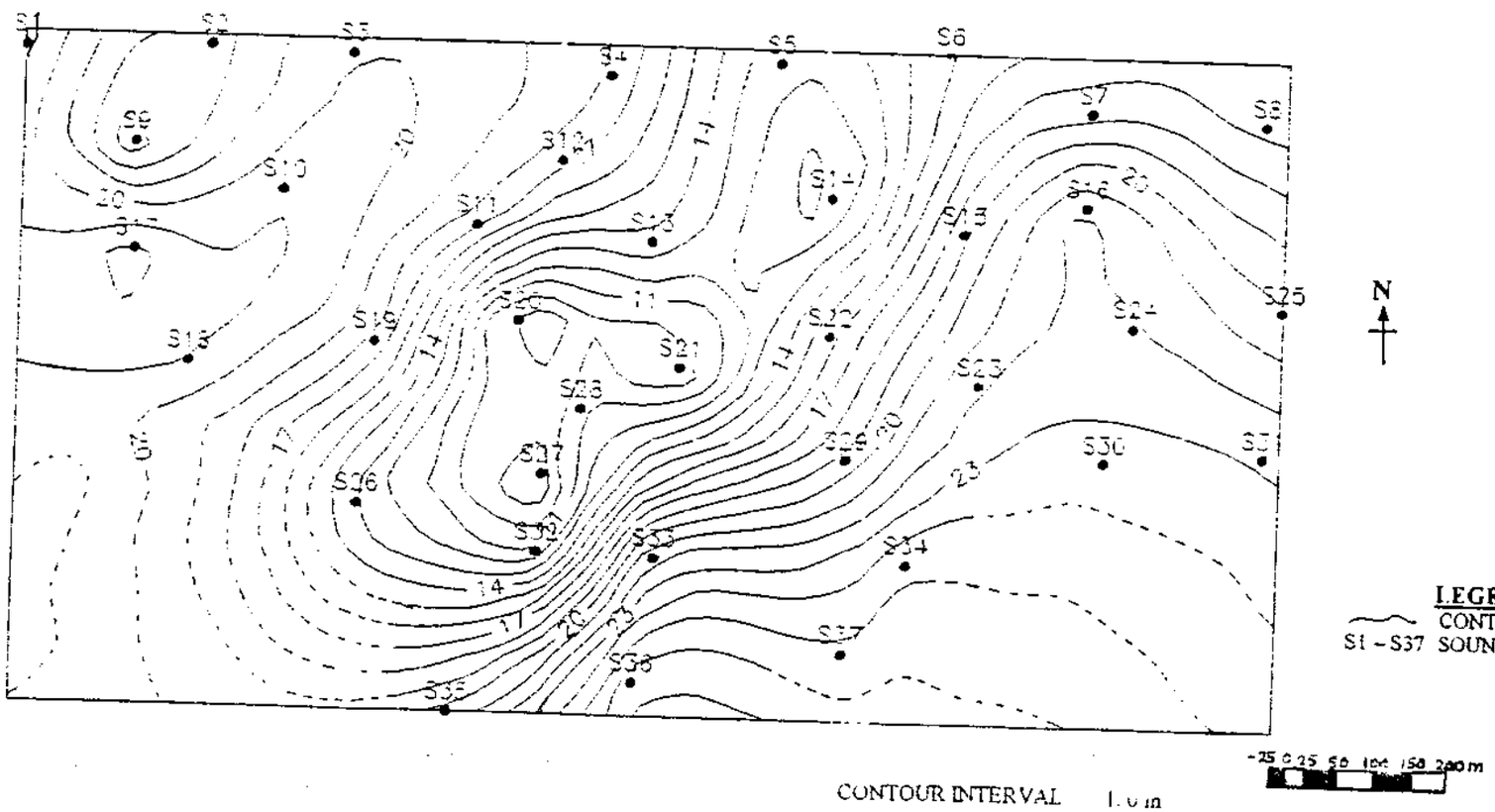


Fig. 5.1 (a) Contour Map of the Aquifer Thickness of the Project Area from Interpreted Two – Electrode Data.

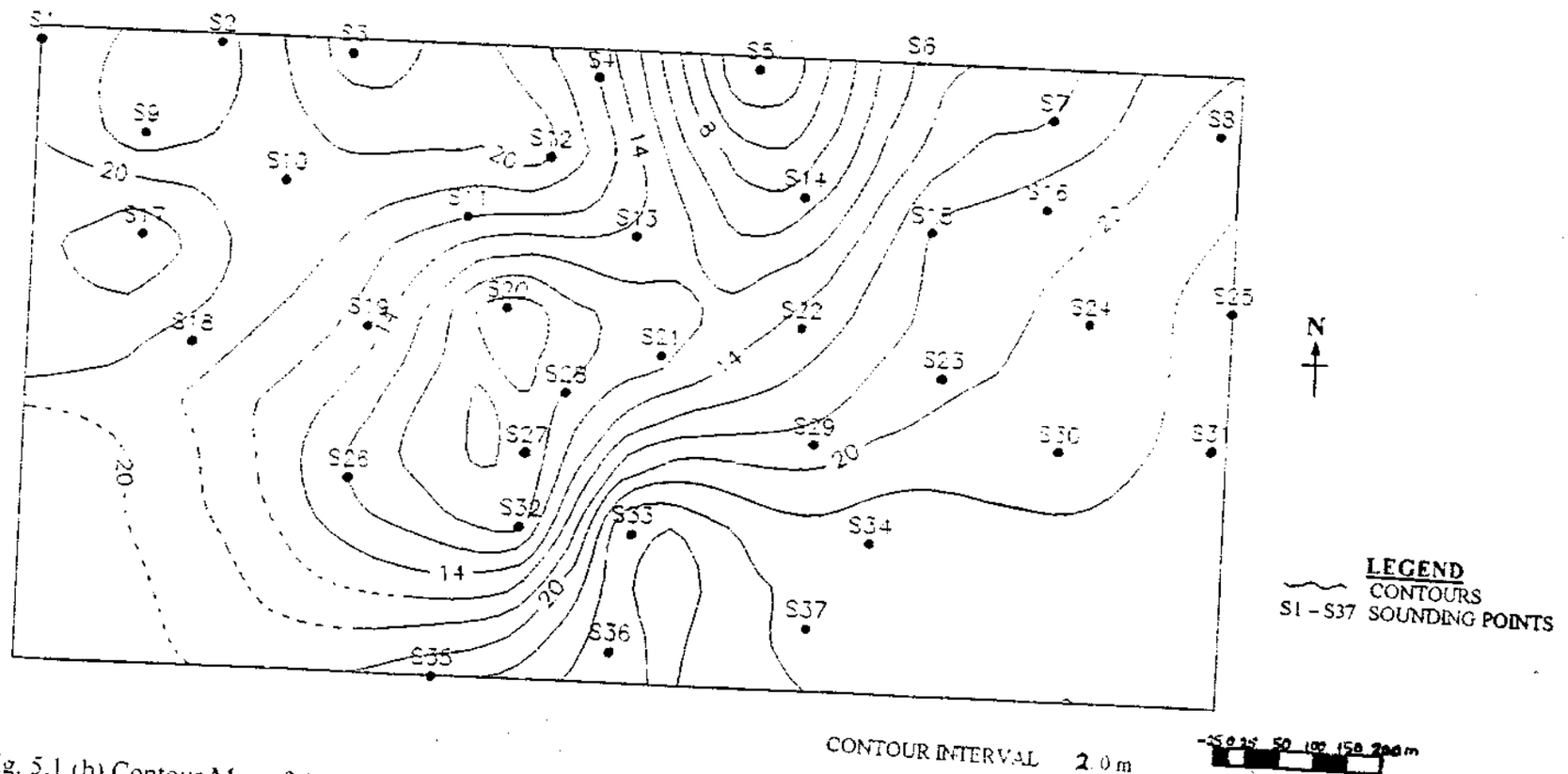


Fig. 5.1 (b) Contour Map of the Aquifer Thickness of the Project Area from Interpreted Schlumberger Data.

5.2 SUGGESTIONS FOR FUTURE RESEARCH

No geophysical method of investigation can give a complete and unique information of an area alone. The two-electrode array and the Schlumberger configurations used in this work cannot be exceptions. To shed more light on and to confirm the deductions made in this work, other geophysical methods of investigation such as the seismic and magnetic methods could be employed for further studies.

The seismic method could be used to delineate more accurately the layeringss and their thicknesses of the various layers in the Main Campus of A.B.U. Zaria. The magnetic method could also be used to delineate the different structures and give approximate depth to magnetic bodies (Spector and Grant, 1970).

More research should be carried out in other areas of the Kubanni Basin by using the two-electrode method and correlate the results obtained with borehole information to confirm the effectiveness and reliability of the two-electrode method.

Also, more research should be carried out for the determination of the resistivity values of the underlying layers just as the new approach employed in this work to come out with a standard and acceptable method.

5.3 CONCLUSIONS

An attempt was made in this work to determine the reliability and effectiveness of the two-electrode method, the geometry of the basement beneath the Main Campus and the groundwater potential of the project area. At the end of it all, the following conclusions were arrived at:

(i) Results of the VES data interpretation for the two-electrode array and the Schlumberger array as discussed and given in Chapter IV have compared very well. The depth-to-basement values obtained from the two sets of interpreted

results have agreed to about 86 %. The agreement for the layer thickness values between the two sets of interpreted results is about 72 % while that for the resistivity values is about 52 %. However, the agreement is better, about 82 %, for the surface layer resistivity values. The procedure for determining the resistivity value of the surface or top layer, depth-to-basement value as well as the layer thickness values and as described in section 4.2.1 using the Ajayi-Makinde method have yielded good results and therefore is a reliable method of interpretation. The procedure adopted in this work based on the method of dimensions to determine the resistivity values of the underlying layers has also yielded results that are reliable, though needs improvement.

(ii) The geometry of the basement beneath the Main Campus of A.B.U. Zaria is undulating with depth values increasing away from the central part of the area towards the southern, western and eastern parts of the study area as depicted in the contour maps of Figs.4.7(a) and (b) and the 3-D cross-sectional view diagrams of Figs.4.8(a) and (b). The undulating nature of the geometry of the basement is also evident along the four profiles shown in Figs.4.3 - 4.6. The depth-to-basement arround Akenzua Hall is also shallow to about 15 m which increases gradually down to the Botanical Garden to about 30 m.

(iii) The aquifer thickness in the Main Campus is variable as shown in Figs.5.1(a) and (b) for the two-electrode array and Schlumberger array respectively. Both maps show a close resemblance between them and the depth-to-basement maps given as Figs.4.7(a) and (b). Areas of maximum aquifer thickness as shown in Figs.5.1(a) and (b) include: the southern end of the Main Campus, the area just to the west and southwest of Danfodio Hall and the area arround the stream dividing Area A (part I) and Area A (part II).

Based on the deductions from the VES data interpretations, a lot has been achieved in this work. The basement geometry as well as the groundwater potential of the Main Campus of A.B.U. Zaria have been deduced. This work has proved that the two-electrode method as used by Makinde (1996) and Ajayi and Makinde (2000) is reliable and effective and can be for use as a geoelectric prospecting method.

REFERENCES

Ajayi, C.O. and Makinde, V. (2000). The "Ajayi - Makinde" Two-Electrode D.C. Resistivity Array. A Brief Brochure to the Patent Office, Abuja.

Akpoborie, I.A. (1972). Hydrogeological Control of Structures along Samaru Creek. Unpublished B.Sc. Thesis. Ahmadu Bello University, Zaria.

Apparao, A. and Roy, A. (1973). Field Results for Direct Current Resistivity Profiling with Two-Electrode Array. Geoexploration, 11(1): 21-44.

Bajeh, I. (1992). Ground Magnetic Investigation of the Kubanni River Basin, Zaria. Unpublished M.Sc. Thesis. Ahmadu Bello University, Zaria.

Brizolari, E. and Bernabini, M. (1979). Comparison Between Schlumberger Electrode Arrangements and Some Focused Electrode Arrangements in Resistivity Profiles. Geophysical Prospecting, 27(1): 233-244.

Eigbefo, C. (1978). Hydrogeology of the Kubanni Drainage Basin, Zaria. Unpublished M.Sc. Thesis. Ahmadu Bello University, Zaria.

Gupta, R.N. and Bhattacharya, P.K. (1963). Unipole Method of Electrical Profiling. Geophysics, 28(4): 608-616.

Hassan, M. (1987). Geoelectrical Investigations of the Western Half of the Kubanni River Basin, Zaria. Unpublished M.Sc. Thesis. Ahmadu Bello University, Zaria.

Hore, P.N. (1970). Weather and Climate, Zaria and Its Region. Ed. by M.J. Mortimore Department of Geography. Occassional Paper No.4. A.B.U. Zaria pp.41-54.

Jain, S.C. and Roy, A. (1973). Comparison of Electrode Arrays in Time Domain Induced Polarization. Geophysical Prospecting, 21(4): 626-634.

Jones, O. And Du Preez, J.W. (1952). Geophysical Survey of the Regional Technical College Site, Zaria. GSN Report No.1019.

Katsube, T.J. and Collett, L.S. (1973). Measuring Techniques for Rocks with High Permitivity and High Loss. Geophysics, 38(1): 92-105.

Keller, G.V. and Frischknecht, F.C. (1966). Electrical methods in Geophysical Prospecting. Pergamon Press. New York.

Klikenbera, K. (1970). Soils of Zaria Area. Ed. By M.J. Mortimore. Department of Geography Occassional Paper No. 4. Ahmadu Bello University, Zaria.

Kumar, R. (1974). Direct Interpretation of Two-Electrode Resistivity Soundings. Geophysical Prospecting, 22(2): 224-237.

Kunetz, G. (1966). Principle of D.C. Resistivity Prospecting Geoexploration Monographs. Series No. 1. Gebrudeo Borntraeger, Berlin.

Makinde, V. (1996). A Field Investigation of a Variant of the Two-Electrode D.C. Resistivity Array Within the Kubanni Basin. Unpublished, Ph.D. Thesis. Ahmadu Bello University, Zaria.

McCurry, P. (1970). Geology of Degree Sheet 21, Zaria. Unpublished M.Sc Thesis. Ahmadu Bello University, Zaria.

Mooney, S.A.G. (1980). Handbook of Engineering Geophysics, Vol.2: Electrical Resistivity. Bison Instruments Inc. Minnesota.

Olufemi, R.O. (1985). Hydrogeology of Jama'a Kubanni Area (Zaria Sheet 102 S.W.). Unpublished B.Sc. Thesis A.B.U., Zaria.

Olugbemiro, R.O. (1985). Hydrogeology of Jama'a Kubanni Area (Zaria Sheet 102 S.W.). Unpublished B.Sc. Thesis. Ahmadu Bello University, Zaria.

Olowu, J. (1967). Preliminary Investigations of the Groundwater Conditions in Zaria Sheet 102 S.W. GSN Report No.1462.

Ososami, I.A. (1968). Assessment of the Groundwater in the Kubanni Valley. Unpublished M.Sc. Thesis. Ahmadu Bello University, Zaria.

Oyawoye, M.O. (1964). Geology of the Nigerian Basement Complex, Journal of Nigerian Mining, Geological and Metallurgical Society Vol. pg.87-102.

Shemang, E.M. (1990). Electrical Depth Soundings at Selected Well-Sites Within the Kubanni River Basin, Zaria. Unpublished M.Sc. Thesis. Ahmadu Bello University, Zaria.

Spector, A. and Grant, F.S. (1970). Statistical Models for Interpreting Magnetic Data. Geophysics, Vol.35, No.2 (April 1970) pg.293-302.

Telford, W.M., Geldart, L.P., Sheriff, R.E. and Keys, D.A. (1976). Applied Geophysics. Cambridge University Press, Cambridge.

Thorp, M.B. (1970). Land Focus and Landscape Evolution of Zaria and Its Region. Ed. by M.J. Mortimore, Department of Geography Occassional Paper No.4, A.B.U., Zaria.

Tokarski, A. (1972). Heterogeneous Terrace Arrangement West of A.B.U. Zaria Occassional Paper No.2 Department of Geology, A.B.U., Zaria.

Truswell, J.F. and Cope, R.N. (1963). The Geology of Parts of Niger and Zaria Provinces, Northern Nigeria. GSN Bulletin 29.

Van Nostrand, R.G. and Cook, K.L. (1966). Interpretation of Resistivity Data. United States Geology Survey Professional Paper 499. U.S Government Printing Office, Washington, D.C.

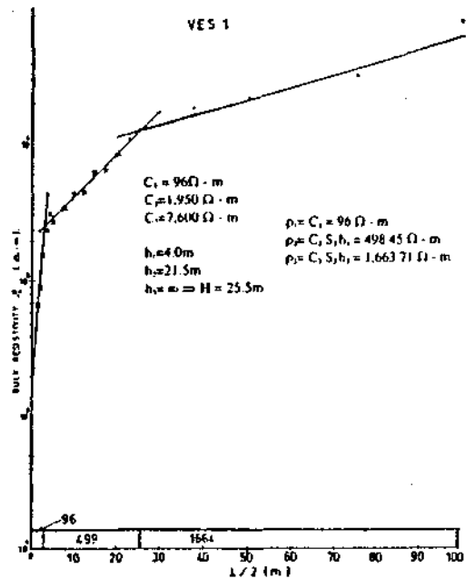
Vingoe, P. (1972). Introduction to Electrical Resistivity Survey. Abem Printed Matter No.900.

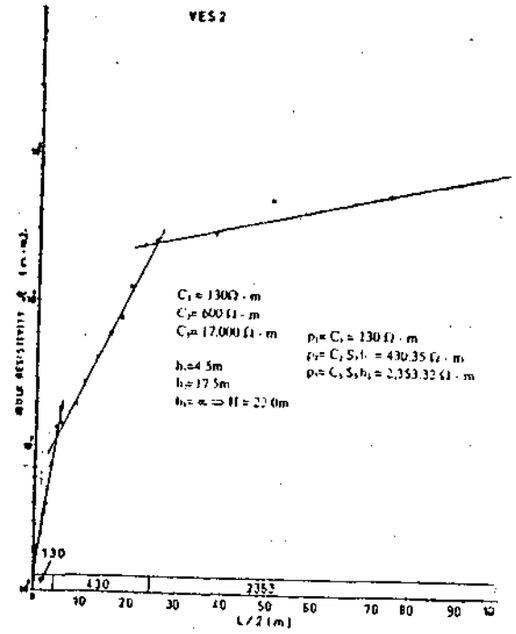
Wright, J.B. and McCurry, P. (1970). The Geology of the Zaria Sheet 102 S.W. and Its Region. In: Mortimore, M.J. (Ed.). Department of Geography Occassional Paper No.4. Ahmadu Bello University, Zaria.

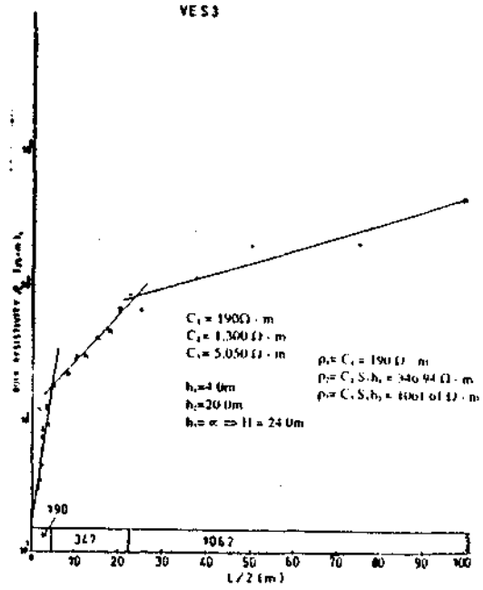
Zohdy, A.A.R. (1969). A New Method for Differential Resistivity Sounding. Geophysics 34(6): 924-943.

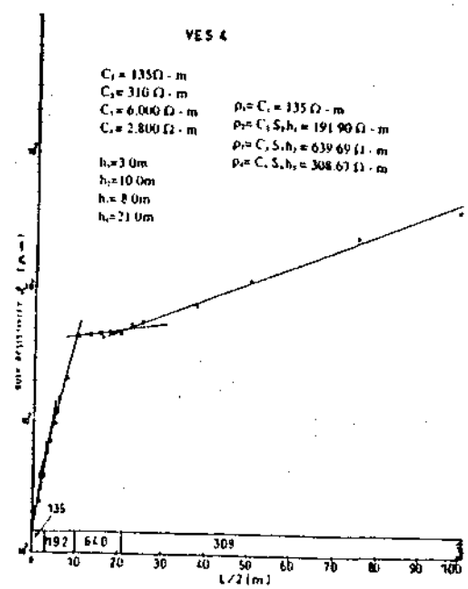
APPENDIX A

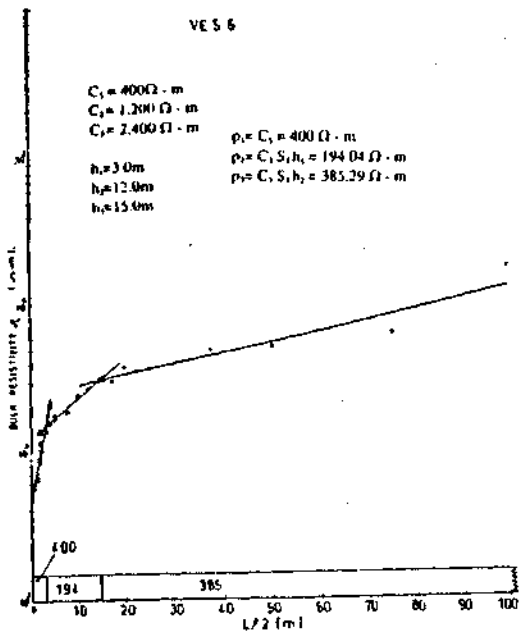
PLOTS OF BULK RESISTIVITY AGAINST L/2 AND INTERPRETATION OF DATA OBTAINED USING TWO-ELECTRODE ARRAY.

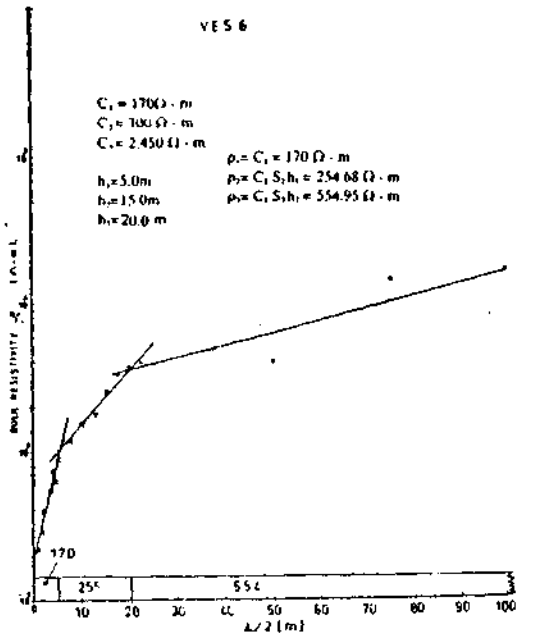


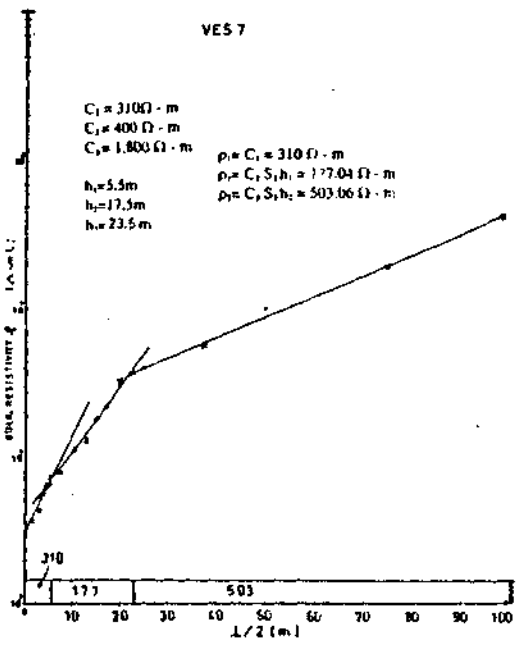


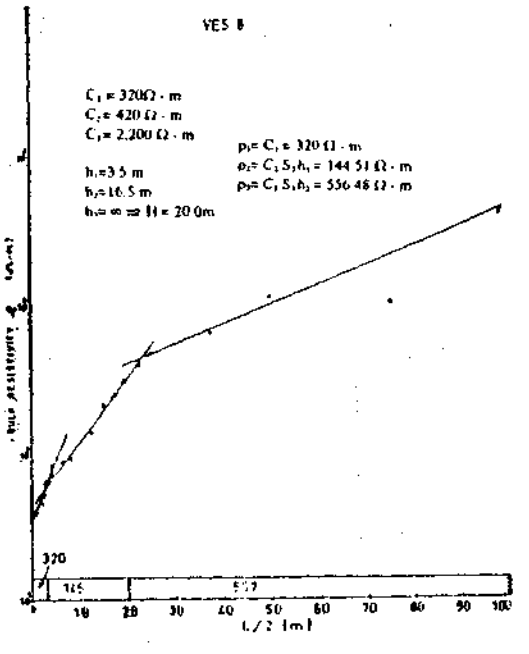


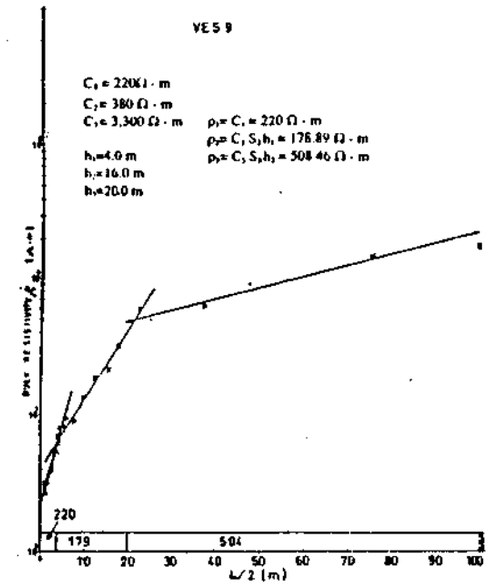


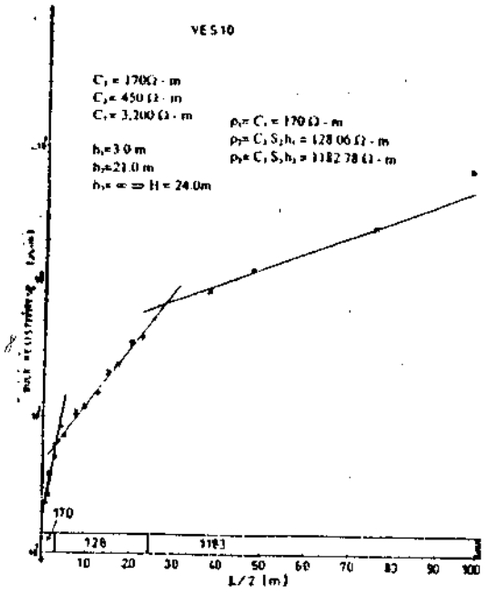

VES 6
C1 = 400Ω - m
C2 = 1,200 Ω - m
C3 = 2,400 Ω - m
h1=3.0m
h2=12.0m
h3=15.0m
ρ1= C1 = 400 Ω - m
ρ2= C1 S1h1 = 194.04 Ω - m
ρ3= C1 S1h2 = 385.29 Ω - m
400
194
385
10 20 30 40 50 60 70 80 90 100
L/2 (m)

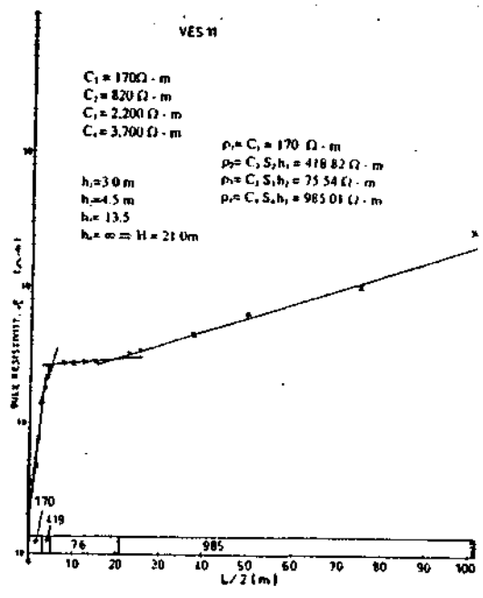

VES 6
C1 = 170Ω - m
C2 = 700 Ω - m
C3 = 2,450 Ω - m
h1=5.0m
h2=15.0m
h3=20.0 m
ρ1= C1 = 170 Ω - m
ρ2= C1 S1h1 = 254.68 Ω - m
ρ3= C1 S1h2 = 554.95 Ω - m
170
554
10 20 30 40 50 60 70 80 90 100
L/2 (m)

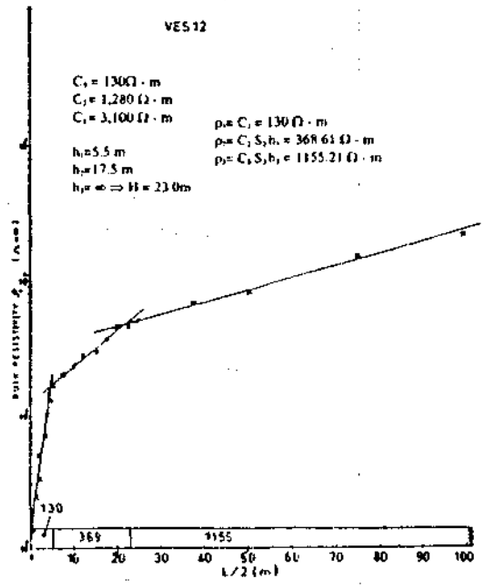

VES 7
C1 = 310Ω - m
C2 = 400 Ω - m
C3 = 1,800 Ω - m
h1=5.5m
h2=17.5m
h3=23.5 m
ρ1= C1 = 310 Ω - m
ρ2= C1 S1h1 = 177.04 Ω - m
ρ3= C1 S1h2 = 503.06 Ω - m
310
177
503
10 20 30 40 50 60 70 80 90 100
L/2 (m)

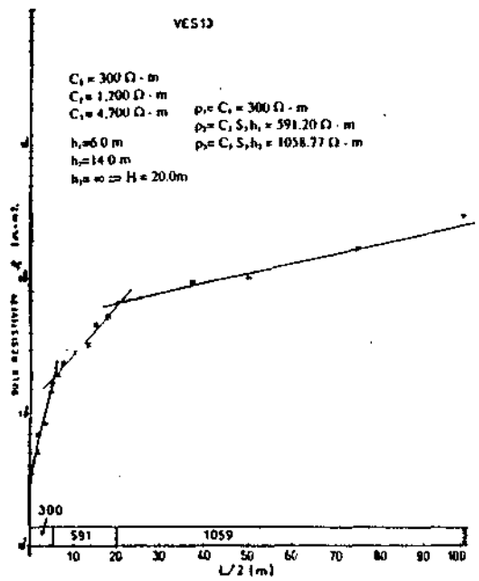

VES 8
C1 = 320Ω - m
C2 = 420 Ω - m
C3 = 2,200 Ω - m
h1=3.5 m
h2=16.5 m
h3= ∞ ≈ H = 20.0m
ρ1= C1 = 320 Ω - m
ρ2= C1 S1h1 = 144.51 Ω - m
ρ3= C1 S1h2 = 556.48 Ω - m
320
10 20 30 40 50 60 70 80 90 100
L/2 (m)

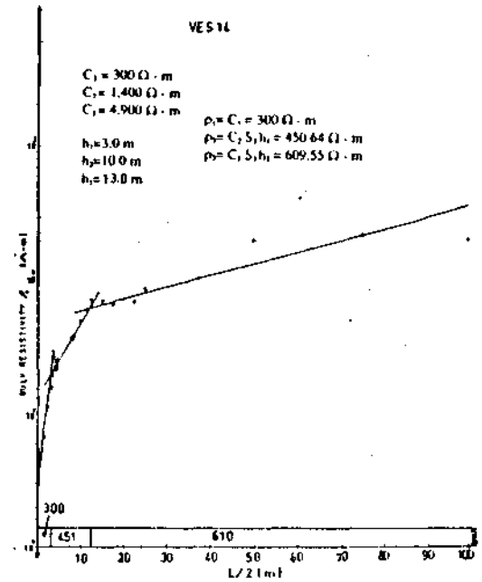

VES 9
C₁ = 220Ω · m
C₂ = 380 Ω · m
C₃ = 3,300 Ω · m
h₁=4.0 m
h₂=16.0 m
h₃=20.0 m
ρ₁= C₁ = 220 Ω · m
ρ₂= C₂ S₂h₂ = 178.89 Ω · m
ρ₃= C₃ S₃h₃ = 508.46 Ω · m
220
179
504
L/2 (m)

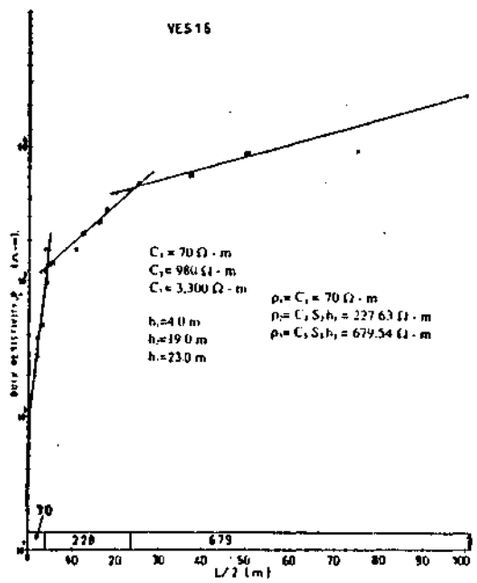

VES 10
C₁ = 170Ω · m
C₂ = 450 Ω · m
C₃ = 3,200 Ω · m
h₁=3.0 m
h₂=21.0 m
h₃= ∞ ⇒ H = 24.0m
ρ₁= C₁ = 170 Ω · m
ρ₂= C₂ S₂h₂ = 128.06 Ω · m
ρ₃= C₃ S₃h₃ = 1382.78 Ω · m
170
128
1383
L/2 (m)

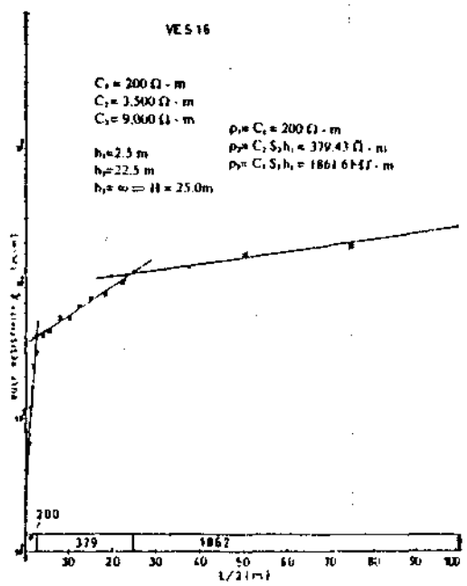

VES 11
C₁ = 170Ω · m
C₂ = 820 Ω · m
C₃ = 2,200 Ω · m
C₄ = 3,700 Ω · m
h₁=3.0 m
h₂=4.5 m
h₃= 13.5
h₄= ∞ ⇒ H = 21.0m
ρ₁= C₁ = 170 Ω · m
ρ₂= C₂ S₂h₂ = 418.82 Ω · m
ρ₃= C₃ S₃h₃ = 75.54 Ω · m
ρ₄= C₄ S₄h₄ = 985.08 Ω · m
170
419
76
985
L/2 (m)

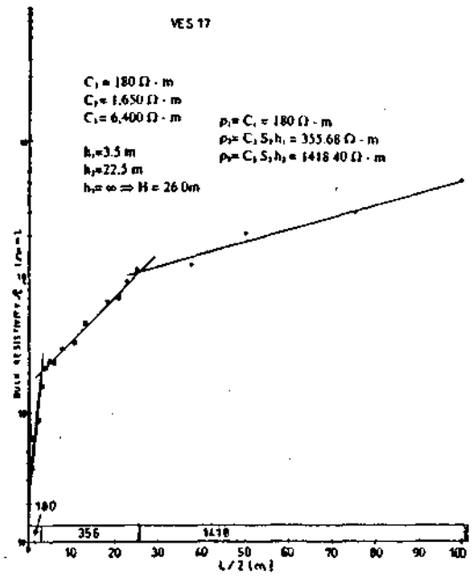

VES 12
C₁ = 130Ω · m
C₂ = 1,280 Ω · m
C₃ = 3,100 Ω · m
h₁=5.5 m
h₂=17.5 m
h₃= ∞ ⇒ H = 23.0m
ρ₁= C₁ = 130 Ω · m
ρ₂= C₂ S₂h₂ = 369.61 Ω · m
ρ₃= C₃ S₃h₃ = 1855.21 Ω · m
130
369
1855
L/2 (m)

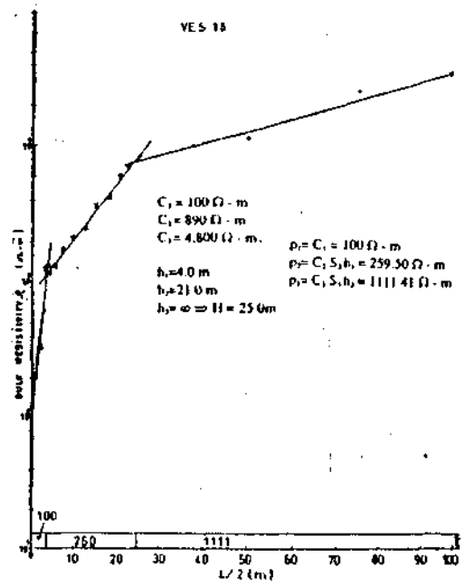

VES 13
C1 = 300 Ω - m
C2 = 1,200 Ω - m
C3 = 4,700 Ω - m
h1=6.0 m
h2=14.0 m
h3 = ∞ ⇒ H = 20.0m
ρ1= C1 = 300 Ω - m
ρ2= C2 S2h2 = 591.20 Ω - m
ρ3= C3 S3h3 = 1058.77 Ω - m
300
591
1059
L/2 (m)

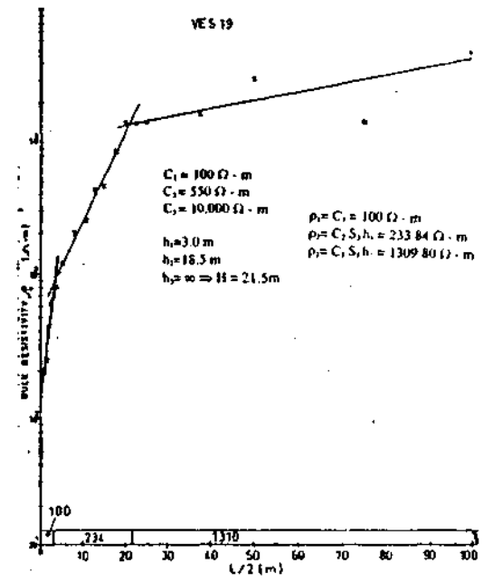

VES 14
C1 = 300 Ω - m
C2 = 1,400 Ω - m
C3 = 4,900 Ω - m
h1=3.0 m
h2=10.0 m
h3=13.0 m
ρ1= C1 = 300 Ω - m
ρ2= C2 S2h2 = 450.64 Ω - m
ρ3= C3 S3h3 = 609.55 Ω - m
300
451
610
L/2 (m)

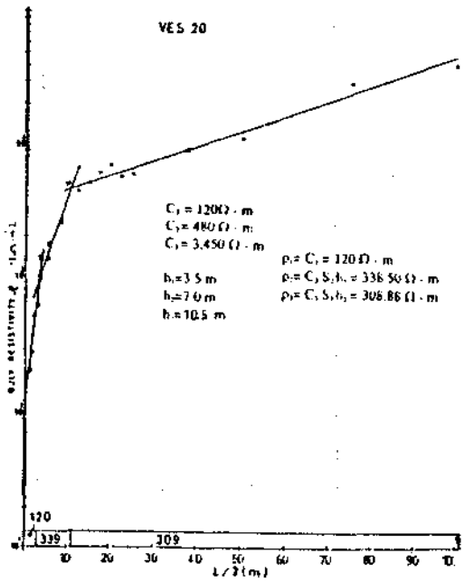

VES 15
C1 = 70 Ω - m
C2 = 980 Ω - m
C3 = 3,300 Ω - m
h1=4.0 m
h2=19.0 m
h3=23.0 m
ρ1= C1 = 70 Ω - m
ρ2= C2 S2h2 = 227.63 Ω - m
ρ3= C3 S3h3 = 679.54 Ω - m
70
228
679
L/2 (m)

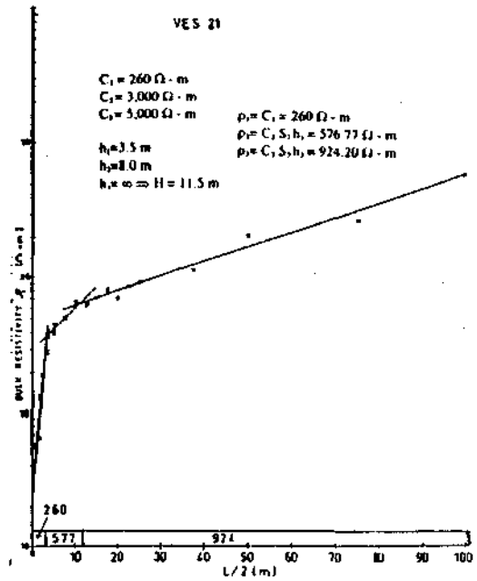

VES 16
C1 = 200 Ω - m
C2 = 3,500 Ω - m
C3 = 9,000 Ω - m
h1=2.5 m
h2=22.5 m
h3 = ∞ ⇒ H = 25.0m
ρ1= C1 = 200 Ω - m
ρ2= C2 S2h2 = 379.43 Ω - m
ρ3= C3 S3h3 = 1861.6[illegible] Ω - m
200
379
1862
L/2 (m)

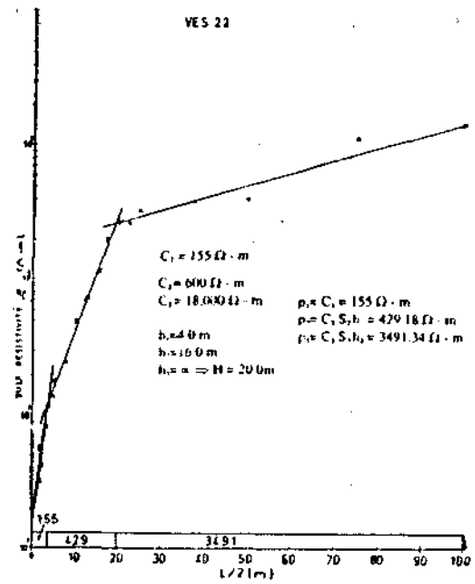

VES 17
C1 = 180 Ω - m
C2 = 1,650 Ω - m
C3 = 6,400 Ω - m
h1=3.5 m
h2=22.5 m
h3= ∞ ⇒ H = 26.0m
ρ1= C1 = 180 Ω - m
ρ2= C2 S2h1 = 355.68 Ω - m
ρ3= C3 S3h2 = 1418.40 Ω - m
180
356
1418
L/2 (m)

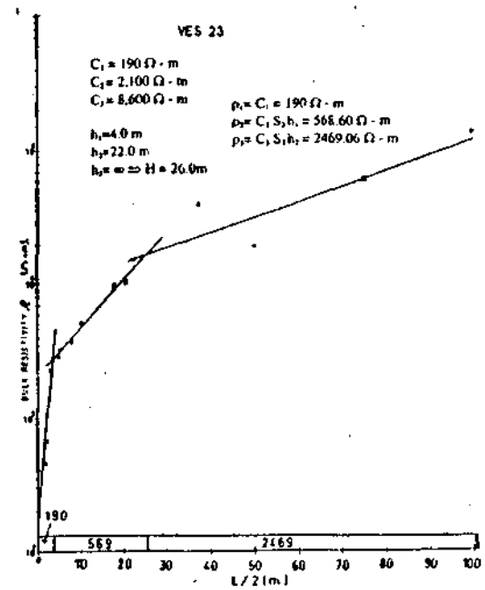

VES 18
C1 = 100 Ω - m
C2 = 890 Ω - m
C3 = 4,800 Ω - m.
h1=4.0 m
h2=21.0 m
h3= ∞ ⇒ H = 25.0m
ρ1= C1 = 100 Ω - m
ρ2= C2 S2h1 = 259.50 Ω - m
ρ3= C3 S3h2 = 1111.41 Ω - m
100
260
1111
L/2 (m)

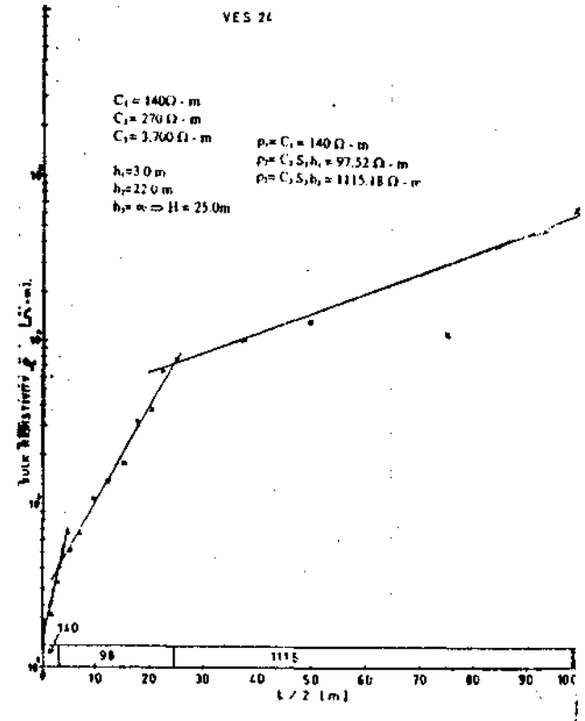

VES 19
C1 = 100 Ω - m
C2 = 550 Ω - m
C3 = 10,000 Ω - m
h1=3.0 m
h2=18.5 m
h3= ∞ ⇒ H = 21.5m
ρ1= C1 = 100 Ω - m
ρ2= C2 S2h1 = 233.84 Ω - m
ρ3= C3 S3h2 = 1309.80 Ω - m
100
234
1310
L/2 (m)

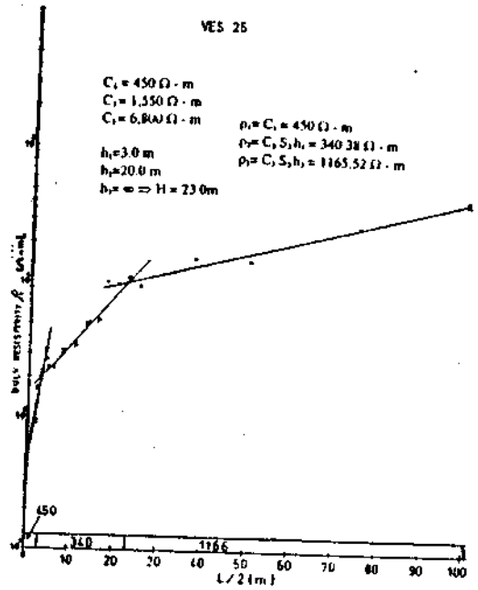

VES 20
C1 = 120Ω - m
C2 = 480 Ω - m
C3 = 3,450 Ω - m
h1=3.5 m
h2=7.0 m
h3=10.5 m
ρ1= C1 = 120 Ω - m
ρ2= C2 S2h1 = 336.50 Ω - m
ρ3= C3 S3h2 = 306.86 Ω - m
120
339
309
L/2 (m)

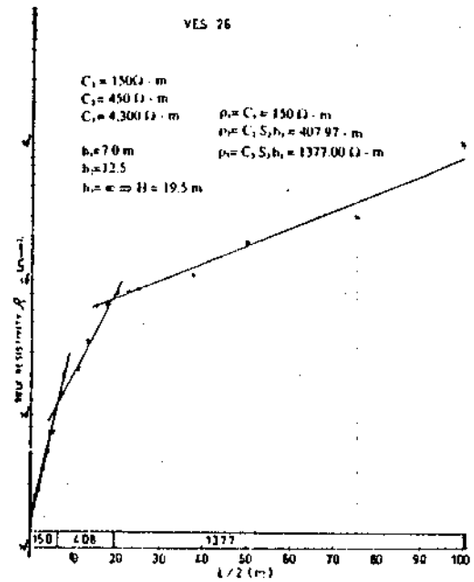

VES 21
C_1 = 260 Ω - m
C_2 = 3,000 Ω - m
C_3 = 5,000 Ω - m
h_1=3.5 m
h_2=8.0 m
h_3= ∞ ⇒ H = 11.5 m
$\rho_1 = C_1$ = 260 Ω - m
$\rho_2 = C_2 S_1 h_1$ = 576.77 Ω - m
$\rho_3 = C_3 S_2 h_2$ = 924.20 Ω - m
260
577
924
L/2 (m)

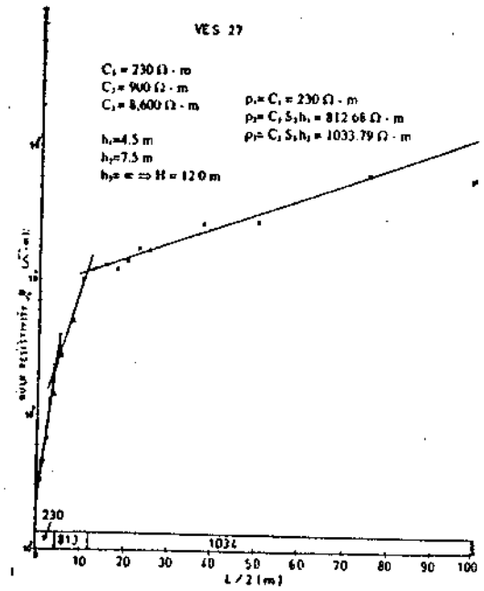

VES 22
C_1 = 155 Ω - m
C_2 = 600 Ω - m
C_3 = 18,000 Ω - m
h_1=4.0 m
h_2=16.0 m
h_3= ∞ ⇒ H = 20.0m
$\rho_1 = C_1$ = 155 Ω - m
$\rho_2 = C_2 S_1 h_1$ = 429.18 Ω - m
$\rho_3 = C_3 S_2 h_2$ = 3491.34 Ω - m
155
429
3491
L/2 (m)

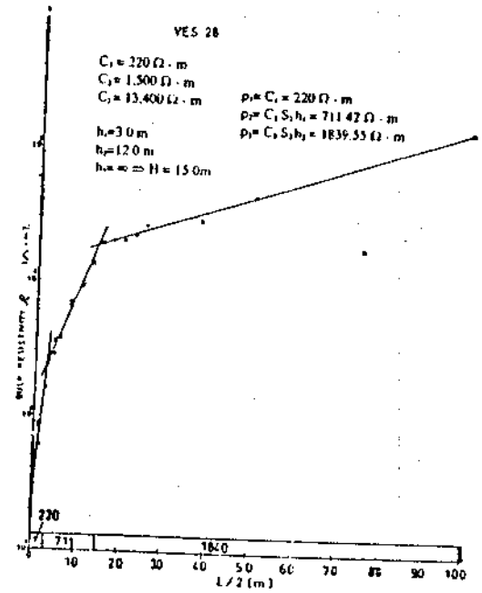

VES 23
C_1 = 190 Ω - m
C_2 = 2,100 Ω - m
C_3 = 8,600 Ω - m
h_1=4.0 m
h_2=22.0 m
h_3= ∞ ⇒ H = 26.0m
$\rho_1 = C_1$ = 190 Ω - m
$\rho_2 = C_2 S_1 h_1$ = 568.60 Ω - m
$\rho_3 = C_3 S_2 h_2$ = 2469.06 Ω - m
190
569
2469
L/2 (m)

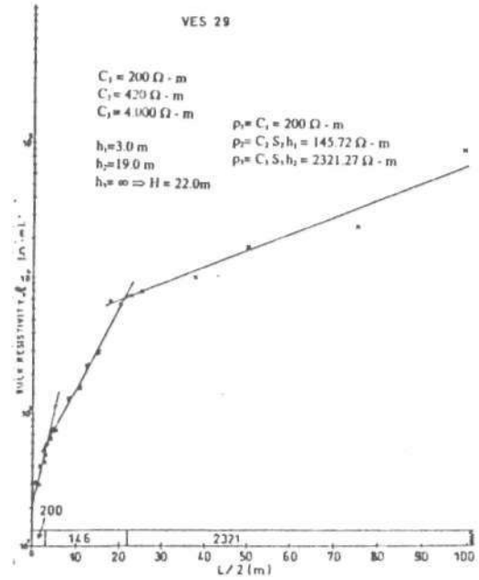

VES 24
C_1 = 140Ω - m
C_2 = 270 Ω - m
C_3 = 3,700 Ω - m
h_1=3.0 m
h_2=22.0 m
h_3= ∞ ⇒ H = 25.0m
$\rho_1 = C_1$ = 140 Ω - m
$\rho_2 = C_2 S_1 h_1$ = 97.52 Ω - m
$\rho_3 = C_3 S_2 h_2$ = 1115.48 Ω - m
140
98
1115
L / 2 (m)

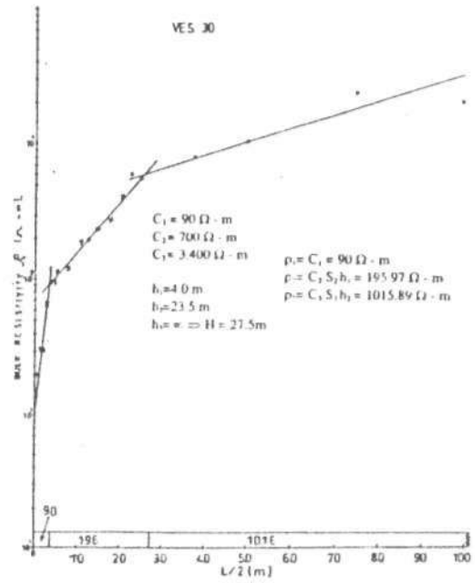

VES 25
C_1 = 450 Ω · m
C_2 = 1,350 Ω · m
C_3 = 6,800 Ω · m
h_1=3.0 m
h_2=20.0 m
h_3= ∞ ⇒ H = 23.0m
$\rho_1 = C_1$ = 450 Ω · m
$\rho_2 = C_2 S_2 h_2$ = 340.38 Ω · m
$\rho_3 = C_3 S_3 h_3$ = 1165.52 Ω · m
450
340
1166
L / 2 (m)

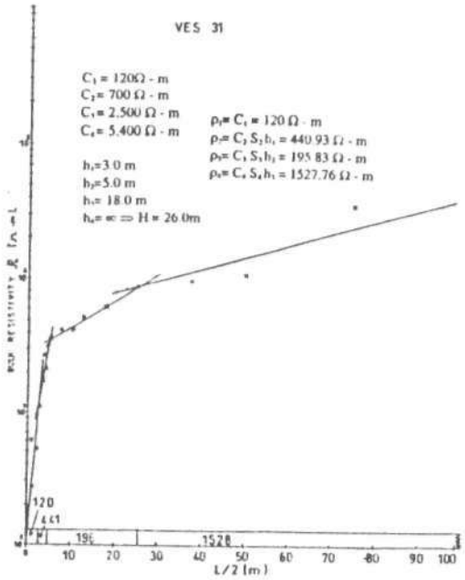

VES 26
C_1 = 150Ω · m
C_2 = 450 Ω · m
C_3 = 4,300 Ω · m
h_1=7.0 m
h_2=12.5
h_3 = ∞ ⇒ H = 19.5 m
$\rho_1 = C_1$ = 150 Ω · m
$\rho_2 = C_2 S_2 h_2$ = 407.97 · m
$\rho_3 = C_3 S_3 h_3$ = 1377.00 Ω · m
150
408
1377
L / 2 (m)

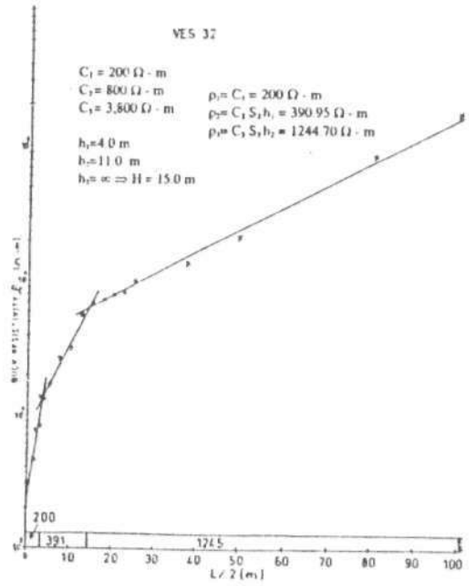

VES 27
C_1 = 230 Ω · m
C_2 = 900 Ω · m
C_3 = 8,600 Ω · m
h_1=4.5 m
h_2=7.5 m
h_3= ∞ ⇒ H = 12.0 m
$\rho_1 = C_1$ = 230 Ω · m
$\rho_2 = C_2 S_2 h_2$ = 812.68 Ω · m
$\rho_3 = C_3 S_3 h_3$ = 1033.79 Ω · m
230
813
1034
L / 2 (m)

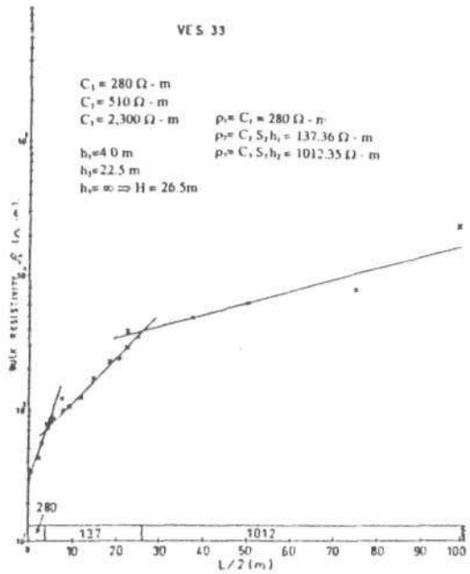

VES 28
C_1 = 220 Ω · m
C_2 = 1,500 Ω · m
C_3 = 13,400 Ω · m
h_1=3.0 m
h_2=12.0 m
h_3 = ∞ ⇒ H = 15.0m
$\rho_1 = C_1$ = 220 Ω · m
$\rho_2 = C_2 S_2 h_2$ = 711.42 Ω · m
$\rho_3 = C_3 S_3 h_3$ = 1839.55 Ω · m
220
711
1840
L / 2 (m)

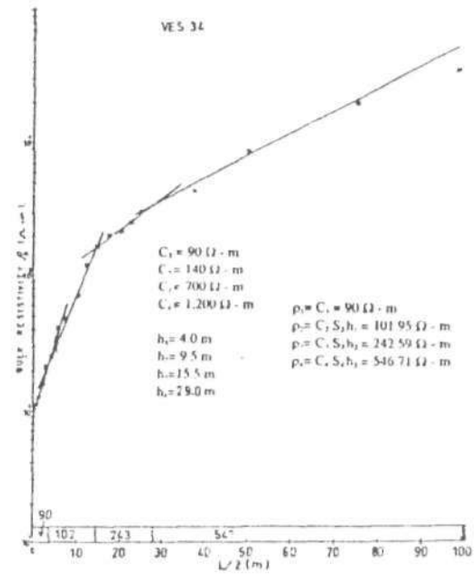

VES 29
C_1 = 200 Ω - m
C_2 = 420 Ω - m
C_3 = 4,000 Ω - m
h_1=3.0 m
h_2=19.0 m
h_3= ∞ ⇒ H = 22.0m
ρ_1= C_1 = 200 Ω - m
ρ_2= $C_2 S_2 h_2$ = 145.72 Ω - m
ρ_3= $C_3 S_3 h_3$ = 2321.27 Ω - m
200
346
2321
L/2 (m)

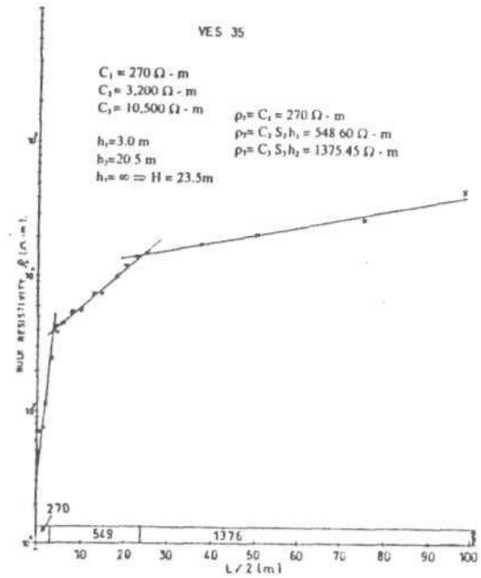

VES 30
C_1 = 90 Ω - m
C_2 = 700 Ω - m
C_3 = 3,400 Ω - m
h_1=4.0 m
h_2=23.5 m
h_3= ∞ ⇒ H = 27.5m
ρ_1= C_1 = 90 Ω - m
ρ_2= $C_2 S_2 h_2$ = 195.97 Ω - m
ρ_3= $C_3 S_3 h_3$ = 1015.89 Ω - m
90
198
1018
L/2 (m)

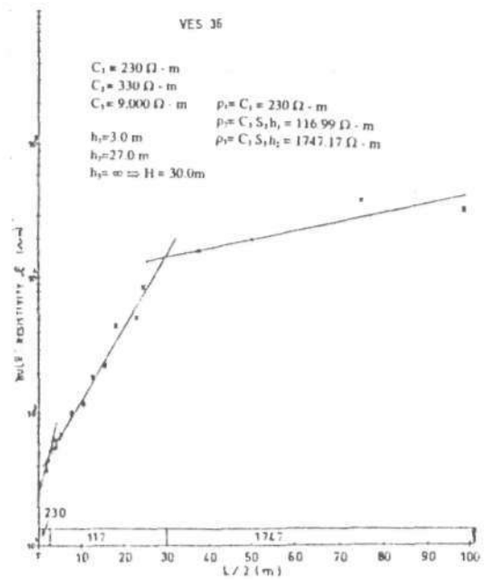

VES 31
C_1 = 120Ω - m
C_2= 700 Ω - m
C_3= 2,500 Ω - m
C_4= 5,400 Ω - m
h_1=3.0 m
h_2=5.0 m
h_3= 18.0 m
h_4= ∞ ⇒ H = 26.0m
ρ_1= C_1 = 120 Ω - m
ρ_2= $C_2 S_2 h_2$ = 440.93 Ω - m
ρ_3= $C_3 S_3 h_3$ = 195.83 Ω - m
ρ_4= $C_4 S_4 h_4$ = 1527.76 Ω - m
120
441
196
1528
L/2 (m)

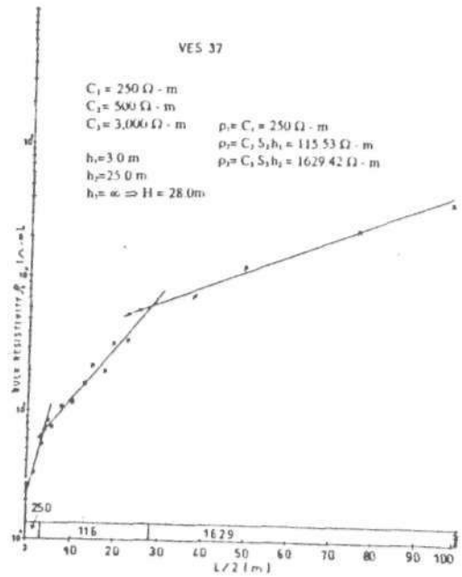

VES 32
C_1 = 200 Ω - m
C_2= 800 Ω - m
C_3= 3,800 Ω - m
h_1=4.0 m
h_2=11.0 m
h_3= ∞ ⇒ H = 15.0 m
ρ_1= C_1 = 200 Ω - m
ρ_2= $C_2 S_2 h_2$ = 390.95 Ω - m
ρ_3= $C_3 S_3 h_3$ = 1244.70 Ω - m
200
391
1245
L/2 (m)


VES 33
C1 = 280 Ω - m
C2 = 510 Ω - m
C3 = 2,300 Ω - m
h1=4.0 m
h2=22.5 m
h3= ∞ ⇒ H = 26.5m
ρ1= C1 = 280 Ω - m
ρ2= C2 S2h1 = 137.36 Ω - m
ρ3= C3 S3h2 = 1012.35 Ω - m
280
137
1012
L / 2 (m)


VES 34
C1 = 90 Ω - m
C2 = 140 Ω - m
C3 = 700 Ω - m
C4 = 1,200 Ω - m
h1= 4.0 m
h2= 9.5 m
h3=15.5 m
h4=29.0 m
ρ1= C1 = 90 Ω - m
ρ2= C2 S2h1 = 101.95 Ω - m
ρ3= C3 S3h2 = 242.59 Ω - m
ρ4= C4 S4h3 = 546.71 Ω - m
90
102
243
L / 2 (m)

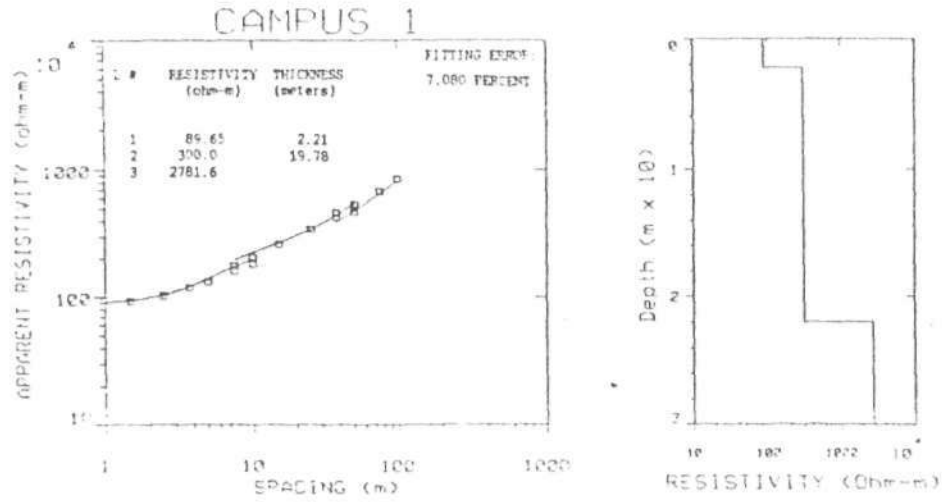

VES 35
C1 = 270 Ω - m
C2 = 3,200 Ω - m
C3 = 10,500 Ω - m
h1=3.0 m
h2=20.5 m
h3= ∞ ⇒ H = 23.5m
ρ1= C1 = 270 Ω - m
ρ2= C2 S2h1 = 548.60 Ω - m
ρ3= C3 S3h2 = 1375.45 Ω - m
270
549
1376
L / 2 (m)

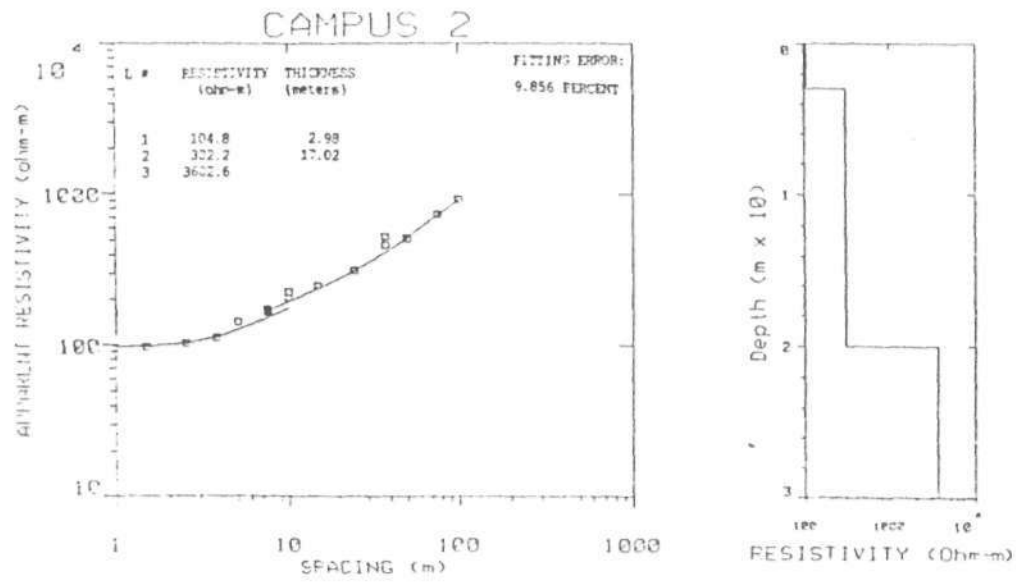

VES 36
C1 = 230 Ω - m
C2 = 330 Ω - m
C3 = 9,000 Ω - m
h1=3.0 m
h2=27.0 m
h3= ∞ ⇒ H = 30.0m
ρ1= C1 = 230 Ω - m
ρ2= C2 S2h1 = 116.99 Ω - m
ρ3= C3 S3h2 = 1747.17 Ω - m
230
117
1747
L / 2 (m)

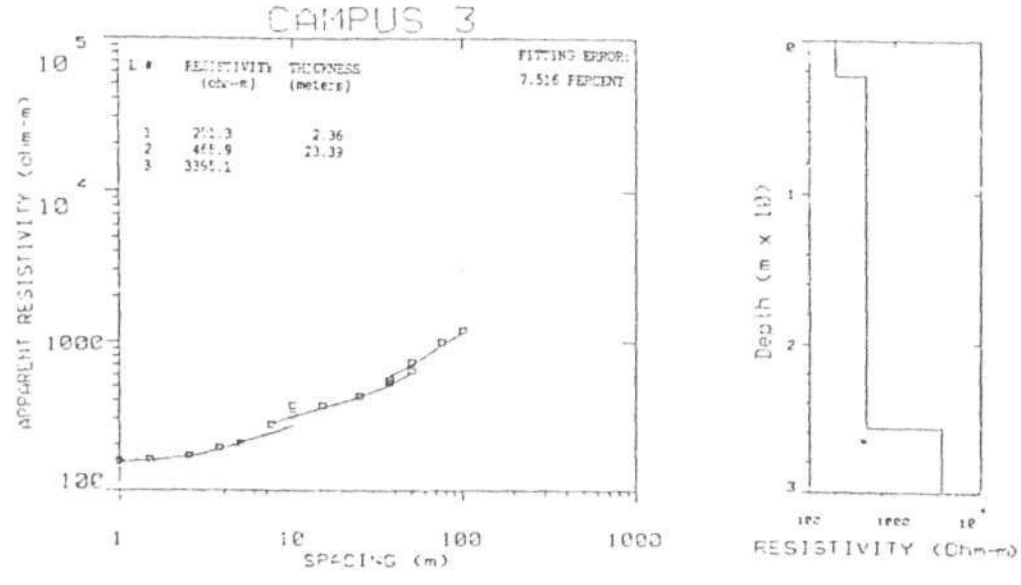

VES 37
C1 = 250 Ω - m
C2 = 500 Ω - m
C3 = 3,000 Ω - m
h1=3.0 m
h2=25.0 m
h3= ∞ ⇒ H = 28.0m
ρ1= C1 = 250 Ω - m
ρ2= C2 S2h1 = 115.53 Ω - m
ρ3= C3 S3h2 = 1629.42 Ω - m
250
116
1629
L / 2 (m)

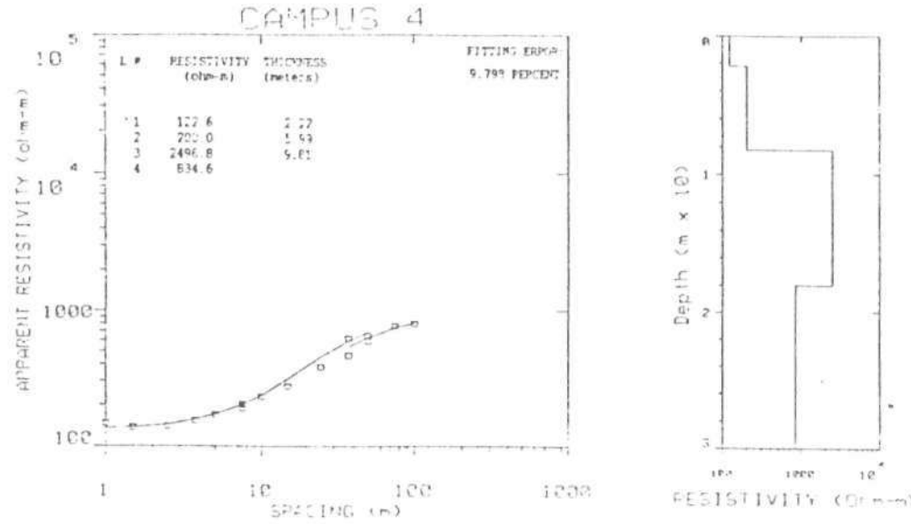
APPENDIX B

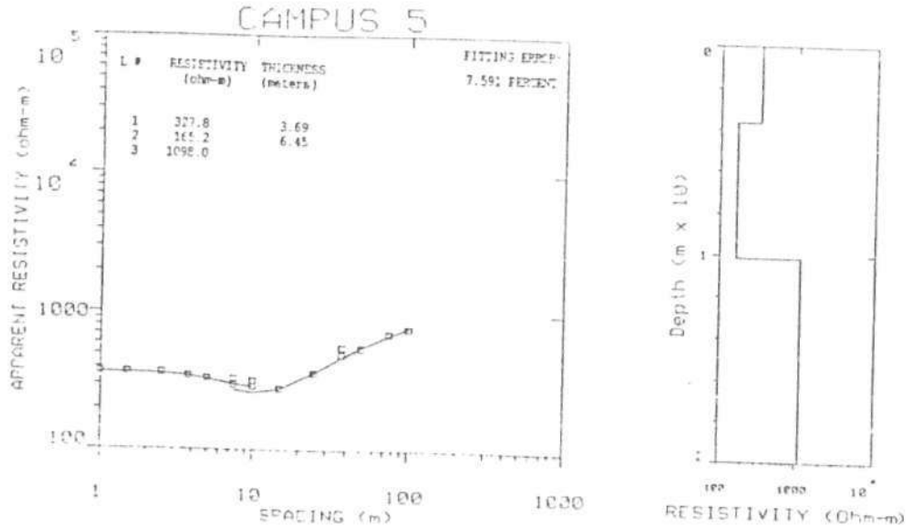
INTERPRETATION OF SCHLUMBERGER DATA.

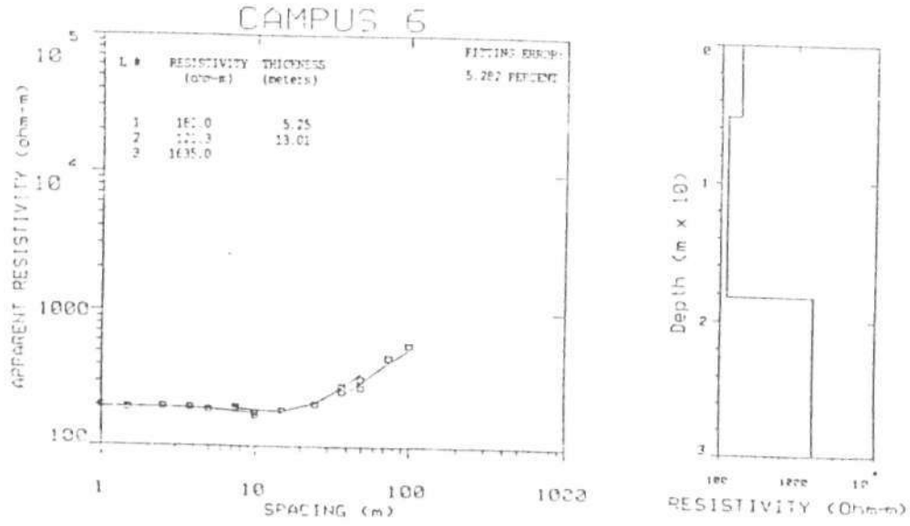


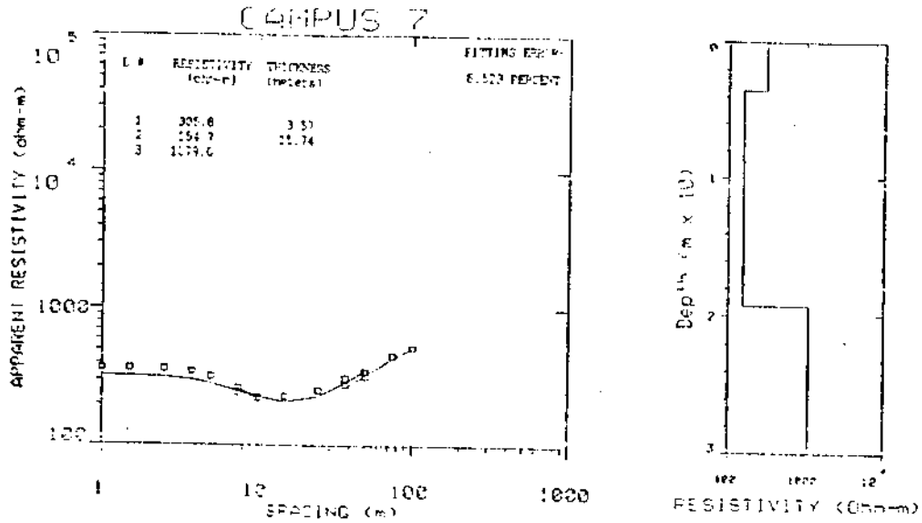


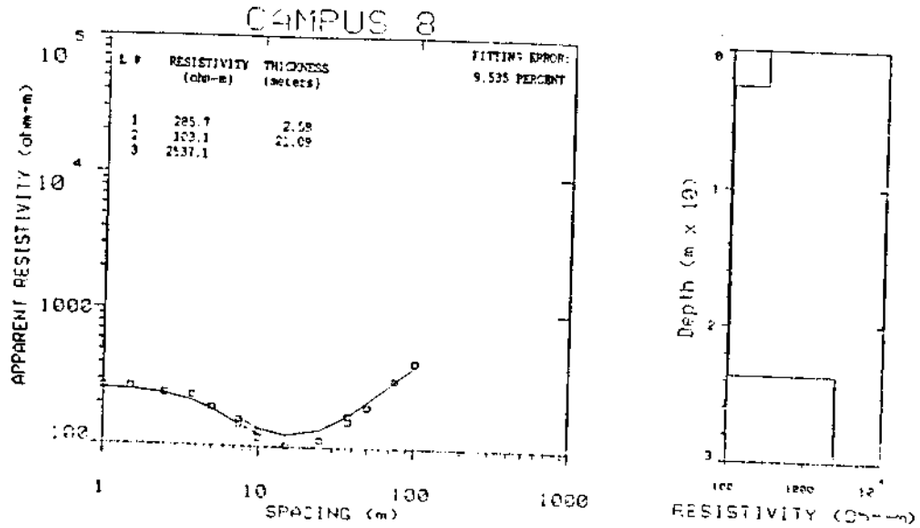


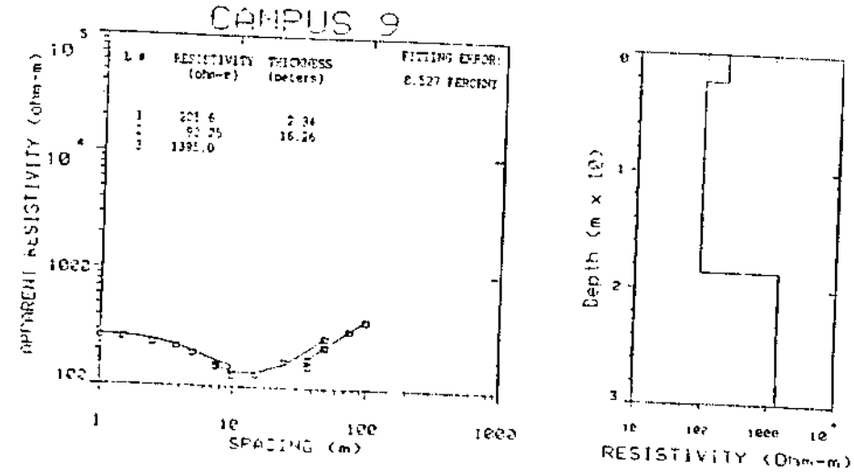

CAMPUS 4
L #
RESISTIVITY (ohm-m)
THICKNESS (meters)
FITTING ERROR:
9.799 PERCENT
1 122.6
2 709.0
3 2496.8
4 834.6
1.27
5.93
9.81
APPARENT RESISTIVITY (ohm-m)
SPACING (m)
Depth (m x 10)
RESISTIVITY (Ohm-m)

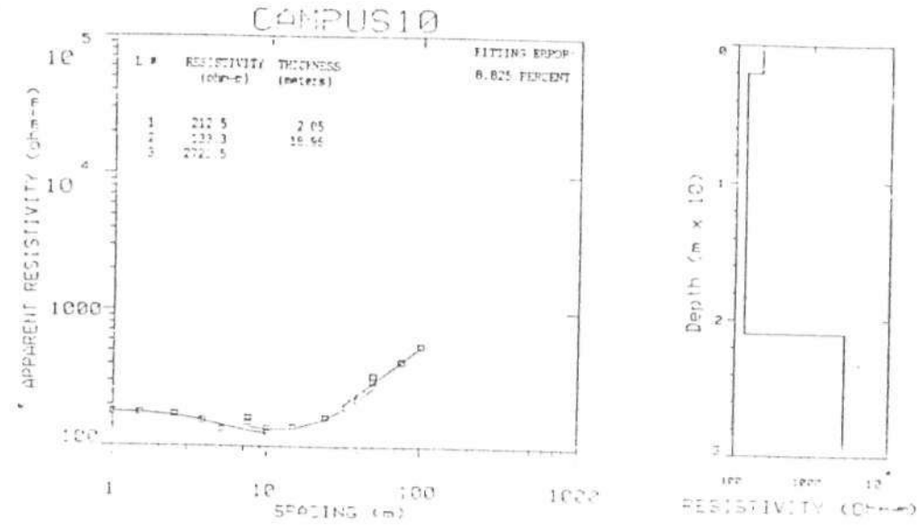

CAMPUS 5
L #
RESISTIVITY (ohm-m)
THICKNESS (meters)
FITTING ERROR:
7.591 PERCENT
1 327.8
2 165.2
3 1098.0
3.69
6.45
APPARENT RESISTIVITY (ohm-m)
SPACING (m)
Depth (m x 10)
RESISTIVITY (Ohm-m)

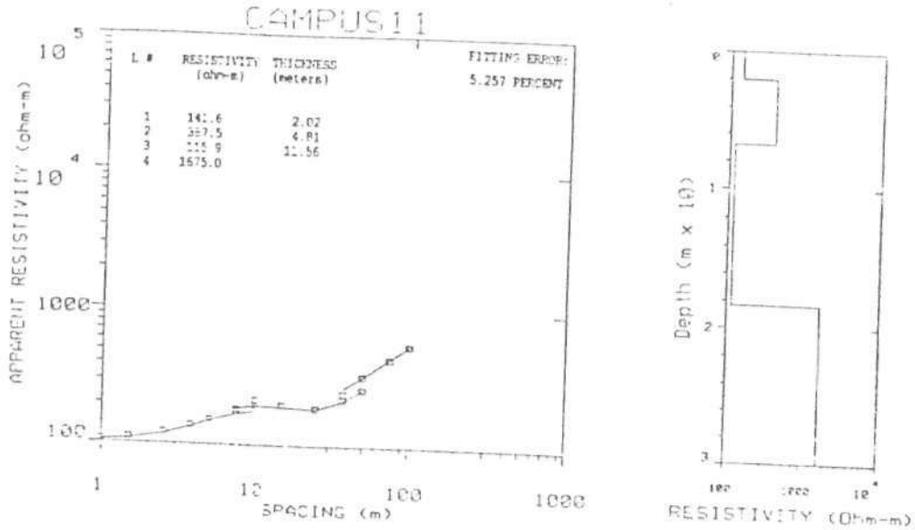

CAMPUS 5
L #
RESISTIVITY (ohm-m)
THICKNESS (meters)
FITTING ERROR:
5.282 PERCENT
1 181.0
2 121.3
3 1635.0
5.25
13.01
APPARENT RESISTIVITY (ohm-m)
SPACING (m)
Depth (m x 10)
RESISTIVITY (Ohm-m)

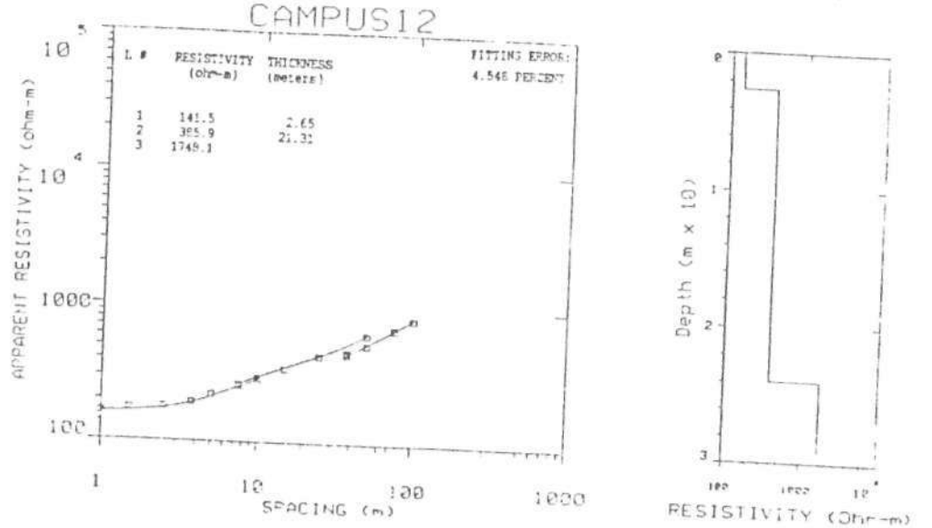

CAMPUS 7
APPARENT RESISTIVITY (ohm-m)
SPACING (m)
RESISTIVITY (Ohm-m)

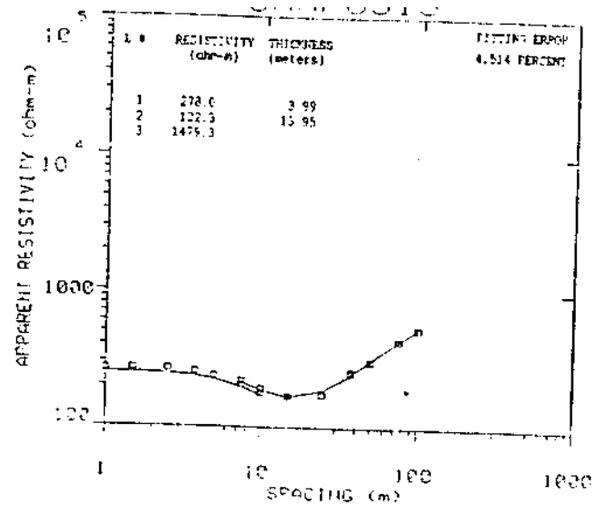

CAMPUS 8
APPARENT RESISTIVITY (ohm-m)
SPACING (m)
Depth (m x 10)

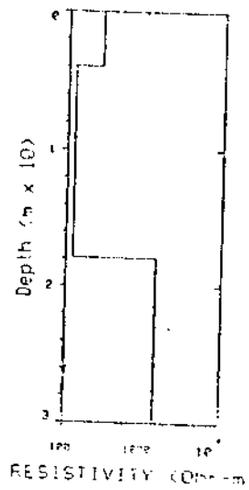

CAMPUS 9
APPARENT RESISTIVITY (ohm-m)
SPACING (m)
RESISTIVITY (Ohm-m)

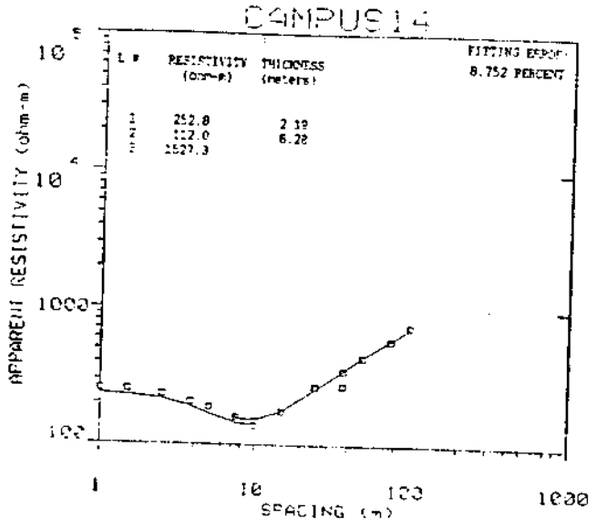

CAMPUS10
L #
RESISTIVITY (ohm-m)
THICKNESS (meters)
FITTING ERROR: 8.825 PERCENT
1 212.5 2.05
2 133.3 10.96
3 872.5
APPARENT RESISTIVITY (ohm-m)
SPACING (m)
Depth (m x 10)
RESISTIVITY (Ohm-m)

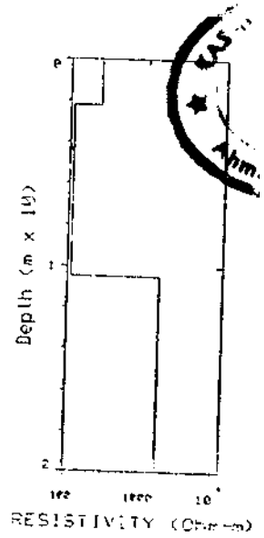

CAMPUS11
L #
RESISTIVITY (ohm-m)
THICKNESS (meters)
FITTING ERROR: 5.257 PERCENT
1 141.6 2.02
2 387.5 6.81
3 115.9 11.56
4 1675.0
APPARENT RESISTIVITY (ohm-m)
SPACING (m)
Depth (m x 10)
RESISTIVITY (Ohm-m)

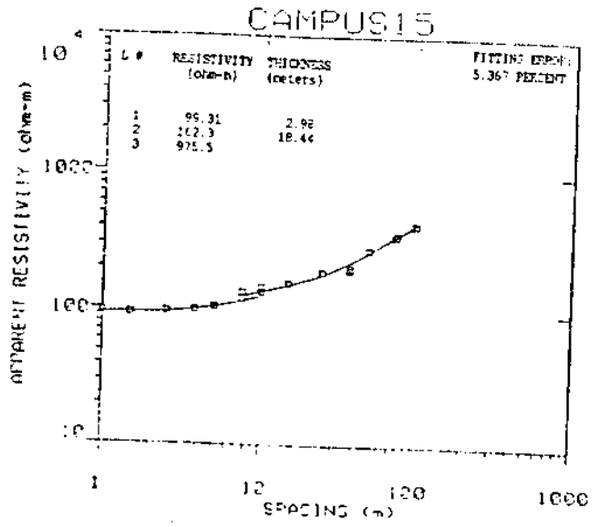

CAMPUS12
L #
RESISTIVITY (ohm-m)
THICKNESS (meters)
FITTING ERROR: 4.548 PERCENT
1 141.5 2.65
2 385.9 21.32
3 1748.1
APPARENT RESISTIVITY (ohm-m)
SPACING (m)
Depth (m x 10)
RESISTIVITY (Ohm-m)

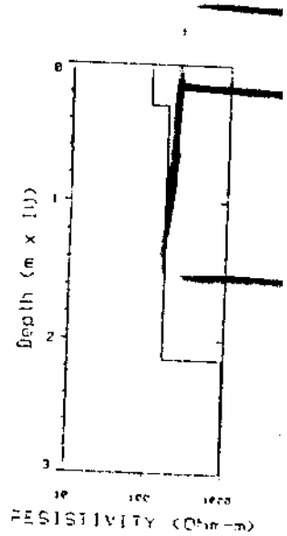

L #
RESISTIVITY (ohm-m)
THICKNESS (meters)
FITTING ERROR
4.514 PERCENT
1 278.0 3.99
2 122.3 15.95
3 1479.3
APPARENT RESISTIVITY (ohm-m)
SPACING (m)

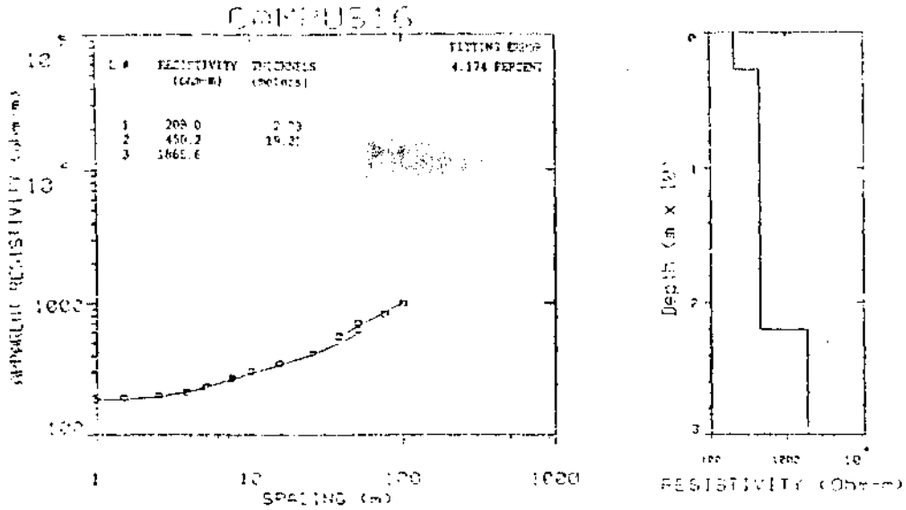

Depth (m x 10)
RESISTIVITY (Ohm-m)

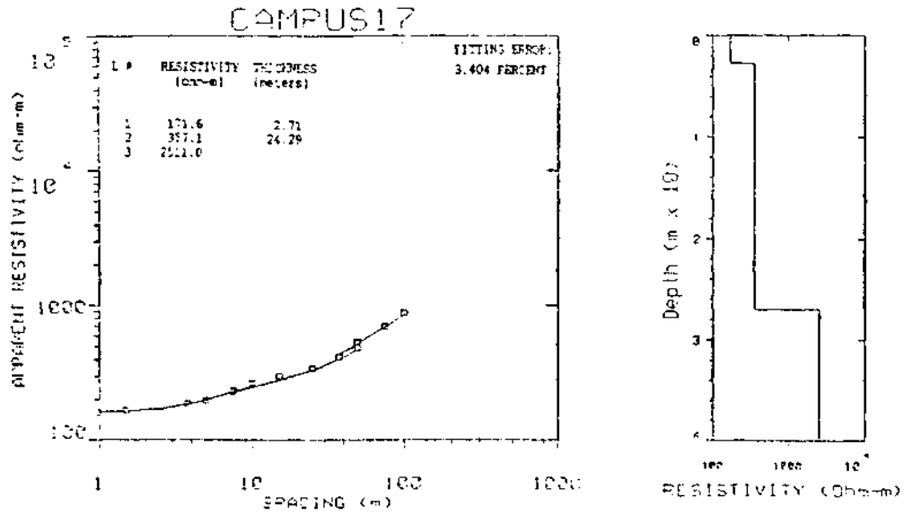

CAMPUS14
L #
RESISTIVITY (ohm-m)
THICKNESS (meters)
FITTING ERROR
8.752 PERCENT
1 252.8 2.19
2 112.0 6.28
3 2527.3
APPARENT RESISTIVITY (ohm-m)
SPACING (m)

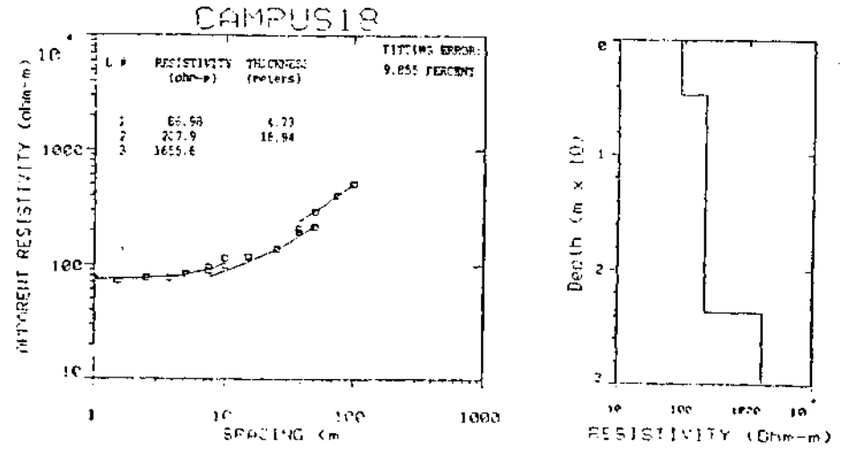

Depth (m x 10)
RESISTIVITY (Ohm-m)

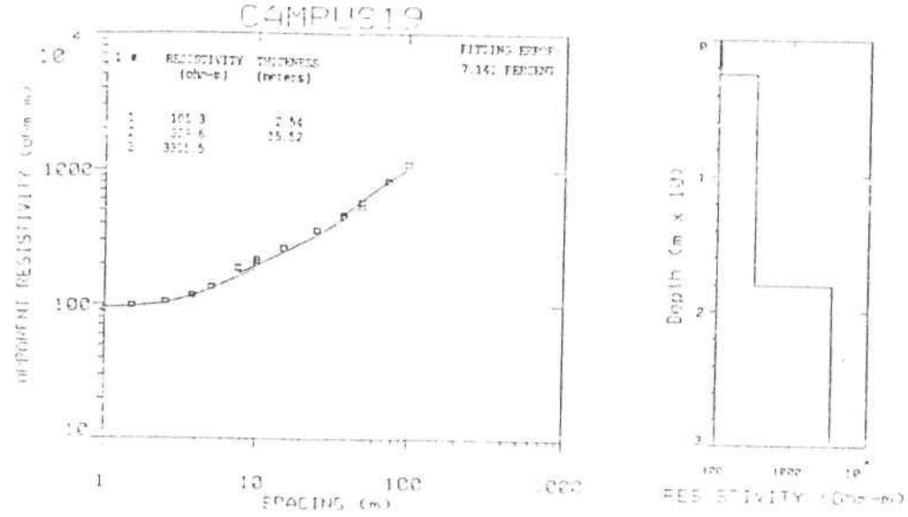

CAMPUS15
L #
RESISTIVITY (ohm-m)
THICKNESS (meters)
FITTING ERROR
5.367 PERCENT
1 99.31 2.98
2 162.3 18.44
3 975.5
APPARENT RESISTIVITY (ohm-m)
SPACING (m)

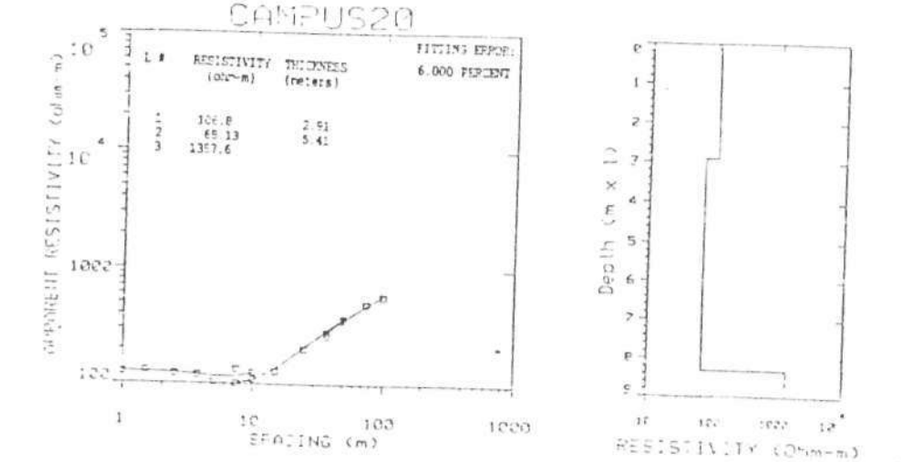

Depth (m x 10)
RESISTIVITY (Ohm-m)

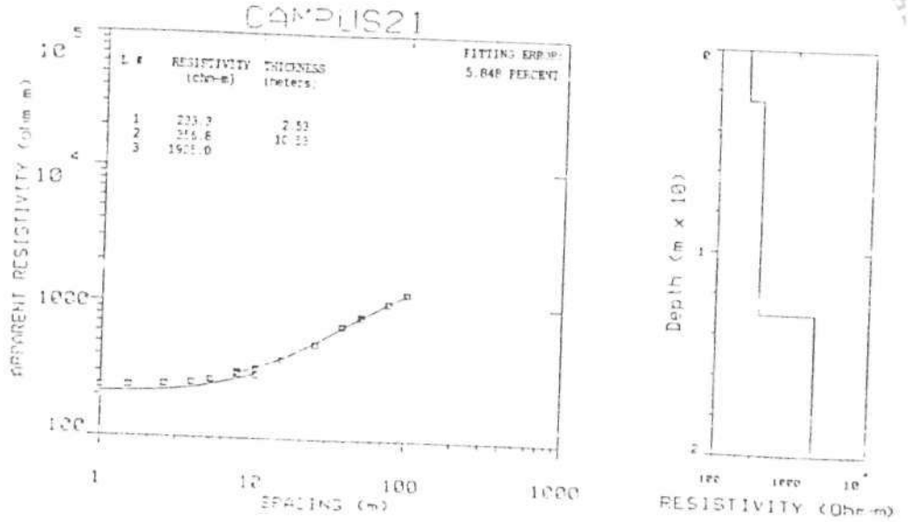

CAMPUS16
L #
RESISTIVITY (ohm-m)
THICKNESS (meters)
FITTING ERROR:
4.174 PERCENT
1 209.0 2.73
2 450.2 19.21
3 1665.6
APPARENT RESISTIVITY (ohm-m)
SPACING (m)
Depth (m x 10)
RESISTIVITY (Ohm-m)

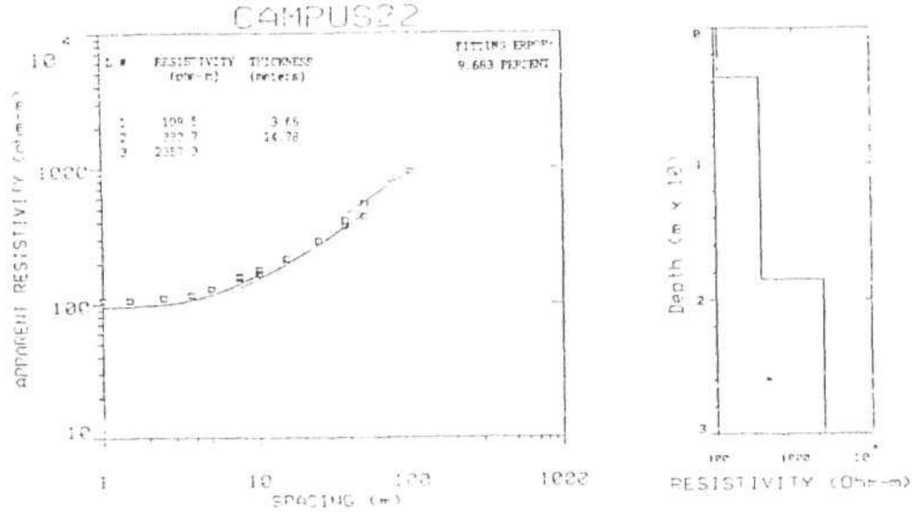

CAMPUS17
L #
RESISTIVITY (ohm-m)
THICKNESS (meters)
FITTING ERROR:
3.404 PERCENT
1 171.6 2.71
2 357.1 24.29
3 2511.0
APPARENT RESISTIVITY (ohm-m)
SPACING (m)
Depth (m x 10)
RESISTIVITY (Ohm-m)

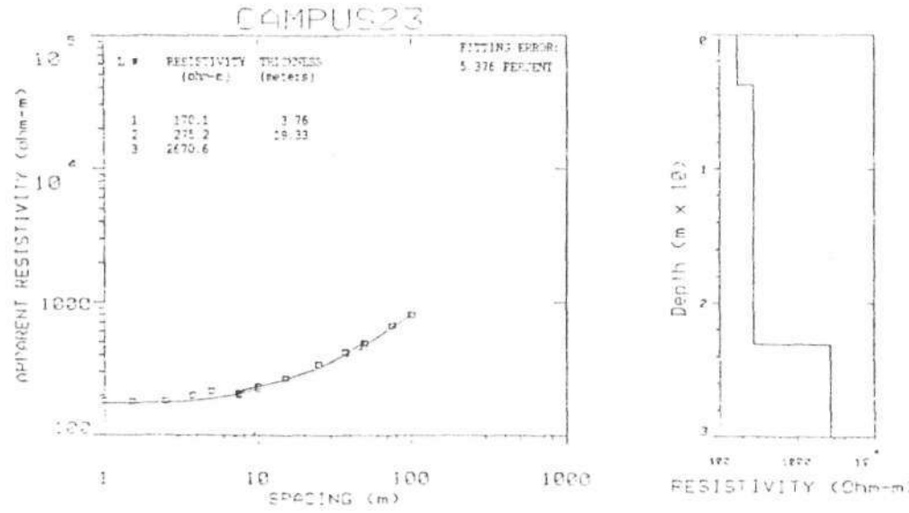

CAMPUS18
L #
RESISTIVITY (ohm-m)
THICKNESS (meters)
FITTING ERROR:
9.855 PERCENT
1 66.98 4.73
2 227.9 16.94
3 1655.6
APPARENT RESISTIVITY (ohm-m)
SPACING (m
Depth (m x 10)
RESISTIVITY (Ohm-m)

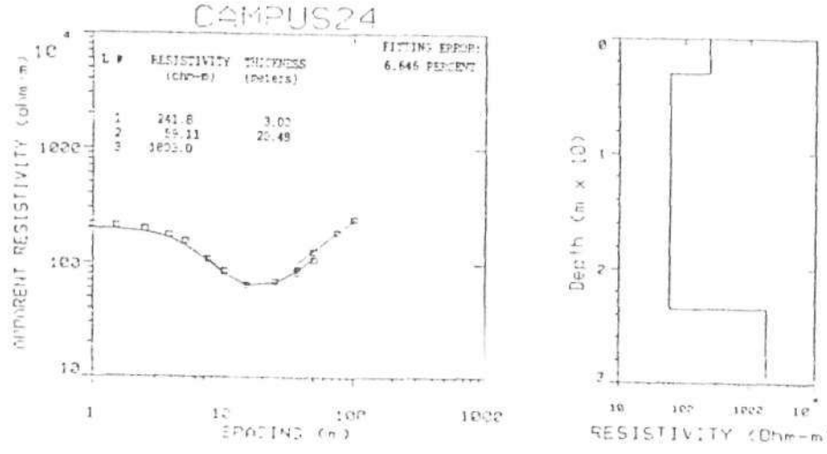

CAMPUS19
L #
RESISTIVITY (ohm-m)
THICKNESS (meters)
FITTING ERROR:
7.341 PERCENT
1
2
3
101.3
2.54
373.6
35.52
3931.5
APPARENT RESISTIVITY (ohm-m)
SPACING (m)
Depth (m x 10)
RESISTIVITY (Ohm-m)

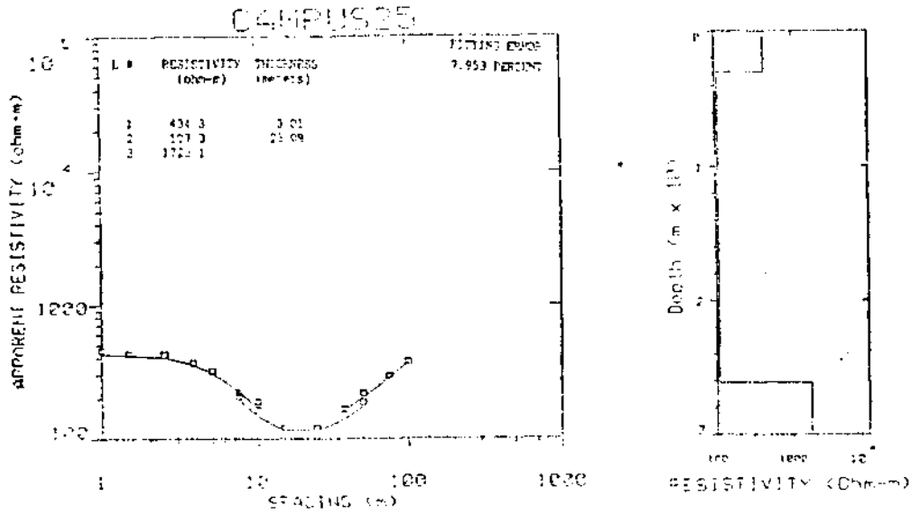

CAMPUS20
L #
RESISTIVITY (ohm-m)
THICKNESS (meters)
FITTING ERROR:
6.000 PERCENT
1
2
3
106.8
2.91
69.13
5.41
1387.6
APPARENT RESISTIVITY (ohm-m)
SPACING (m)
Depth (m x 1)
RESISTIVITY (Ohm-m)

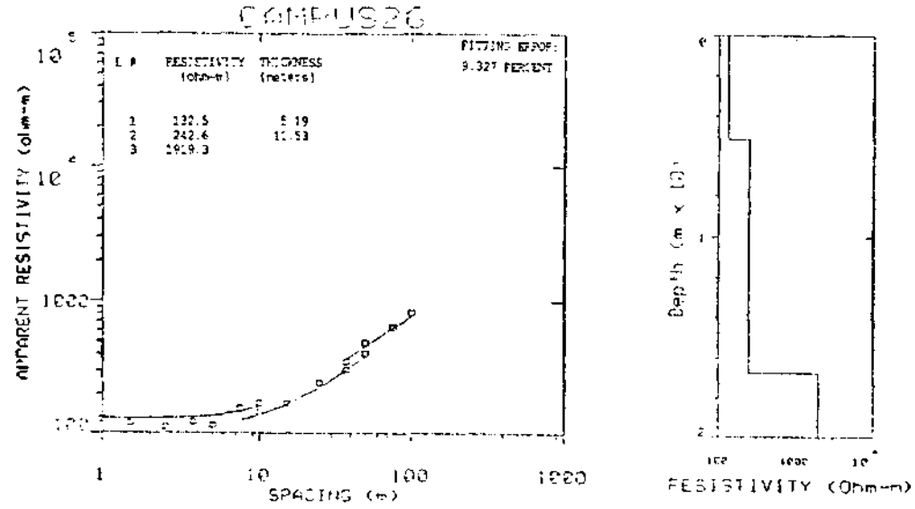

CAMPUS21
L #
RESISTIVITY (ohm-m)
THICKNESS (meters)
FITTING ERROR:
5.848 PERCENT
1
2
3
223.7
2.53
216.8
10.33
APPARENT RESISTIVITY (ohm-m)
SPACING (m)
Depth (m x 10)
RESISTIVITY (Ohm-m)

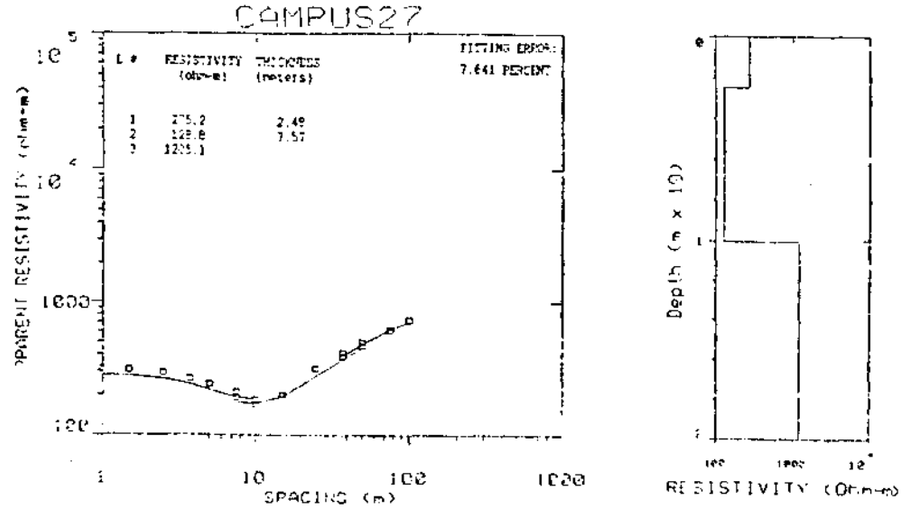

CAMPUS22
L #
RESISTIVITY (ohm-m)
THICKNESS (meters)
FITTING ERROR: 9.683 PERCENT
1 109.5 3.69
2 332.7 14.78
3 2357.3
APPARENT RESISTIVITY (ohm-m)
SPACING (m)
Depth (m x 10)
RESISTIVITY (Ohm-m)

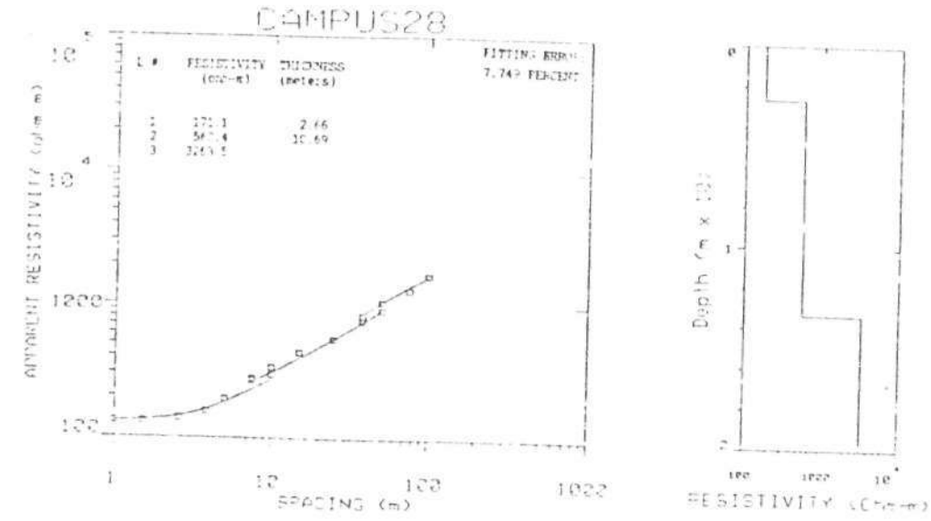

CAMPUS23
L #
RESISTIVITY (ohm-m)
THICKNESS (meters)
FITTING ERROR: 5.376 PERCENT
1 170.1 3.76
2 275.2 18.33
3 2670.6
APPARENT RESISTIVITY (ohm-m)
SPACING (m)
Depth (m x 10)
RESISTIVITY (Ohm-m)

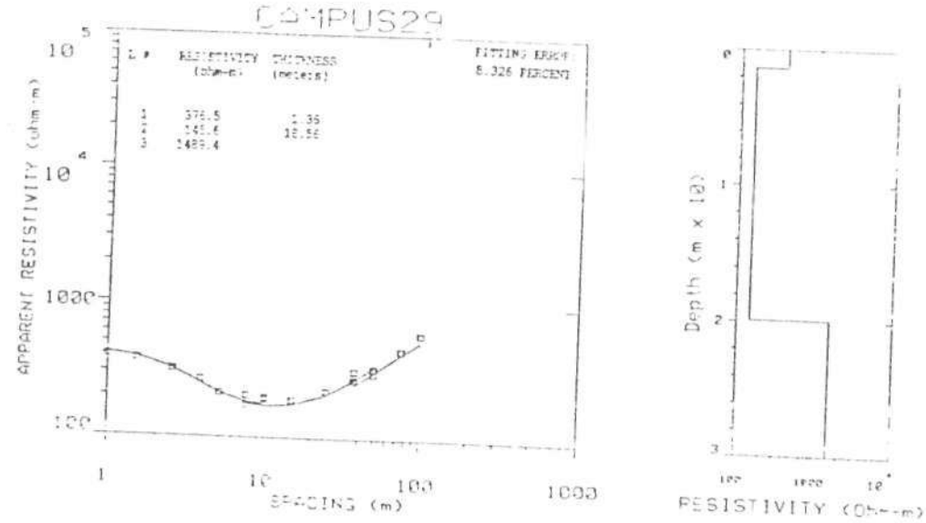

CAMPUS24
L #
RESISTIVITY (ohm-m)
THICKNESS (meters)
FITTING ERROR: 6.646 PERCENT
1 241.8 3.02
2 59.11 20.48
3 1803.0
APPARENT RESISTIVITY (ohm-m)
SPACING (m)
Depth (m x 10)
RESISTIVITY (Ohm-m)

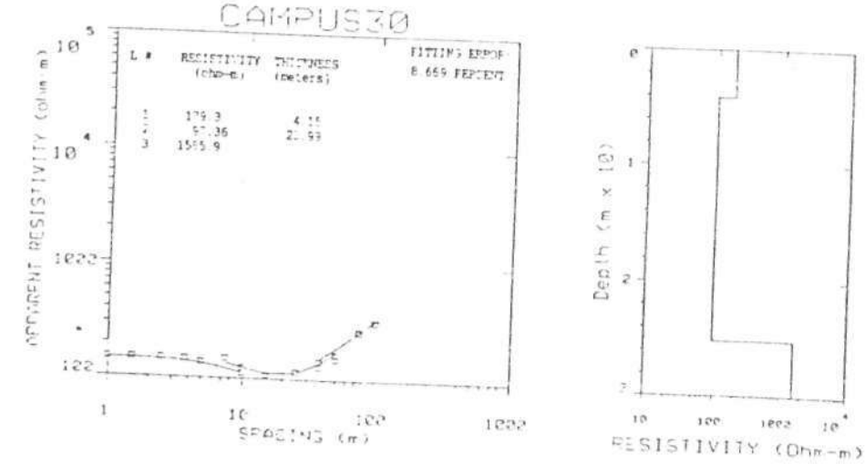

CAMPUS25
APPARENT RESISTIVITY (ohm-m)
SPACING (m)
Depth (m x 10)
RESISTIVITY (Ohm-m)

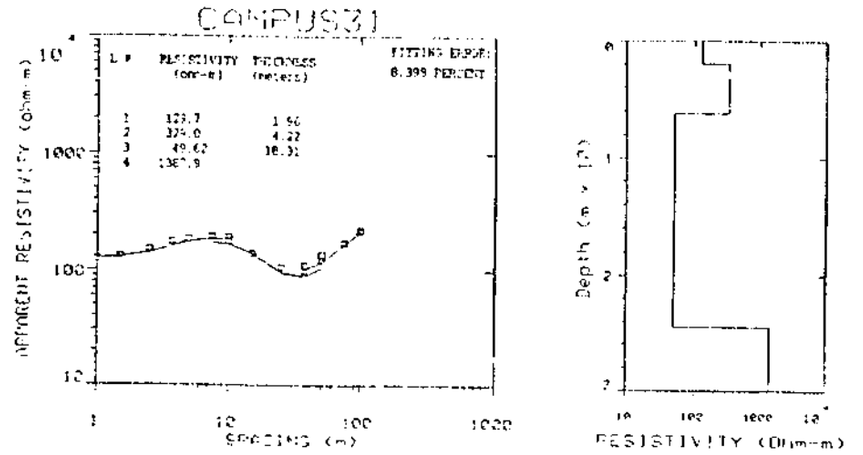

CAMPUS26
APPARENT RESISTIVITY (ohm-m)
SPACING (m)
Depth (m x 10)
RESISTIVITY (Ohm-m)

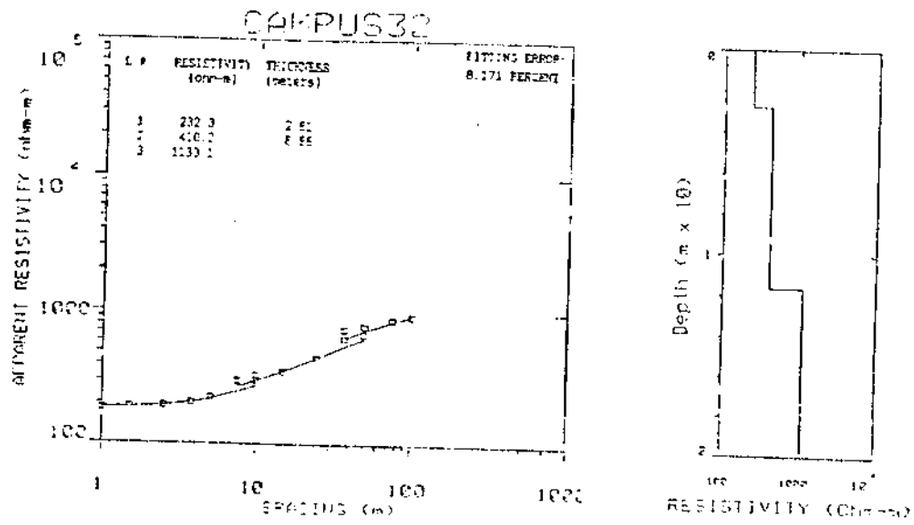

CAMPUS27
APPARENT RESISTIVITY (ohm-m)
SPACING (m)
Depth (m x 10)
RESISTIVITY (Ohm-m)

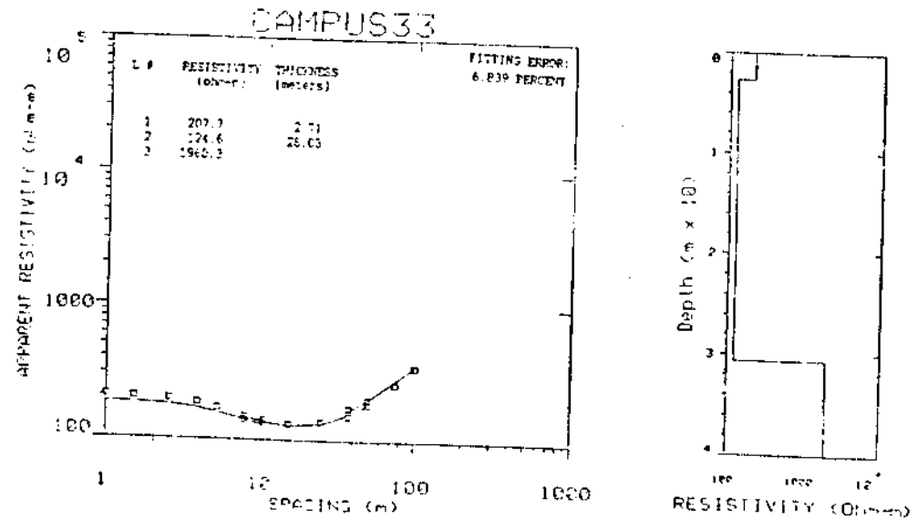

CAMPUS28
APPARENT RESISTIVITY (ohm-m)
SPACING (m)
Depth (m x 10)
RESISTIVITY (Ohm-m)

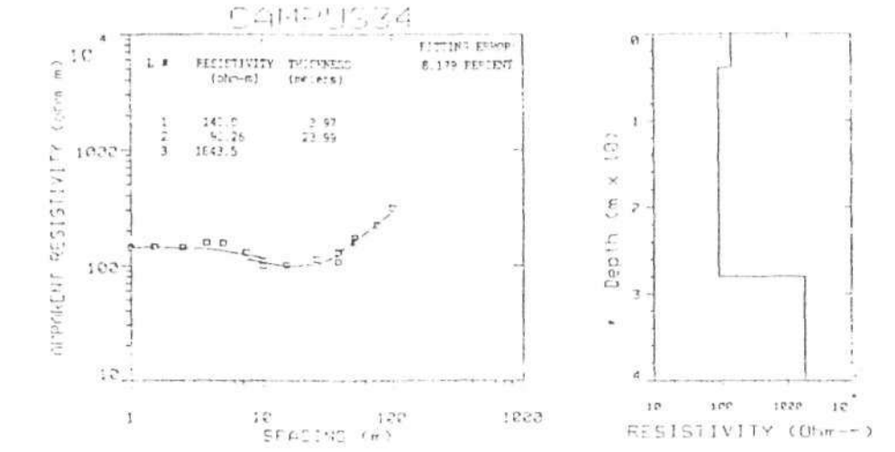

CAMPUS29
APPARENT RESISTIVITY (ohm-m)
SPACING (m)
Depth (m x 10)
RESISTIVITY (Ohm-m)

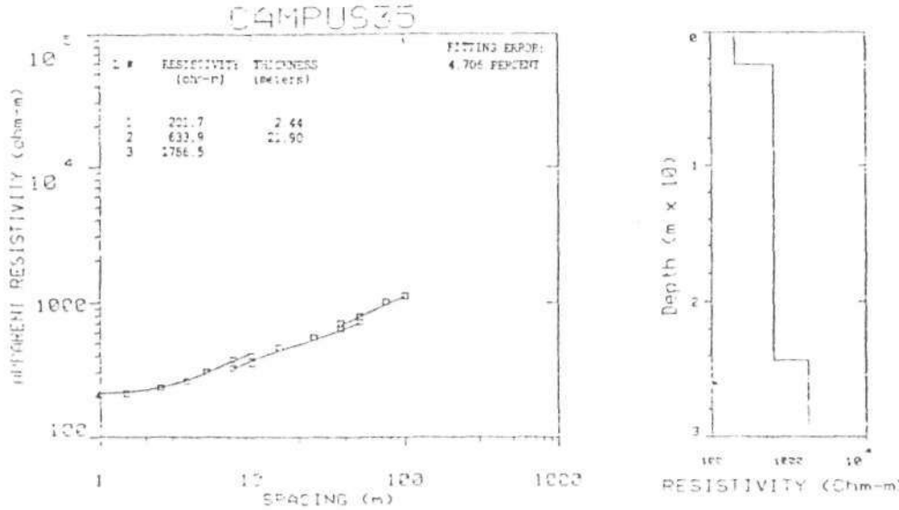

CAMPUS30
APPARENT RESISTIVITY (ohm-m)
SPACING (m)
Depth (m x 10)
RESISTIVITY (Ohm-m)

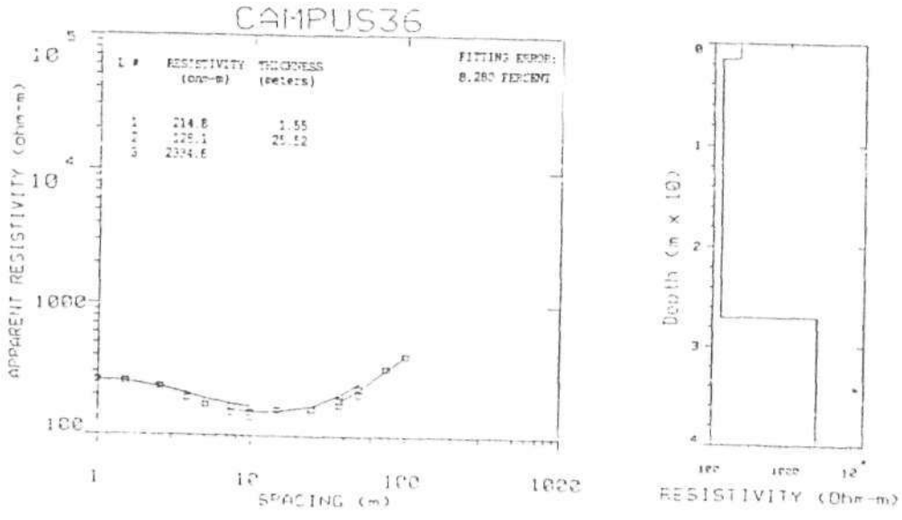

CAMPUS31
APPARENT RESISTIVITY (ohm-m)
SPACING (m)
Depth (m x 10)
RESISTIVITY (Ohm-m)

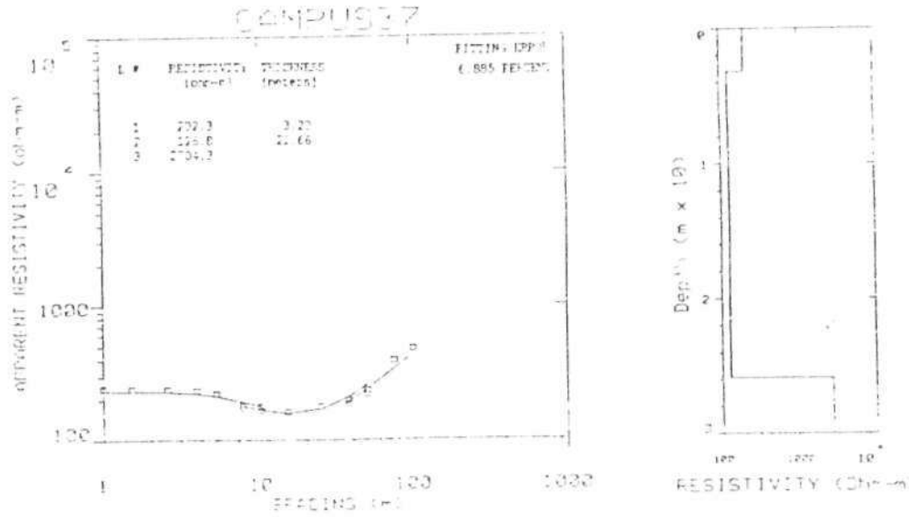

CAMPUS32
APPARENT RESISTIVITY (ohm-m)
SPACING (m)
Depth (m x 10)
RESISTIVITY (Ohm-m)


CAMPUS33
APPARENT RESISTIVITY (ohm-m)
SPACING (m)
Depth (m x 10)
RESISTIVITY (Ohm-m)


CAMPUS34
APPARENT RESISTIVITY (ohm-m)
SPACING (m)
Depth (m x 10)
RESISTIVITY (Ohm-m)


CAMPUS35
APPARENT RESISTIVITY (ohm-m)
SPACING (m)
Depth (m x 10)
RESISTIVITY (Ohm-m)


CAMPUS36
APPARENT RESISTIVITY (ohm-m)
SPACING (m)
Depth (m x 10)
RESISTIVITY (Ohm-m)


COMPUSET
APPARENT RESISTIVITY (ohm-m)
10
100
1000
1
10
100
1000
SPACING (m)
RESISTIVITY (ohm-m)